INSTRUMENTED MONITORING AND DYNAMIC TESTING OF METU
CABLE STAYED PEDESTRIAN BRIDGE AND COMPARISONS AGAINST
ANALYTICAL MODEL SIMULATIONS

A THESIS SUBMITTED TO
THE GRADUATE SCHOOL OF NATURAL AND APPLIED SCIENCES
OF
MIDDLE EAST TECHNICAL UNIVERSITY

BY

TANER ÖZERKAN

IN PARTIAL FULFILLMENT OF THE REQUIREMENTS
FOR
THE DEGREE OF MASTER OF SCIENCE
IN
CIVIL ENGINEERING

JULY 2005

Approval of the Graduate School of Natural and Applied Sciences

_____

Prof. Dr. Canan Özgen
Director

I certify that this thesis satisfies all the requirements as a thesis for the degree of Master of Science.

_____

Prof. Dr. Erdal Çokca
Head of Department

This is to certify that we have read this thesis and that in our opinion it is fully adequate, in scope and quality, as a thesis for the degree of Master of Science.

_____

Asst. Prof. Dr. Ahmet Türer
Supervisor

Examining Committee Members

Prof. Dr. Çetin Yılmaz	(METU,CE)	_____
Asst. Prof. Dr. Ahmet Türer	(METU,CE)	_____
Assoc. Prof. Dr. Cem Topkaya	(METU,CE)	_____
Asst. Prof. Dr. Alp Caner	(METU,CE)	_____
Asst. Prof. Dr. Ferhat Akgül	(METU,ES)	_____

I hereby declare that all information in this document has been obtained and presented in accordance with academic rules and ethical conduct. I also declare that, as required by these rules and conduct, I have fully cited and referenced all material and results that are original to this work.

Name, Last Name   : Taner ÖZERKAN

Signature   :

ABSTRACT

INSTRUMENTED MONITORING AND DYNAMIC TESTING OF METU
CABLE STAYED PEDESTRIAN BRIDGE AND COMPARISONS AGAINST
THE ANALYTICAL MODEL SIMULATIONS

ÖZERKAN, Taner

M.S., Department of Civil Engineering

Supervisor   : Asst. Prof. Dr. Ahmet Türer

July 2005, 125 pages

This study includes structural instrumentation and monitoring of a 48.5 meters long cable-stayed pedestrian bridge located on Eskişehir road near METU campus. The objectives of the study are (1) to monitor the bridge responses during erection and operation stages so that the strain changes are determined during important events such as transportation, lifting, cabling, mid-support removal, slab concrete pouring and tile placement, (2) to determine existing cable forces using vibration frequencies, and (3) comparison of the experimental and analytical results for model updating.

A total of 10 vibrating wire type strain gages were used for strain readings in steel members. The readings are taken at various stages of construction at every 10 to 30 minutes intervals. The bridge responses were monitored about three months and large strain changes in the order of 300 to 500 $\mu\varepsilon$ were recorded during important events (e.g., transportation, lifting, cabling, mid-support removal, deck cover placement).

The deck and tower natural vibration frequency measurements are conducted in two main directions. Two different FE models are constructed using two levels of complexity. FEM analysis results are compared against measured natural frequencies of the bridge and tower.

Simplistic analytical model is modified to include temporary support removal in order to perform staged construction simulation and investigate cable force variations. Actual cable tensile forces are obtained using measured cable natural vibration frequencies. The cable frequencies are measured using a CR10X data logger and a PCB 393C accelerometer. Existing cable forces are compared against analytical simulations and symmetrically placed cables.

Keywords: Structural Monitoring, Cable-Stayed Bridge, Dynamic Analysis of Cables, Cable Forces.

ÖZ

ODTÜ ASMA YAYA ÜST GEÇİDİNİN ÖLÇÜME DAYALI İZLENMESİ VE DİNAMİK TESTLER İLE HAZIRLANAN ANALİTİK MODELLERİN KARŞILAŞTIRILMASI

ÖZERKAN, Taner

Yüksek Lisans, İnşaat Mühendisliği Bölümü

Tez Yöneticisi : Yrd. Doç. Dr. Ahmet Türer

Temmuz 2005, 125 sayfa

Bu çalışma Eskişehir yolu üzerinde ODTÜ kampüsü yakınında bulunan 48.5 metre uzunluğundaki asma yaya üst geçidinin yapısal olarak izlenmesini içerir. Bu çalışmanın amaçları; (1) önemli olaylar örneğin köprü parçalarının nakli, kaldırılması, kablolanması, köprü orta ayağının kaldırılması, döşeme betonunun dökümü ve döşeme karolarının yerleştirilmesi sırasında meydana gelen birim deformasyon değişikliklerinin saptanması için yaya üst geçidinin yapısal davranışlarını inşaa ve işletme halinde izlemek, (2) kablolardaki eksenel yüklerin, kabloların titreşim frekanslarını kullanarak belirlemek ve (3) model kalibrasyonu için deneysel sonuçların analitik model sonuçları ile karşılaştırmaktır.

Çelik elemanlar üzerinden birim deformasyonları okumak için toplam 10 adet titreşim telli birim deformasyon ölçer kullanılmıştır. Çeşitli inşaa aşamalarında her 10 dakika ve 30 dakika da bir okumalar alınmıştır. Köprü yapısal davranışları yaklaşık üç ay boyunca izlenmiş ve önemli olaylar; köprü gövdesinin nakli, kaldırılması, askı kablolarının takılması, köprü orta ayağının kaldırılması ve köprü döşemesinin kaplanması sırasında yaklaşık olarak 300 ile 500$\mu\varepsilon$ arasında büyük birim deformasyonlar kaydedilmiştir.

Analitik model simulasyonu ile karşılaştırmak için köprü gövdesi doğal titreşim frekans ölçümleri hem düşey hem de yatay olmak üzere köprü orta noktasından alınmış ve köprü kulesinin de dinamik analizleri hem boyuna hem de dik yönde olmak üzere köprü tabanından 15 metre yükseklikte yapılmıştır.

Kablo doğal titreşim frekansları kablolardaki eksenel yüke göre değişir. Kablolardaki kuvvetleri ve paralel olarak yerleştirilmiş kablolardaki eksenel kuvvet farklılıklarını hesaplayabilmek için kablo doğal titreşim frekansları, CR10X data toplama aleti ve PCB 393C tipi aksonometre kullanılarak ölçülmüştür. Ölçülen kablo kuvvetleri sonlu elemanlar yöntemi ile oluşturulmuş statik model sonuçları ile karşılaştırılmıştır.

Anahtar Kelimeler: Yapısal Sağlık İncelemesi, Asma Köprüler, Kabloların Dinamik Analizi, Kablo Kuvvetleri.

This thesis is dedicated to

My mother and father

Cahide & H. Ahmet ÖZERKAN

ACKNOWLEDGMENTS

I would like to express my deepest appreciation to my supervisor, Asst. Prof. Dr. Ahmet TÜRER, for his invaluable support, guidance, criticism, and insight throughout the research. Also, I underline that my career may have been a linear one without his priceless encouragement.

I wish also thank to Asst. Prof. Dr. Habib Tabatabai at Department of Civil Engineering & Mechanics, University of Wisconsin, Milwaukee, for valuable knowledge about field instrumentation and monitoring of bridges and I would also thank to Mrs. Tuba EROĞLU for her supports in dynamic analysis experiments on the METU Bridge.

Finally, I would like to thank my parents, Mrs. Cahide ÖZERKAN and Mr. H. Ahmet ÖZERKAN, who give me all chances to go forward and encourage me to start this Master of Science program. They make all things which their children want by dedicating their life. I could not able to accomplish this research without their love and supports.

TABLE OF CONTENTS

LIST OF TABLES

Table

LIST OF FIGURES

Figure

LIST OF ABBREVIATIONS

A/D   Analog to digital converter

cm   Centimeter

COUPLERL   Coupler load

COVERL   Cover load

DAS   Data acquisition system

dia   Diameter

DL   Dead load

dofs   Degrees of freedom

DSI   Devlet Su İşleri (General Directorate of State Hydraulic Works)

EIVAR22   The changes of the bending stiffness values about 2 axis

EIVAR33   The changes of the bending stiffness values about 3 axis

FE   Finite element

FEM   Finite element model

FFT   Fast Fourier transformation

Hz   Hertz (1/sec)

KGM   Karayolları Genel Müdürlüğü (General Directorate of Highway)

METU   Middle East Technical University

M.D   Mode shape of the bridge deck

M.T   Mode shape of the tower

P.STRESSL   Prestressing load

LIST OF SYMBOLS

A	:	Cross-section area
c	:	User defined ($c = \sqrt{\dfrac{EIg}{wL^4}}$)
E	:	Modulus of elasticity
F	:	Prestressing load
f_n	:	Measured resonant vibration frequency
F_y	:	Yield strength
g	:	Gravity acceleration
L	:	Total length of the bridge member
m	:	Mass per unit length
n	:	Vibration mode referring to f_n
I	:	Moment of Inertia
T	:	Axial load in the cable
t_2	:	Outside width of non-prismatic sections
t_3	:	Outside depth of non-prismatic sections
α	:	Coefficient of thermal expansion
Δf	:	Frequency domain resolution
ΔT	:	Temperature difference
ξ	:	User defined ($\xi = \sqrt{\dfrac{T}{EI}}L$)
ρ	:	Unit weight of cables per unit length

CHAPTER 1

INTRODUCTION

This section summarizes the objectives and scope of the thesis. Brief description of the study and general issues about instrumented monitoring and analytical modeling are presented.

1.1 Objectives and Scope of the Study

The following are the main objectives of this thesis:

❖ Investigate the level of strain changes at the bridge girders during construction and service stages (such as transportation, lifting, cabling, mid-support removal, deck surface concreting and tile placement).

❖ Determine axial forces and axial force differences on the cables.

❖ Instrumented monitoring of bridge girders to investigate bridge response to temperature induced forces.

❖ Investigate the bridge natural frequencies and mode shapes by conducting simplistic dynamic measurements. Modal updating (calibration) of the analytical model in order to conduct structural identification.

❖ Investigate the usage of long-term monitoring systems and instrumentation methods.

The main scope of the thesis is given below:

❖ Instrumentation of the bridge members at the factory using strain gages, data transmission cables, CR10X data logger, and battery.

❖ Collect data from strain gages during transportation, cabling, temporary supports removal, slab concreting and tile placement processes.

❖ Conduct simplistic dynamic experiments on the deck and tower in order to obtain natural frequencies and mode shapes.

❖ Measure the resonant frequencies of the cables in order to obtain axial forces and compare field experiment and analytical models' results.

1.2 Description of the study

Cable stayed bridges are among the world's architecturally pleasing and technically innovative structures. Moreover, they are economical if they are properly designed; therefore, cable-stayed bridges have found wide applications all over the world since 1955.

One of the main reasons for investigation of the METU Bridge is that cable-stayed bridges are rarely seen in Turkey and steel bridge construction constitutes less than 1% of Turkey bridge inventory (Kara Yolları Genel Müdürlüğü (KGM), General Directorate of Highway – 2000). The METU Bridge is also conveniently located very close to the campus making it possible to make frequent trips. The owners have permitted instrumentation; therefore, the study took off by instrumentation at the factory. The study

would give an idea for the level of construction stresses that occur in cable stayed pedestrian bridge.

One of the important chances of this thesis study was that monitoring the bridge response from factory to the service stages which is rarely seen even in big projects. Therefore, instrumentation of the METU Bridge was performed from the beginning at the factory and continued at the construction stages as data were recorded during erection and service stages (such as transportation, lifting, cabling, mid-support removal and concreting and tile placement at different times).

Dynamic tests were performed on the deck and tower of the bridge to find natural vibration frequencies and mode shapes. Cable forces are calculated indirectly using resonant vibration frequencies of the cables and these results are compared against symmetric cables and analytical model results. This study would be a mile stone for future studies in similar structures. The instrumented monitoring and dynamic analysis results are given in Chapter 4.

Another main reason of the investigation of the METU Bridge is to test analytical modeling capabilities and FEM calibration using dynamic field test results of the bridge. Designers can benefit from staged construction modeling investigated in this study since the cable forces and effects on the bridge change as cables are tensed one by one and temporary supports are removed.

1.3   Instrumented Monitoring

The instrumentation was carried out at the factory right after the bridge was manufactured in two separate pieces for easy transportation. The two pieces are combined on the construction site. Five strain gages and 5 thermocouples were mounted on each piece of the bridge; however, due to transportation and cabling constraints, only five of the gages were monitored during transportation and lifting until both pieces were assembled together at METU site. The other five strain gages were connected to the data logger after the two bridge segments were combined together on temporary supports.

Dynamic tests are carried out using CR10X data logger and a PCB-393C accelerometer. The tests were carried out using a single accelerometer which was intelligently placed on the bridge to capture certain modes at a time. The center of the bridge deck versus edges of the deck distinguishes torsional modes. Placing the accelerometer in horizontal direction captures only the modes in transverse direction. Excitation of the bridge deck was provided by jumping on the bridge deck (two people jumping about 180 kg mass). Lateral excitation of the deck, tower, and cables were provided by hitting the members laterally using a wooden log.

1.4 Structural Modeling & Updating

Finite element modeling is a mathematical tool which may be used to simulate the physical behavior of the structures. Using FE modeling, the structure is divided into several small segments. The three-dimensional (3D) finite element models (FEM) are constructed using shell and frame elements. The tower, the deck, cables, and girders are modeled. Frame/cable members are used to simulate beam and truss behavior and shell members are used to simulate membrane and plate behavior. The model dynamic analysis is performed by eigenvalue analysis. The eigenvalue analysis is used to calculate the natural vibration frequencies (eigenvalues) of the FE model and the corresponding mode shapes (eigenvectors).

Simplifications and approximates made when creating the initial FE model causes deviations from the actual measured responses. The analytical model is updated to match field measured dynamic test results. The FE model updating studies involve changing the model structural parameters within SAP2000 structural analysis program such as boundary conditions of the deck and tower supports, elastic modulus of the cables, unit mass of the deck cover. Calibration process was done until a relatively good correlation was obtained between analytical model and experimental results.

CHAPTER 2

GENERAL INFORMATION ABOUT CABLE-STAYED BRIDGES

2.1 Bridge Architecture

The structural system of cable-stayed bridges can be divided into four main components [5] as shown in Figure 2-1.

1. The stiffening girder with the bridge deck,

2. The cable system,

3. The towers (or pylons),

4. The anchor blocks (or anchor piers)
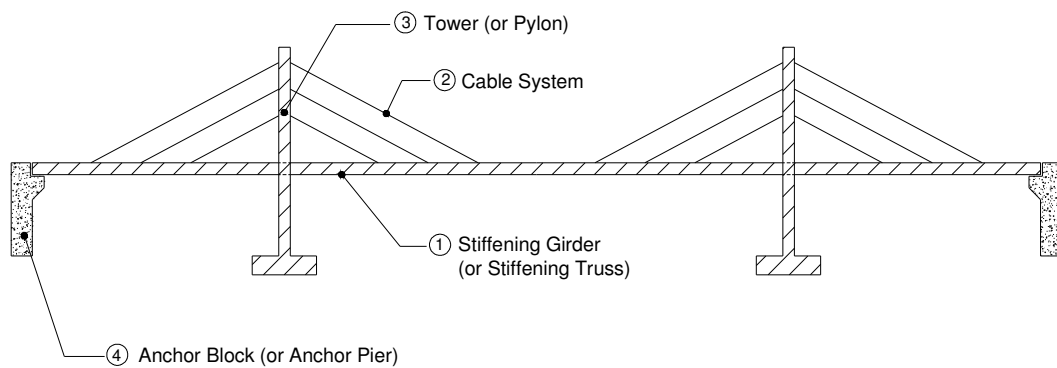
Figure 2-1: Structural system definition of cable-stayed bridges [5]

Aesthetic design has become an important part of bridge design and includes the combination of three basic factors which are given as follows [3].

1- Function

2- Sound structural design

3- Appropriate aesthetic treatment

The above considerations can be summarized as follows:

1. Safety, ecology, compatibility with the environment, slenderness, reduced mass, and the simplicity of details are the factors to be considered in the aesthetic design.

2. Safety measures which are related to safety margins should be considered in design.

3. Landscape and environment are important point of view, therefore, the overall view of the bridge should appear to be in balance and the bridge should fit into the surrounding terrain.

4. Slenderness is another main objective of aesthetic view of bridges. Designers should kept the span/depth ratio of superstructure and width/height ratio of piers to a minimum.

5. Designer also should keep details of the bridge as simple as possible. In the design of modern cable-stayed bridges, an important aim is to produce an aesthetically appealing bridge which matches all conditions which are mentioned at previous pages with its surroundings.

Classical principles of aesthetics for bridge architecture are given by Vitruvius [3], and generally most of cable-stayed bridges satisfy these principles.

1) Harmony of scale,

2) Arrangement or expression of function

3) Element of beauty resulting from fitting adjustment of members,

4) Symmetry or proper balance of parts,

5) Simplicity,

6) Economy, considering cost.

Selection of cable arrangement type is one of the important factors of the aesthetic design of the bridge. The harp arrangement of parallel cables generally is preferable and usually provides the most attractive solution. Towers which are being visible from many points on land are the most noticeable part of the bridge. The height of the tower is usually determined by the clear height of the deck, span lengths and the selected inclination of the cables.

2.2   Structural Advantages

Cable-stayed bridges have found wide applications all over the world since the last few decades. Bridge engineering has been developed to a great extent with the introduction of the cable-stayed bridges.

Stiffening girders and prestressed or post-tensioned stay cables which attached from the tower to the deck stiffening girders and hang from the tower to anchor blocks are the main structural characteristics of cable stayed

systems. The substructure is smaller and economical since massive anchorages are not required in cable-stayed bridges [3].

The orthotropic system (i.e. of or relating to a bridge deck consisting of steel plates supported by ribs underneath [21] (www.bartleby.com) enables to reduce the depth of the girders. The orthotropic type deck also acts as transverse beams, which increases the lateral bending stiffness of the deck.

Another structural characteristic of orthotropic system is that the geometry of this system is stable under any load case on the bridge, and all cables are always in state of tension. Also, the continuity of the bridge over many spans is provided by using orthotropic deck system [3]. Cable-stayed bridges are preferred between girder type and suspension type bridges for long spans.

2.3 Comparison of Cable-Stayed and Suspension Bridges

The cable-stayed bridge differs from suspension bridge in terms of deck supporting and anchorage zone type. In suspension bridges the deck is supported from loosely hug main cables with vertical suspenders which behave as truss members. However, in cable-stayed bridges the deck is supported directly from the towers with stay cables. In cable stayed bridges, the deck can be made lighter and more slender because orthotropic deck system increases the bending stiffness of the deck. This provides a significantly stiffer structure [3].

The superiority of the cable-stayed bridge over the suspension bridge was proposed and developed by Gimsing [5]. The study was carried out to find the proportion of costs and quantities of steel required. The investigation results have shown that the cable-stayed bridges with fan system give the minimum cost, while the cost of the suspension bridge is 24% higher (for shorter distances). Analysis results about quantities of steel required are given in Table 2-1.

Table 2-1: Required quantities of steel for different span length [3]

Bridge System	Span (m)	Required Cable Steel (tons)	Required Structural Steel (tons)
Suspension	1000	7500	23000
Cable-stayed	1000	3900	25000
Suspension	2000	3600	55000
Cable-stayed	2000	1900	94000

The results of the investigation [3] are given as follows;

1. The required quantities of steel of the cable-stayed bridge are less than suspension bridge for main span of 1000m. However, the required quantities of steel of the suspension bridge are less than cable-stayed bridge for main span of 2000m.

2. Cable-stayed bridge has a greater deflection at mid-span than does the suspension bridge for main span of 2000m. However, the suspension bridge has a greater deflection for a main span of 1000m.

The comparison between the deck system of both bridge types shows that the suspension bridge needs more bending and torsional stiffness, while the cable-stayed bridges need more steel area for thrust [3].

The other main advantage of the cable-stayed bridges over the suspension bridges (for shorter distance) is the required concrete for anchorage zone. Suspension bridges need larger or heavier anchorages to provide the stability.

2.4   Structural Details

2.4.1   Stiffening Girders and Trusses

Bending moments and normal force components from the inclined cables acting on the deck should be considered for a proper design. The deck system are usually designed as box-sections due to their torsional contributions and to provide convenient anchorages for stay cables. Another advantage of using box-sections is the reduction of the truss members. Intermediate stiffeners of the webs are placed inside box girders to prevent torsional and shear buckling and for aesthetic reasons. The rigidity of box-sections is increased by using diagonal bracing outside the sections [3].

11

2.4.2 Towers

Several types of towers are used from early cable-stayed bridges to present ones. The main types of towers are listed below [3].

1. Trapezoidal portal frames,

2. Twin towers,

3. A – frames,

4. Single towers.

The frequent usage of towers goes from portal type to single or twin ones because of the investigation results and the cost of the construction. The investigations show that the horizontal forces of the stay cables and the wind load which the cable transfers to the top of the towers are relatively small. The inclined stay cables, which behave as restraint at the tower connection, also prevent tower from moving laterally.

The single or twin towers with no cross-members are stable under wind load cases. When tower is placed at the bridge end and cables are anchored on anchor block, the lateral movement is prevented placing the cable anchorage level above the tower's base support level. The stretching of the cable enables to increase of the tension forces on the cable. Most towers of modern cable-stayed bridges consist of a single rectangular box built with thick steel plates by means of welding or bolting.

2.4.3 Tower Base Bearings

The connections between the towers, cables, deck, and piers determine the structural behavior of the cable-stayed bridges. Pinned connections can be used to minimize the bending moments at the base of the tower but these type connections may not be preferred since they are expensive and complicated for pinned construction and erection. A fixed base, attached either to the deck or pier, would generate large bending moments and must be taken into consideration for proper design [3].

Although pinned connections have some difficulties in application, they are usually preferred when the tower foundations are in weak soil where moment transfer to the foundation would be prevented.

2.4.4 Types of Cables

A cable may be composed of one or more structural ropes, parallel wire strands, or locked-coil strands which are shown in Figure 2-2 [4]. There are several types of cables which are used in bridges. The form or configuration of the cable mainly depends on its material characteristics and purpose of usage: it may be solid bars or composed of one or more structural ropes, structural strands, locked coil strands, or parallel wire strands.

A solid bar as a stay cable can be used for the cable stayed bridges with small spans. An assembly of wires formed helically around a central wire in

one or more symmetrical layers is called as a strand with the exception of a parallel wire strand. A rope is formed by lots of strands which are helically placed around a core and is covered by a material is complies with ASTM A-603 standard specifications. Significant differences between a rope and a strand are given as follows [4], [5].

1. In contrast to the strand, a rope provides high curvature capability.

2. The modulus of elasticity of a strand is higher than that of a rope.

3. A strand has higher breaking strength than a rope at equal sizes.

4. The wires in a strand are larger than those in a rope of the same diameter.
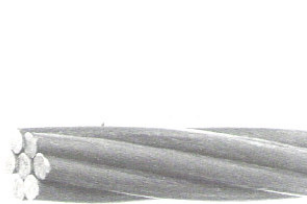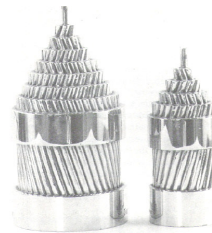
a) Multi-wire strand	b) Multi-wire helical strand
c) Rope of twisted strands	d) Cross-section of a locked coil strand
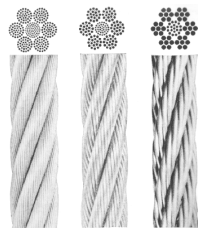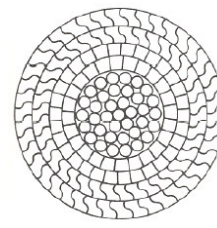
Figure 2-2: Main types of cables [4], [5]

2.4.5 Cable Supports on the Tower

The connection between towers and cables can be either fixed or movable or a combination of both. Although fixed type connections can cause high restraint forces on supports, fixed supports increases the stiffness of the system.

2.4.6 Cable Supports on the Deck

The supports should be fixed because the cable connections should provide full transfer of loads. Also, protection against weather, adjustments, initial tensioning, and ease of access for inspection are the main considerations to make a proper design.

2.4.7 Modulus of Elasticity of Cables

Modulus of elasticity of a strand or a rope with the exception of a solid bar can be determined from a specimen and computed on the gross metallic area, including the zinc coating. Modulus of elasticity of a solid bar can be taken as $2*10^5$ Mpa [3].

CHAPTER 3

DESCRIPTION OF THE STRUCTURE

3.1   General

The newly constructed 48.5 meters long METU cable-stayed pedestrian steel bridge is designed and constructed to enable safe crossing of Eskişehir highway between Middle East Technical University and DSI (General Directorate of State Hydraulic Works) sides. The bridge elevation is shown in Figure 3-1 and Figure 3-2 which includes the adjacent metro station. The structure, weighing approximately 190 tons (about 100 tons for the tower and 90 tons for the deck and cables), comprised a 2.63m wide deck suspended by a 43.12 meters tall tower on parallel placed 12 steel cables.
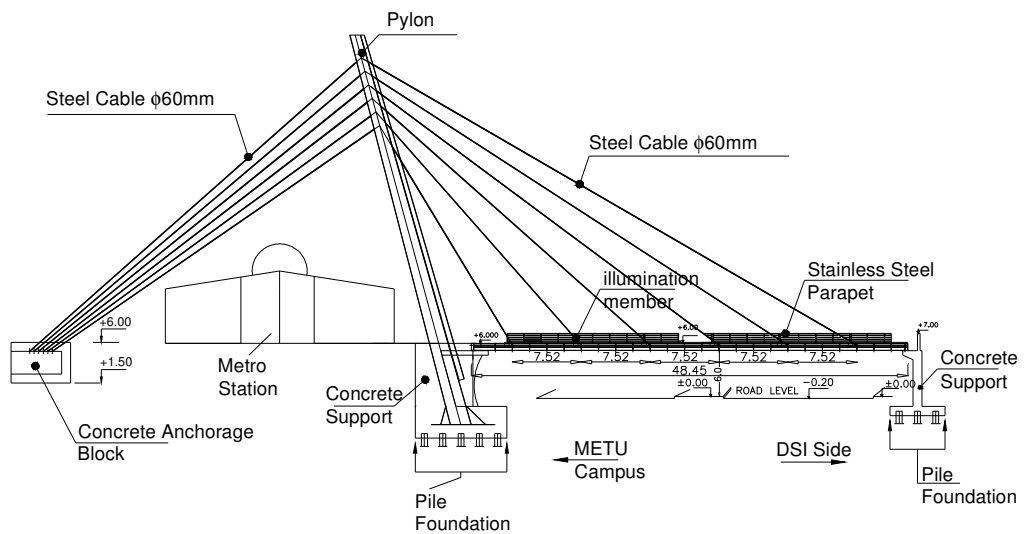
Figure 3-1: Longitudinal cross section of the bridge

(a)

SECTION A-A

(b)

SECTION C-C

THIS DETAIL WAS APPLIED AT THE CABLE CONNECTIONS
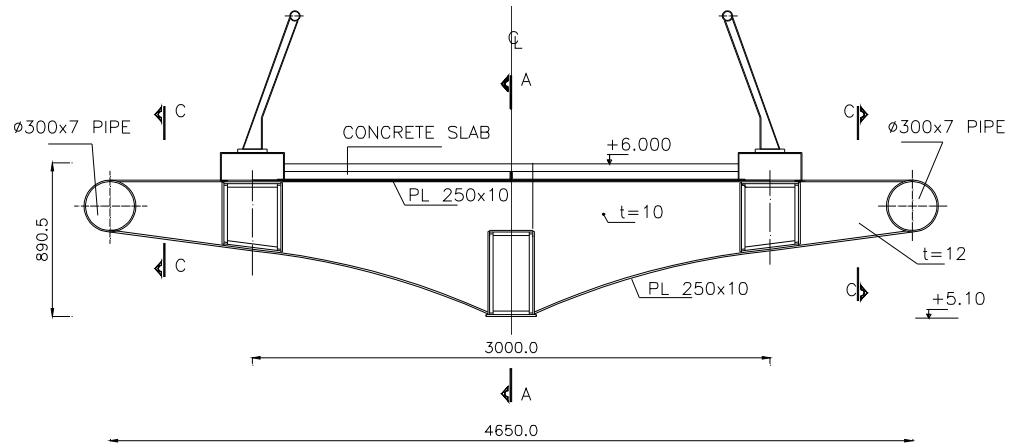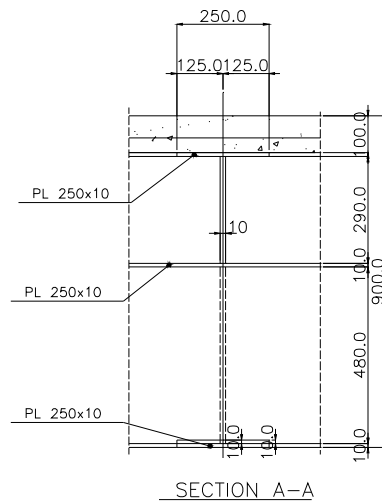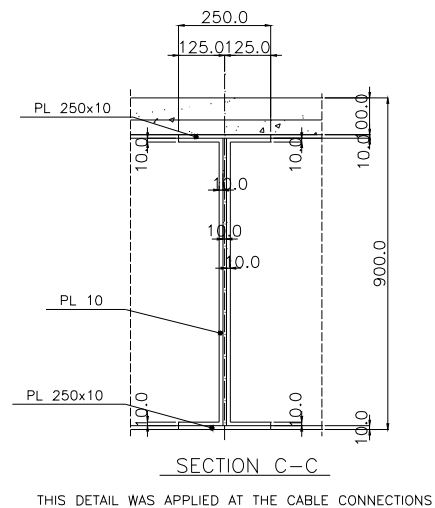
(c)

Figure 3-2: Cross section of the bridge

3.2 Description of the Bridge Deck

The bridge deck is supported by three hollow box sections and two pipe sections form the main load carrying members in the longitudinal direction. The box and pipe beams are connected in transverse direction using variable height built-up girders using 10mm thick web and 10x250mm steel plates (Figure 3-2a). The transverse beams that are placed at every 1.88 meters

17

supports the deck from twelve locations using parallel placed stay cables between two concrete abutments.

Three hollow box sections of the bridge deck are built up from 10 mm thick steel plates and the webs and flanges are stiffened using 20mm thick plates at the junction of transverse beams (at every 1.88 meters). The outer diameters of pipe sections are 300mm and the thicknesses of the sections are 7mm. Additional ϕ80mm outer diameter and 6mm thick pipe sections are used as truss members underneath the bridge slab (Figure 3-3a). The bridge deck is approximately 6m above the road surface and aesthetic lighting at six points is provided. The edges of deck are secured with stainless steel hand rails for pedestrian safety.

The 10mm thick steel slab is covered by ϕ6mm mesh reinforced about 5 cm thick mortar layer and tiling (Figure 3-3b) following the stay cables installation and mid-support removal.

(a)   (b)

Figure 3-3: The bottom and top views of the bridge deck

3.3 Description of the Cable System

DYWIDAG 47mm diameter bar tendons are used for the cables for the METU pedestrian bridge. The benefits of the DYWIDAG system are: fast installation and stripping, rugged thread resisting handling abuse, threadability even when dirty, higher strength and lighter weight than coil rod [22]. The cables have lengths varying from 28.31 m up to 62.22 m, and are made of high-strength, low relaxation steel BS 4486. There are twelve cables anchored at 0.5 m intervals on the concrete anchorage block which is located on M.E.T.U. campus side. The other ends of these cables are anchored to the tower at approximately 1.50m intervals from the elevation 30.11m to 37.60m. The twelve cables located between the tower and deck are anchored to the deck at 7.52m intervals along the bridge span length. The axes of the two sets of 12 cables coming from the bridge and anchor block intersect on the tower central axis. Technical data of DYWIDAG type prestressing steel bar tendons (threadbar) is given below in Table 3-1. Modulus of Elasticity of tendons is given as E = 205,000 N/mm^2 ± 5% in its specifications [22].

Table 3-1: Technical data of DYWIDAG type bar tendons [22]

Nominal Diameter	Steel Grade	Ultimate Strength f_{pu}	0.1% Proof Strength=Yield Strength,Fy	Cross Sectional Area	Diameter over Threads	Thread Pitch	Bar Weight
mm	N/mm^2	kN	kN	mm^2	mm	>mm	kg/m
15	900/1100	195	159	177	17	10	1.44
20	900/1100	345	283	314	23	10	2.56
26.5	950/1050	579	523	551	30	13	4.48
32	950/1050	844	764	804	36	16	6.53
36	950/1050	1069	967	1018	40	18	8.27
40	950/1050	1320	1194	1257	45	20	10.21
47	950/1050	1822	1648	1735	52	21	14.10

Manufactured in accordance with the German Certificate of Approval (Deutsches Institut für Bautechnik), the tendon bar and coupler system is also in conformance with BS 4486 (High Tensile Steel Bars for Prestressing of Concrete) [22].

The threadbar's are hot rolled, quenched and tempered, followed by cold working and further tempering, to achieve the necessary performance. Dywidag 26.5mm-47mm prestressing steel threadbar's also have a fatigue resistance exceeding 2 million load cycles, over a tensile range of 630-682N/mm^2 as specified in BS4447 (Performance of Prestressing Anchorages). Stress relaxation when loaded to 70% f_{pu} is less than 3.5% over a 1000 hour period in accordance with BS4486 [22]. The 3-D view and cross section of the DYWIDAG bar tendons are given in Figure 3-4.
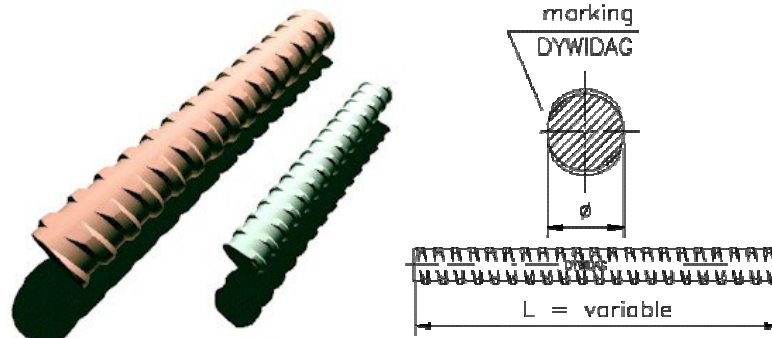
Figure 3-4: 3-D view and cross section of the DYWIDAG bar tendon [22].

Couplers enable "prestressing steel threadbar" to be coupled or extended, reliably and efficiently. It is important that the two threadbar meet centrally within the coupler, and remain so during installation, to ensure correct load transfer. Coupler strength is 92% tensile strength of the bar in accordance with BS 4447 [22]. Precautions should be taken to ensure that the coupler remains centrally located. This can be achieved through the use of grub screws and/or a centre pin. Marking the two bars with paint or similar at half a coupler length prior to engagement provides visual confirmation of centralization and is recommended as good working practice [22]. The types of connection and accessories of prestressing steel threadbar are given in Figure 3-5, and Figure 3-7.
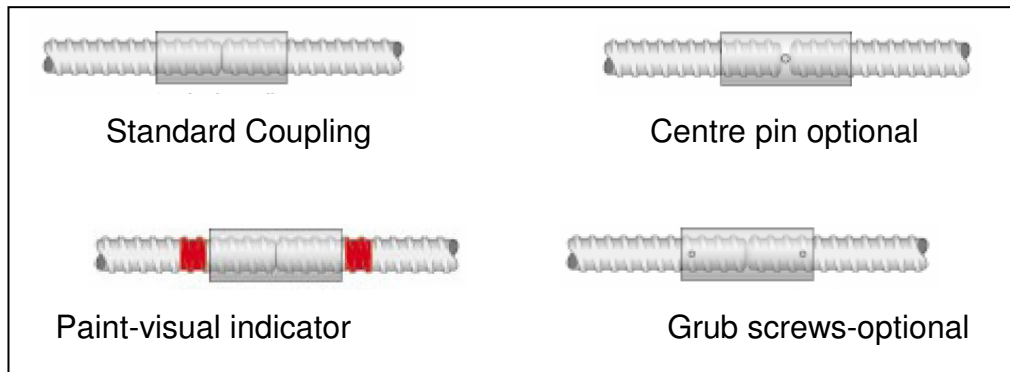
Figure 3-5: Types of connections of solid bar cables [22]
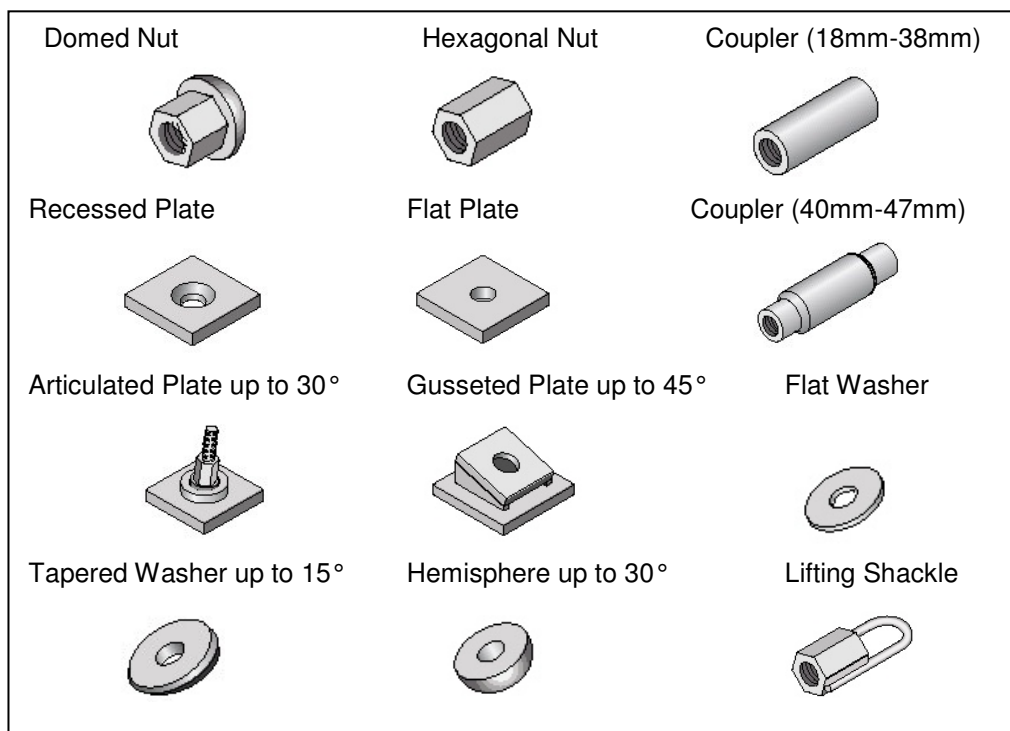
Figure 3-6: Accessories of prestressing steel threadbar [22]

Table 3-2: Technical properties of accessories [22]

Nominal Diameter	Steel Grade	Recessed Plate Stock Size*	Domed Nut AF	Length	Flat Plate Stock Size	Hexagonal Nut AF	Length	Coupler Dia.	Length
mm	N/mm^2	mm	mm	Mm	mm	mm	mm	mm	mm
15	900/1100				120x120x12	30	50	30	105
20	900/1100				120x120x12	36	70	40	130
26.5	950/1050	130x130x35	46	55	130x130x35	46	80	50	150
32	950/1050	160x160x40	55	70	160x160x40	55	90	62	180
36	950/1050	180x180x45	60	90	180x180x45	60	110	67	220
40	950/1050	220x220x50	70	125	220x220x50	70	120	71	250
47	950/1050	260x260x50	80	140	260x260x50	80	140	85	265

Table 3-3: Dimensions of stressing equipments [22]

Nominal Diameter	Steel Grade	Dimension A	Dimension B
mm	N/mm2	mm	Mm
15	900/1100	50	50
20	900/1100	60	55
26.6	950/1050	35	60
32	950/1050	50	70
36	950/1050	65	85
40	950/1050	50	125
47	**950/1050**	**67**	**140**
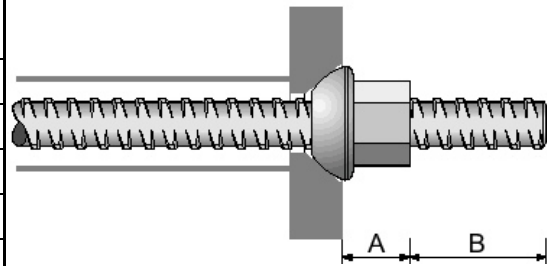
Dimension **B** is the minimum threadbar projection required for stressing

Table 3-4: Jack selection chart [22]

Jack Properties			Bar Diameter mm						
Capacity	Stroke	Weight	15	20	26.5	32	36	40	47
300kN	50mm	21kG	yes	yes	yes				
600kN	100mm	44kG			yes	yes	yes		
1100kN	50mm	46kG			yes	yes	yes	yes	yes
1100kN	150mm	54kG			yes	yes	yes	yes	yes
1500kN	250mm	95kG						yes	yes
2000kN	100mm	160kG						yes	yes

In this bridge, standard couplings are used to connect each part of the threadbar of the cable. The cables are connected to the bridge deck using fixed type connections as shown in Figure 3-7.

Figure 3-7: The cable connection to the bridge deck stiffening girder

It is a difficult part of the erection to join the cables from the deck or anchor block to the tower. Pipe sections which are shown in the following Figure 3-8 are used to anchor the cables with the help of three cranes (Figure 3-9).

Figure 3-8: The tool which enables to connect cables and anchor the structure parts

Figure 3-9: The process of connection of the cables and anchoring of structural parts.

According to the various longitudinal cable arrangements, cable-stayed bridges could be divided into the following four basic systems (Figure 3-10).
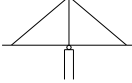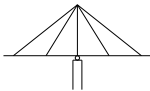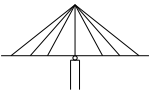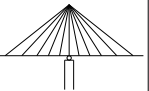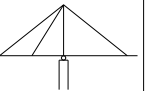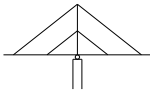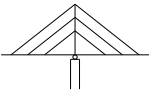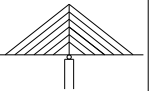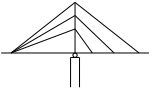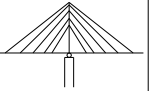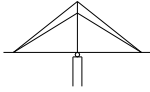
Stay System		Single	Double	Triple	Multiple	Variable
		1	2	3	4	5
1	Bundle or Converging or Radial					
2	Harp or Parallel					
3	Fan					
4	Star					

Figure 3-10: Arrangement of the stay cables [3}

Figure 3-11: Arrangement of the Investigated bridge stay cables

METU Bridge uses fan (intermediate) cable arrangement system. This arrangement system represents a modification of the harp system. The cables are connected to the tower at different heights with fixed connections and placed parallel to each other in harp system. The Nord Bridge in Germany is a typical example of this arrangement.

3.4 Description of the Tower and Support Systems

The tower has a rectangular tapered cross section; mainly welded connections are used. Thirty millimeter thick rectangular plate members and 10mm thick stiffeners are placed at every six meters and every at every one meter from the elevation of +7.87 meters (Figure 3-12 and Figure 3-13). The tower supports 24 stay cables; twelve of them are fixed to anchorage block and other twelve are connected to the bridge.
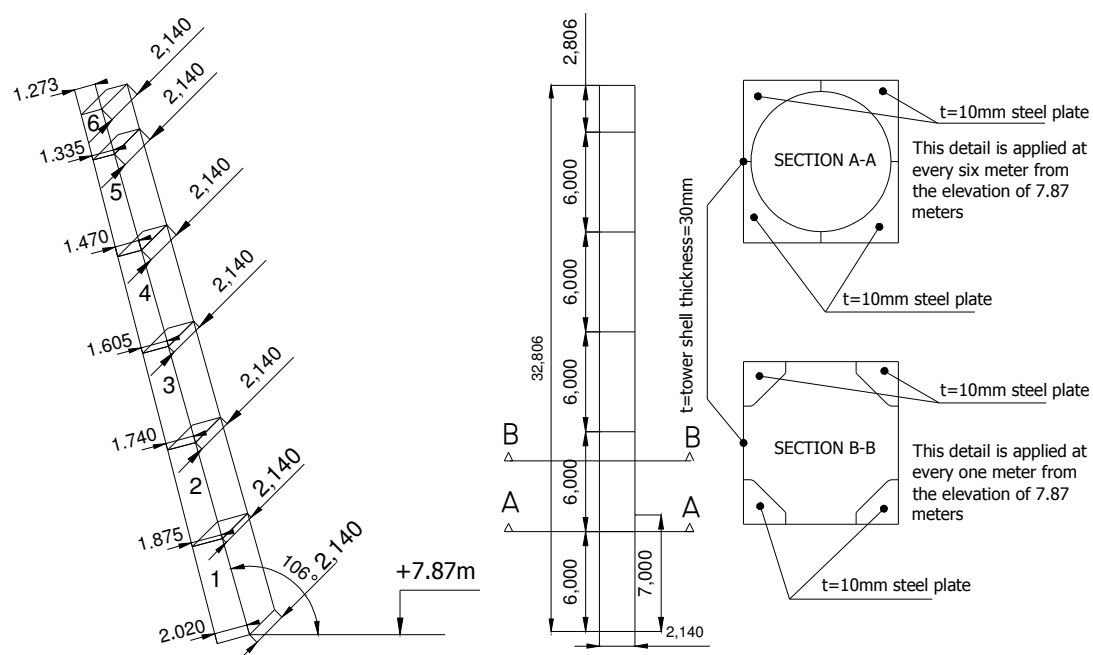
Figure 3-12: Details of the bridge tower

Stairs to the tower exist inside the tower for maintenance purposes and a circular safety fence was constructed around of the stairs to prevent falling down (Figure 3-13).

Figure 3-13: Inside view of the tower

The tower is embedded in concrete abutment - foundation (Figure 3-14) and is stiffened by 30mm thick steel flanges at the elevation of -3.10 meter inside the concrete as shown in Figure 3-15 sections A and B. Piled foundation system is selected due to bad soil conditions. A total of twenty-five concrete piles with 60cm diameter are used under the tower abutment.

A total of nine concrete piles with 60cm diameter are used under the other (DSI) side of the bridge abutment. General location of abutments and piles are shown as Figure 3-14, Figure 3-15, Figure 3-16, and Figure 3-17.

Figure 3-14: 3-D views of the METU and DSI side abutments
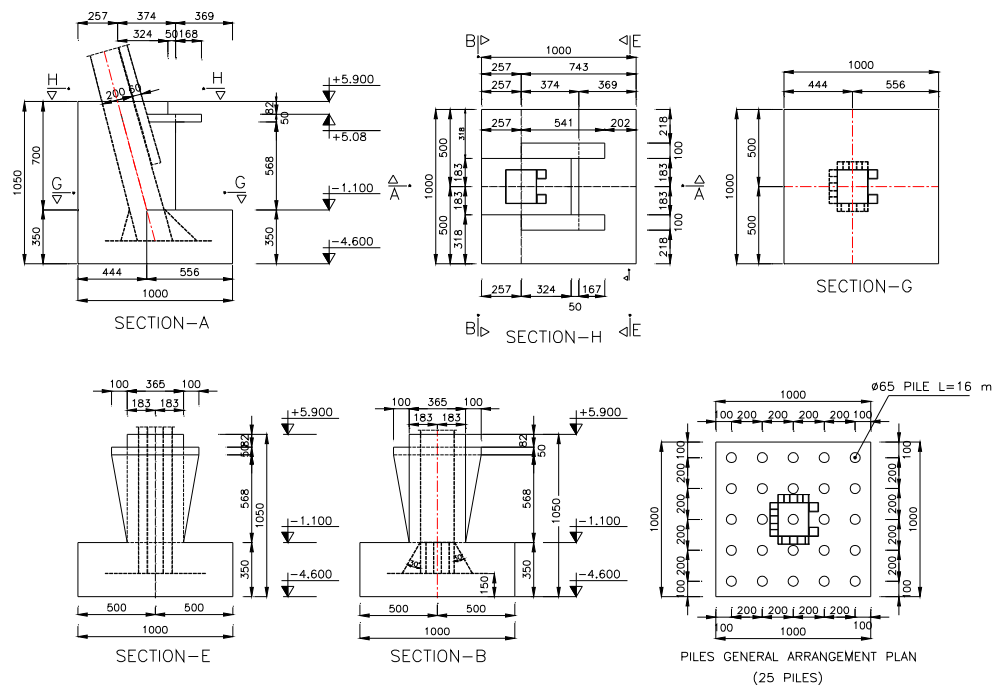
Figure 3-15: Cross sections of the METU side abutment
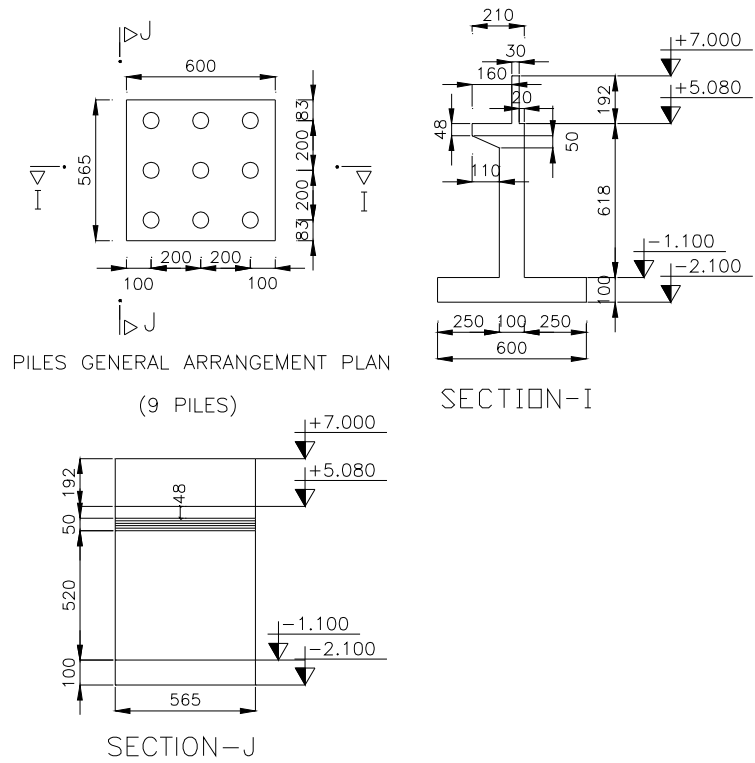
Figure 3-16: Cross sections of the DSI side abutment
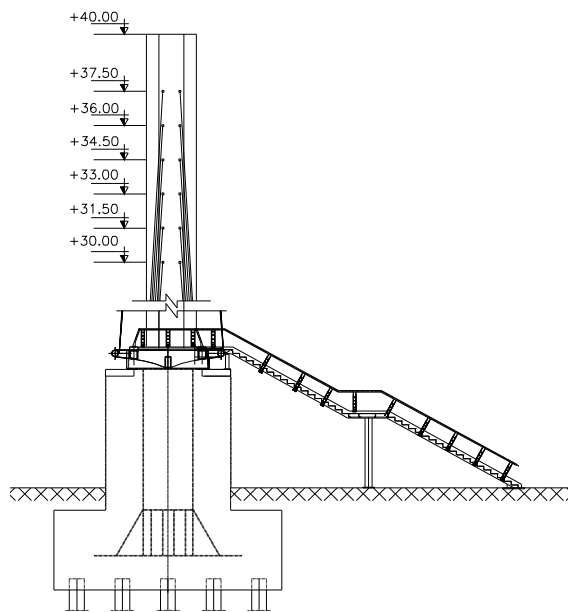
Figure 3-17: Cross section of METU side abutment

30

3.5   Description of the Anchor Block

Cable supported bridges can also be characterized by the cable anchorage system similar to the cable configuration. In the earth anchored systems, both the vertical and horizontal component of the cable force is transferred to the anchor-block. In the self-anchored systems, the horizontal component of the cable force is transferred to the bridge deck, whereas the vertical component is taken by the tower support [3].

In principle both earth anchoring and self-anchoring systems can be applied in suspension bridges as well as in cable stayed bridges. However, in actual practice earth anchoring is primarily used for suspension bridges and self-anchoring for cable stayed bridges. Earth anchored system is used for the studied METU pedestrian bridge and detailed drawings of the anchor block are provided in Figure 3-18 and Figure 3-19 [3].

Figure 3-18: Several view of at the anchor block

ANCHOR BLOCK PLAN VIEW

SECTION-D

PILES GENERAL ARRANGEMENT PLAN
(9 PILES)
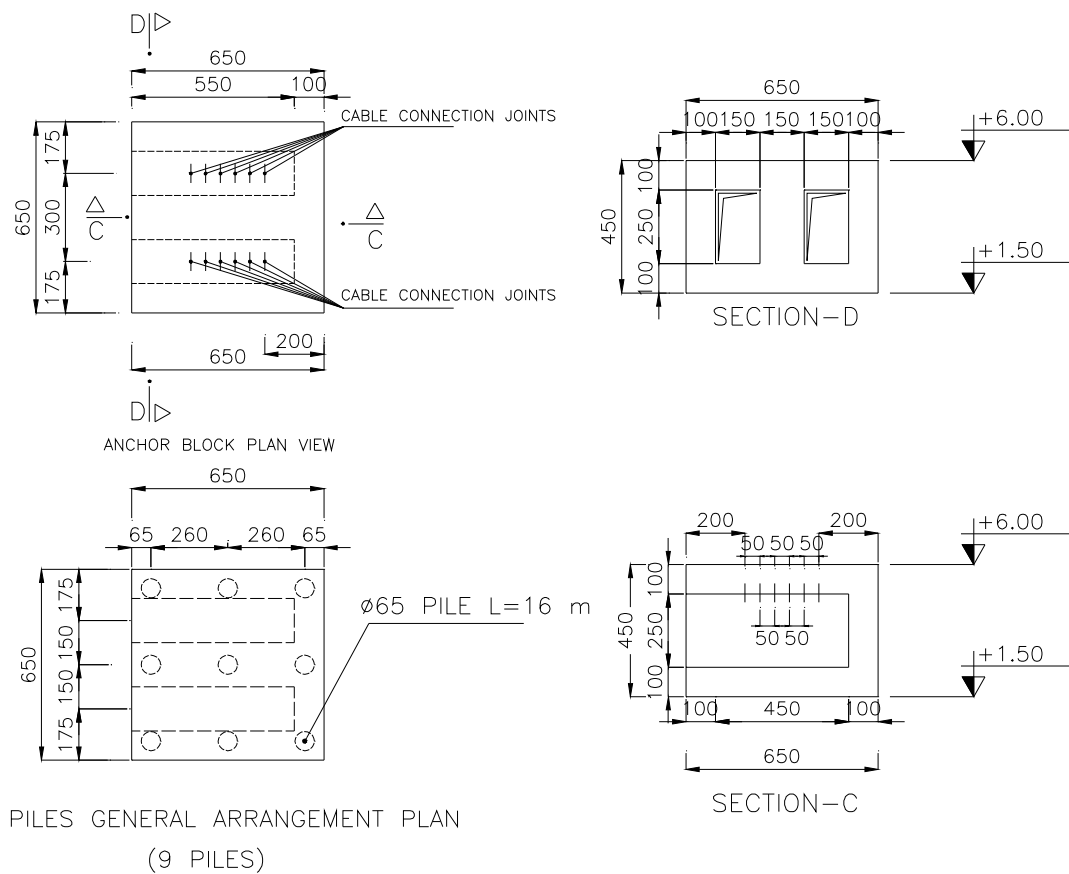
SECTION-C

Figure 3-19: Cross sections of the anchor block

3.6 Construction Process of the Bridge

The anchorage block and tower were constructed before the bridge deck was brought to the construction site. Lifting and placement of the bridge deck on its supports, cabling, temporary supports removal, and tile placement of the deck processes followed the transportation process (Figure 3-20). Lifting of the bridge in two separate segments was performed by using a 100 tons capacity crane. Each segment was fastened tightly at center from four points of the pipe sections which have 300mm outer diameter. The lifting process was performed very slowly to prevent each deck segment from hitting the temporary piers and abutments. Placement of the stiffening girder on supports was followed by careful adjustment which was performed using two ropes tied at the ends of the girder. Two workers climbed up the temporary mid-support for adjustment of the deck segment placement. The process of lifting and placement are shown in Figure 3-21. There were two temporary piers, one was beside of the tower support (METU side) and the other was placed at the median of Eskişehir highway. Temporary support at METU side was removed after the first four parallel cables were anchored the tower and deck. Mid-support at the median was removed after the remaining two parallel cables were anchored from the tower to deck. The final stage of the construction, the deck tile placement, was completed after cabling and temporary support removal processes. Cabling, temporary support removal, and tile placement processes are shown in Figure 3-22.

33

Figure 3-20: Transportation process

Figure 3-21: Lifting process

Figure 3-22: Cabling, support removal and tile placement process

CHAPTER 4

INSTRUMENTED MONITORING AND DYNAMIC TESTS

This chapter summarizes the instrumentation work carried out during monitoring studies. Dynamic testing related information is also summarized. The strain-temperature measurements, maximum strain variations during construction stages, and dynamic test results are presented and discussed.

4.1   Instrument Types for Monitoring and Dynamic Tests

Components of the measurement system used for monitoring and field testing are data acquisition system (DAS), data transmission cables, strain gages, accelerometer, notebook computer and other tools and consumables such as epoxies, strings, pliers, pincers, screwdriver, ducktape etc. (Figure 4-1). Further details about the vibrating wire strain gages, data acquisition system, and accelerometer used in this study are given in the following sections. The information includes working principles, system components, and technical properties. Technical specifications of the instruments are listed in Appendix-C.

Figure 4-1: Equipments used for strain readings and dynamic field tests

4.1.1 Vibrating Wire Strain Gage

Vibrating wire strain gage consists of a steel wire tensed between the two edges of the gage that are connected to the mounting blocks which are usually arc welded or epoxy bonded to the surface of member to be monitored. Deformation of the member under loading produces relative movement between the two mounting blocks, which causes wire tension to change. Similar to a guitar string, the natural vibration frequency of the wire changes as a function of the strain. The resonant frequency is measured by an electromagnetic coil placed around the wire and connected through a signal cable to readout unit, which measures the resonant frequency of wire and then converts to the strain [19]. The vibrating wire working principle is briefly illustrated in Figure 4-2.
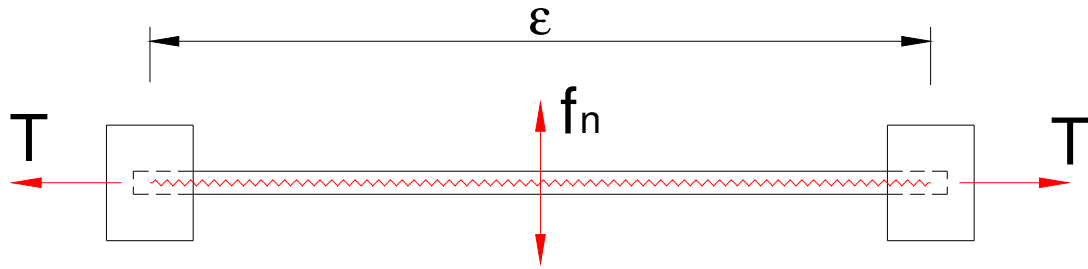
Figure 4-2: Work principle of vibrating wire strain gage

The vibrating wire is protected inside a stainless steel tube with "o" ring seals at both ends for water proofing. The electronic coil clips over the center of the tube and a thermistor is encapsulated with the coil to permit the measurement of temperature. A space bar and welding jig is used to correctly space the mounting blocks during welding. Cover plates can be used to protect the gage from accidental damage [19].

4.1.2 Data Acquisition System (DAS)

A complete data acquisition system mainly consists of a) power supply, b) data retrieval components, and c) software components. Campbell CR10X data acquisition system is used in this study. The DAS is programmable and automatically collects data at certain intervals over long periods of time. Multiplexers are used to increase the number of sensors that can be monitored by limited number of channels on a data logger. The CR10X can control up to six multiplexers, each capable of handling 16 to 32 sensors. In practice, the data logger usually controls one or two multiplexers, and additional DAS and multiplexers are employed if there are more sensors due to memory constraints. A power supply provides regulated 12V power to the

logger and sensors. Power is drawn from a battery that is charged from AC mains power or a solar panel. Any 12V DC source can power the CR10X. Logger-Net software is used to create monitoring programs and to retrieve data from the logger to PC. Dynamic measurements of the bridge were taken using the burst mode readings. Burst measurements can be made up to 750Hz for a maximum of 1000 data points. CR10X data logger has 6 differential or 12 single ended channels as shown in Figure C.2 at Appendix-C. Full scale input range of the data logger can be chosen as ±2.5mV, ±7.5mV, ±25mV, ±250mV and ±2500mV [17], [18]. Data Acquisition chart is given in Figure 4-3.

Ch 1
Ch 2
Ch 3
Ch 4
Ch 5
Ch 6
Ch 8 | Multi-plexer |——| A / D | ▭⇒ | DAS Memory |
Ch 9
Ch 10
Ch 11
Ch 12   ⇓
Ch 13 | Computer |
Ch 14
Ch 15
Ch 16 | 12 bit Analog to Digital Converter |
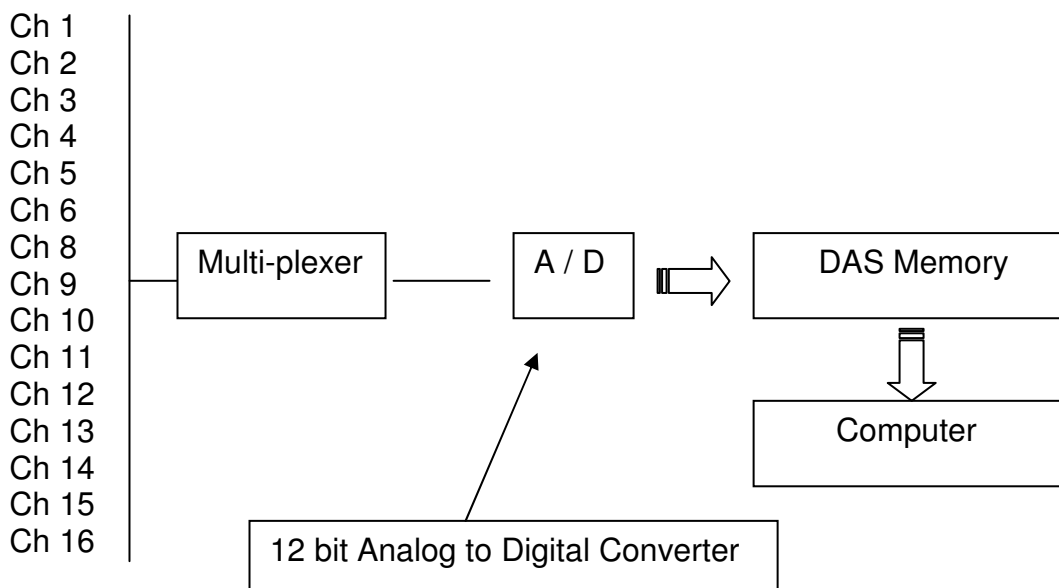
Figure 4-3: Data acquisition chart

4.1.3 Accelerometer

Accelerometers are sensors to measure acceleration of vibrations and can be used to obtain natural frequencies of structures. PCB 393C type accelerometer was used in conjunction with CR10X data logger. Technical properties of accelerometers should be investigated in order to match the test requirements of the structure being tested as well as being in compliance with the DAS. Important technical parameters of an accelerometer can be listed as: amplitude (measurement) range, frequency range, voltage sensitivity, and resolution [20]. Amplitude range is measured in units of gravitational acceleration (g) and frequency range is measured in Hz (1/sec). Some technical features of PCP 393C accelerometer used in this study are given as follows:

Voltage Sensitivity   : 1109 mV/g

Measurement Range   : ± 2.5 g

Frequency Range   : 0.025 - 800 Hz

Resolution   : 100 μg

Diameter   : 2.25" (5.72cm)

Height   : 2.16" (5.49cm)

Detailed information about PCB 393C model accelerometer can be found in Appendix-C [20].

4.2 Strain gage instrumentation

The instrumentation process was carried out at the factory right after the two separate parts of the bridge deck were manufactured. Five strain gages together with five thermocouples were mounted on each one of the two bridge segments; however, due to transportation and cabling constraints, only five of the gages were monitored until both pieces were assembled together at the construction site. A total of ten gages were installed on the bridge segments at three different cross-sections along its length as shown in Figure 4-4a. The layout of the gages at the bridge cross section is shown in Figure 4-4b. Gage number 3 was placed in transverse direction while the others were placed parallel to the bridge length. Five gages located on segment #2 at section C-C were not recorded during transportation. Recording of those five gages was started after the gage cables were connected to data acquisition system (DAS) the next day when two bridge segments were placed together on temporary supports. The main structural girders of the bridge was monitored during important events such as transportation, lifting, cabling, temporary supports removal, and deck surface covering (tile placement). Long-term monitoring was performed through the first three months of the service stage. Ten channels of vibrating wire strain gages and ten temperature transducers were used to record strain and temperature data. Data was recorded at every ten minutes during transportation and lifting processes and in 30 minutes intervals during following construction and service stage [14].

Data Acqusition System (DAS)

METU CAMPUS
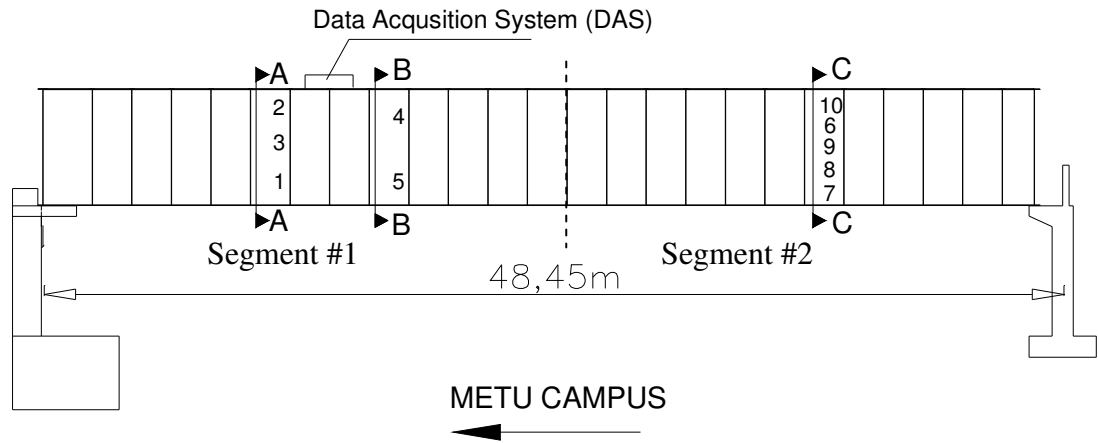
a) Gage locations along the length
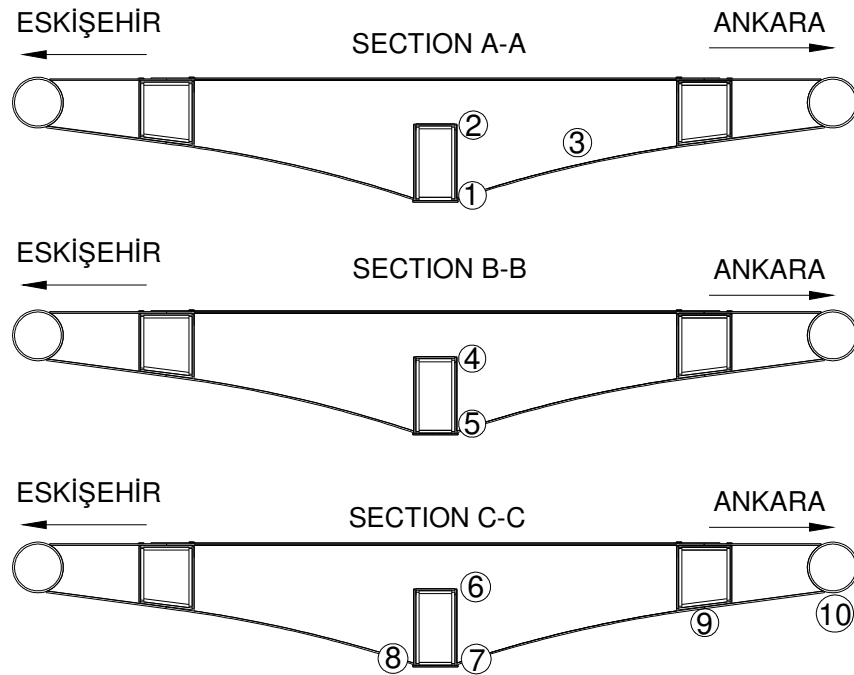
b) Gage locations at A, B and C sections

Figure 4-4: Gage locations shown on longitudinal and cross sections

4.3 Strain Monitoring Results

The three months of strain gage records are processed and maximum strain changes during major events are determined. A sample strain readings window during the transportation and lifting process on March 16th, 2003 is shown in Figure 4-5 for 5 gages. Similarly, strain variations at all major events are processed for all gages and summarized in Table 4-1 (The recorded strain changes for all 10 strain gages through the construction and service stages are given in Appendix-A). Briefly, the maximum strain changes were obtained during the lifting process at gage locations #1 and #4 (Table 4-1) while the minimum strain changes were obtained during deck concreting and tile placement at gage location #7. The discussion of the results using Table 4-1 is given in Chapter 6.
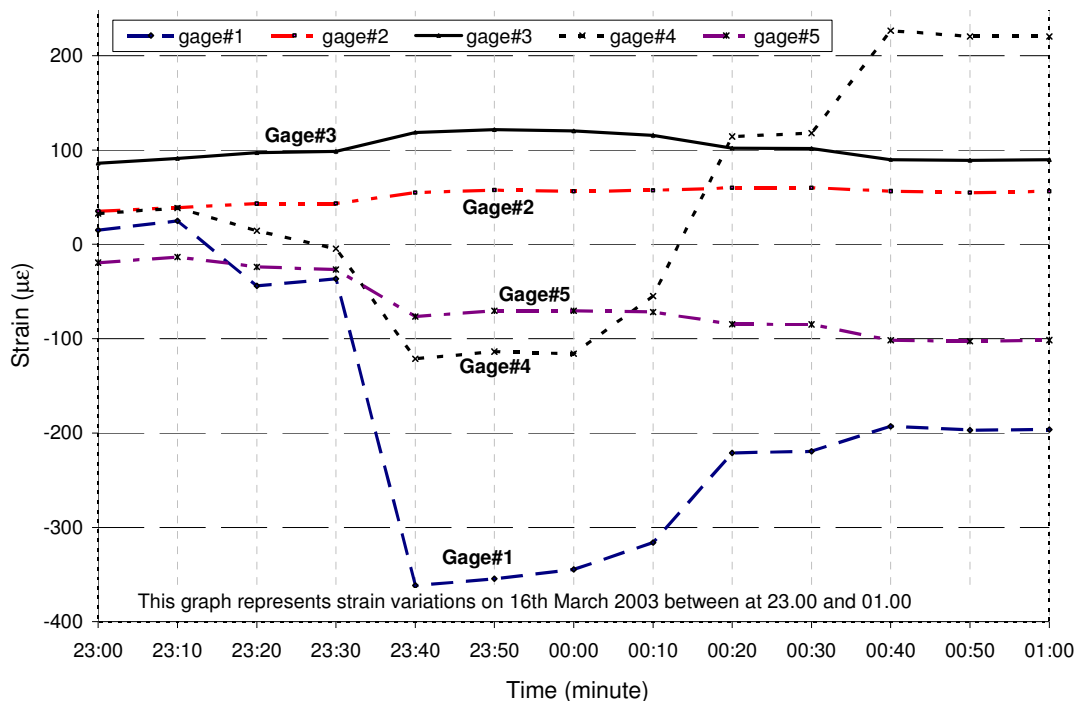
Figure 4-5: Strain changes during transportation and lifting process

43

Table 4-1: Strain changes for important events at each gage locations [14]

Event	Date	Strain gage numbers and strain values ($\mu\varepsilon$)									
		1	2	3	4	5	6	7	8	9	10
Transportation	16.03.03	10.9	0.0	0.0	82.5	0.0	-	-	-	-	-
Lifting	16.03.03	381.8	21.1	28.9	348.0	88.8	-	-	-	-	-
Cabling	03.05.03	273.0	36.0	41.0	103.0	124.0	168.3	97.1	61.2	51.0	43.0
Supp.removal	12.05.03	8.3	14.0	8.6	8.4	7.9	8.2	5.5	6.8	5.2	5.1
Tile placement	20.05.03	14.8	8.0	14.0	19.4	10.0	2.6	1.5	4.1	1.7	4.1

Analytical model of one segment of the bridge deck is developed to compare strain levels occurred at the first five gage locations. FE model input data is given at Section 5 and comparisons between experimental and analytical results are given in Chapter 6.

4.4 Bridge Dynamic Tests

The dynamic tests conducted on the METU Bridge can be grouped under three main sections: the dynamic measurements taken from the a) bridge deck, b) cables, and c) tower. The details of testing and results of measurements are given in the following sections. Field dynamic tests were conducted by using PCB 393C type accelerometer, CR10X data logger, lap-top computer, and clamps.

4.4.1 Vibration Measurements of the Bridge Deck

This section includes vertical, lateral, and torsional vibration measurements of the bridge deck. The vertical bridge deck vibration measurements were carried out close to the two third length of the bridge deck at two different lateral positions to distinguish between bending and torsional mode shapes. Placement of the accelerometer at the central line of the bridge mostly eliminates torsional vibrational modes capturing only bending modes. When the accelerometer is placed off-centered close to the sides of the bridge, torsional modes may be more dominantly obtained and reveal themselves. Lateral modes of the bridge deck can be similarly obtained by placing the accelerometer in horizontal direction at the parapet level. Locations of the accelerometer where vibration measurements were taken are shown in Figure 4-6 and Figure 4-7.
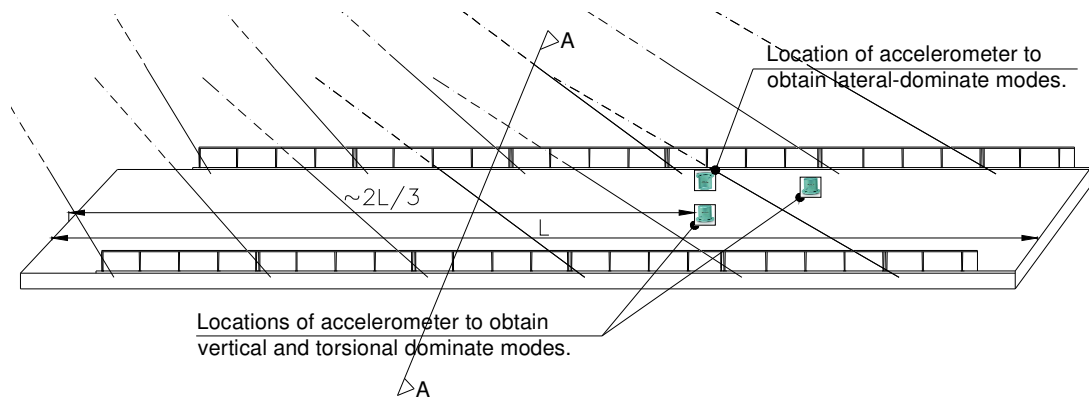
Figure 4-6: Locations of accelerometer in longitudinal section
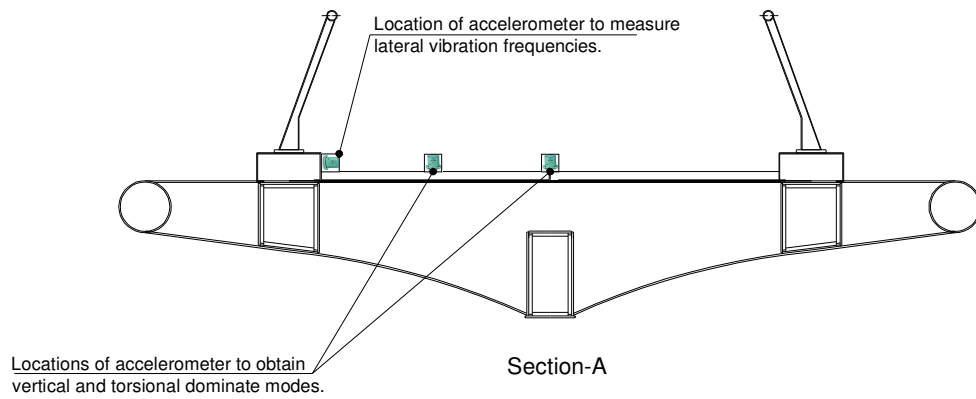
Figure 4-7: Locations of accelerometer in cross section

The recording rate of vibration measurements was selected to be 100Hz and the duration as 10 seconds, which would give Nyquest frequency of 50Hz. The frequency domain resolution (Δf) is obtained as 0.1 Hz. The impact load on the bridge deck generates almost equal excitation in all frequencies between 0-50 Hz. The response of the bridge is in free-decay form and fast Fourier transform (FFT) would yield resonant mode frequencies. The dominant vibration modal frequencies in vertical, lateral and torsional direction impact tests are obtained by selecting peak points as shown in Figure 4-9, Figure 4-10, and Figure 4-11, respectively. The experimentally obtained modal frequencies are matched against analytically obtained modal frequencies in order to determine the matching mode shapes.

A lateral mode at 4.50 Hz, torsional mode at 6.50 Hz, and two bending (vertical) modes at 3.10 Hz and 4.85 Hz can be heuristically identified just by looking at the frequency domain data in Figure 4-9, Figure 4-10, and Figure 4-11.

Figure 4-8: Dynamic test views on the deck
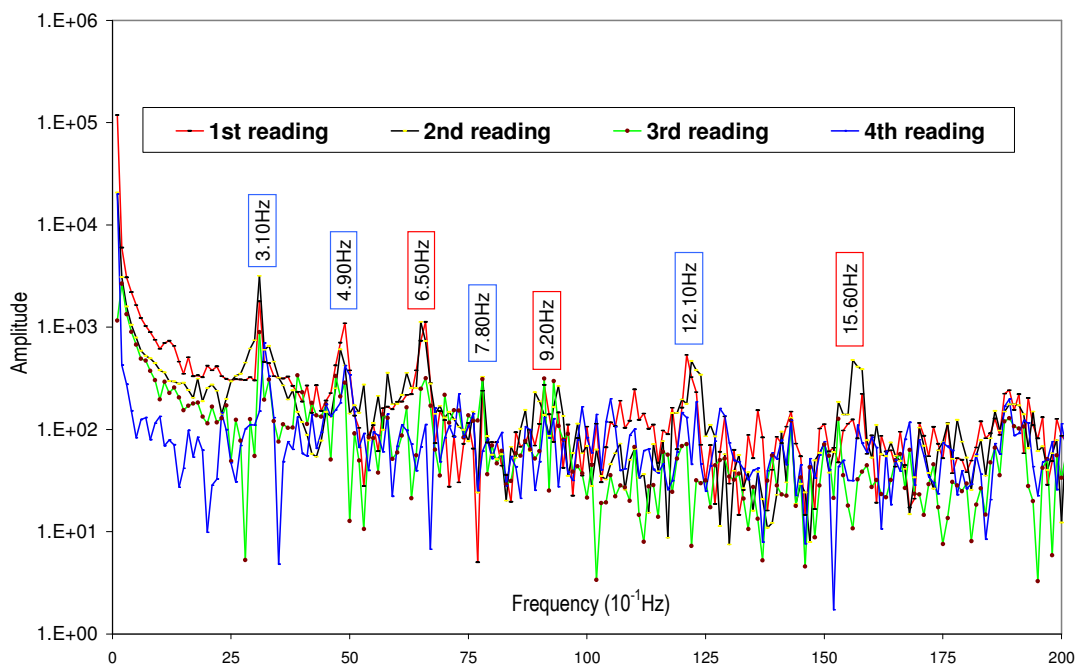
Figure 4-9: Vertical vibration measurements of the bridge deck
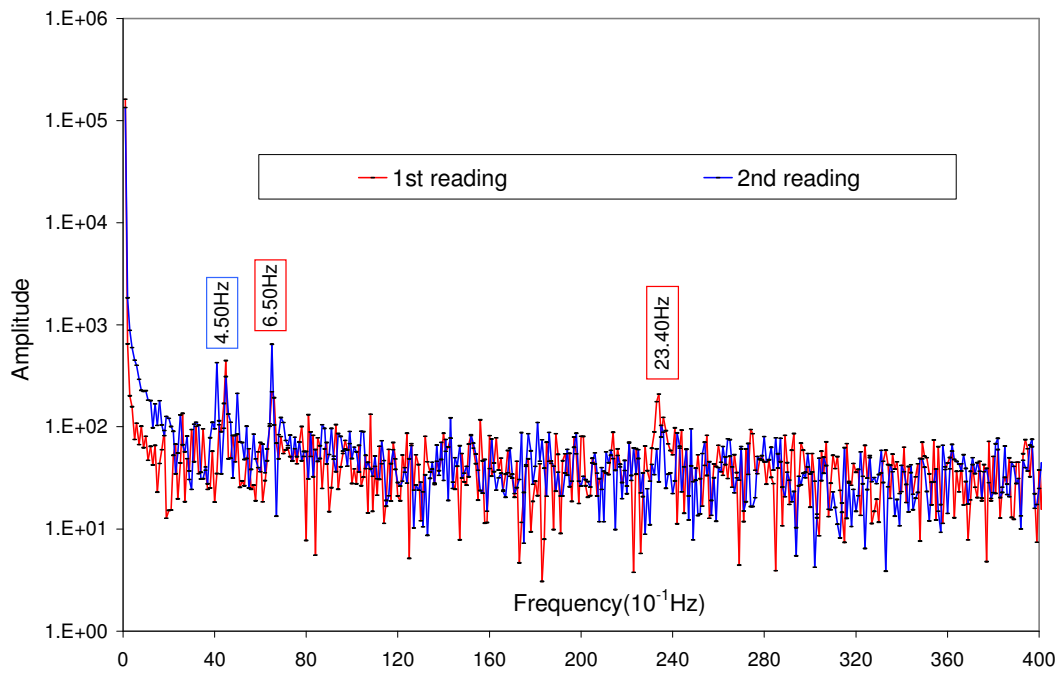
Figure 4-10: Lateral vibration measurements of the bridge deck
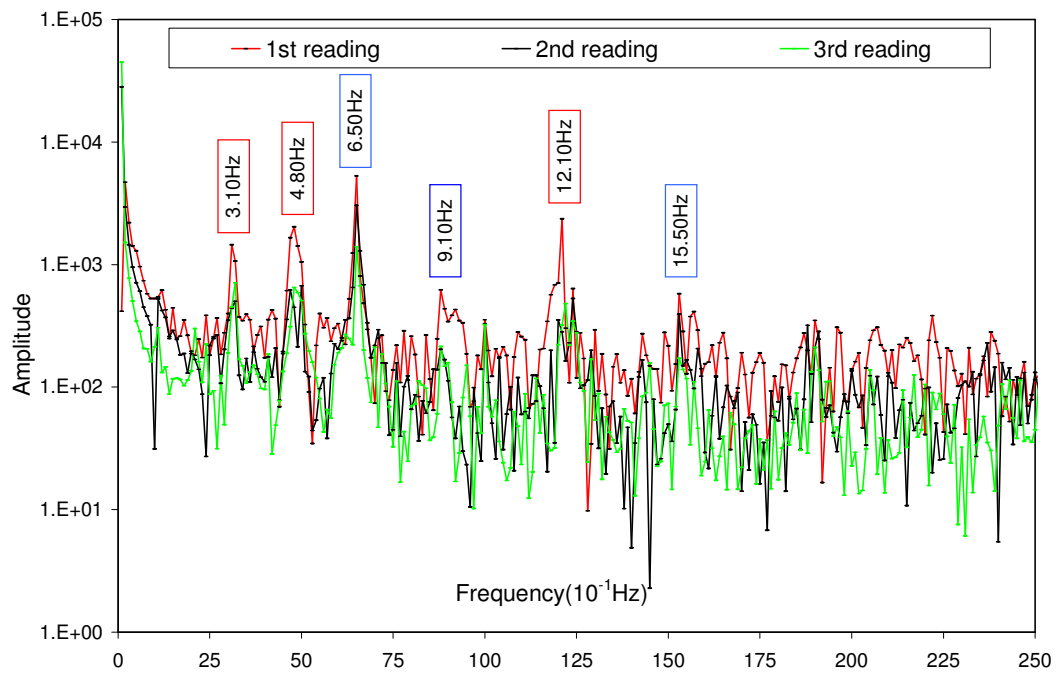
Figure 4-11: Torsional vibration measurements of the bridge deck

48

4.4.2 Vibration Measurements of Cables

Determination of cable axial load is a costly procedure which should also be practical and reliable. The cable axial load can be determined in many different ways: A method involving attachment of strain gages to stranded systems or wire is generally not appropriate and reliable since the gage should not be affected by temperature changes and stability of readings becomes an issue. The lift-off method can be used but this method is usually costly because it includes removal and/or modification of parts of cable anchorage system. Another method is to pre-install calibrated load cells under the cable anchorage during construction. However, the initial cost of these load cells is high and possible drift in readings cause problems [11]. Finally, measurement of cable vibration frequencies, which is used in this study, may be used to determine existing cable forces. In this method, the cables are excited by means of an impact force induced by a wooden log to generate transverse direction free vibration. An accelerometer attached to the cables is used to measure their transverse direction vibration frequencies. Vertical direction excitation and vibration measurements of the cables were also measured however no significant difference is observed when compared against transverse direction cable test measurements. Similar to the deck measurement test setup, CR10X data logger and PCB 393C accelerometer are used. 10 seconds of data is measured at 100 Hz to collect 1000 data points for each measurement. The cables are numbered starting from the longest ones (DSI side) towards shorter ones (METU side) as shown in Figure 4-12.
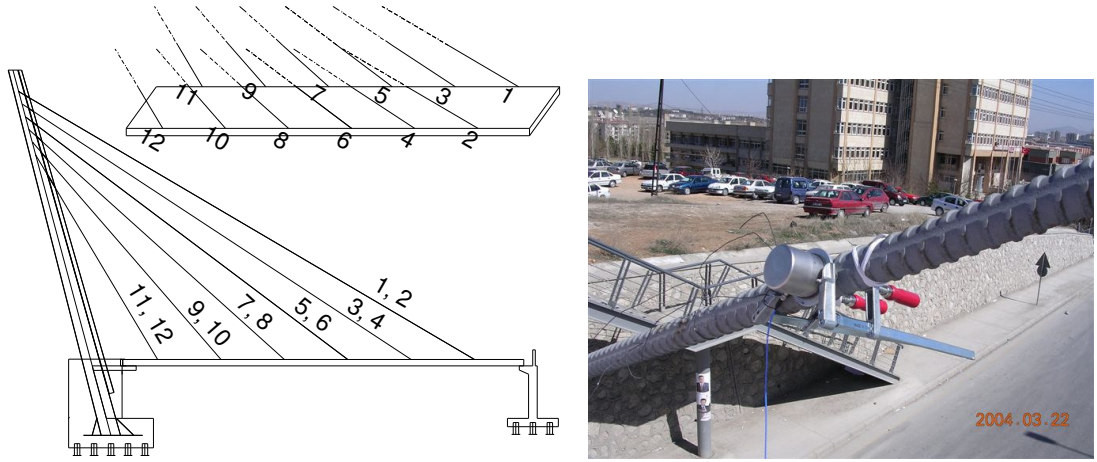
Figure 4-12: Cables applied vibration measurement test

The relationship between natural vibration frequencies of cables and axial tensile load on cables can be determined by the analogy of transverse vibration of piano wire (String Theory). Natural vibration frequencies of a cable can be calculated using Equation (4.1) [6]. The variable 'n' is used for the nth mode shape.

$$f_n = \frac{n}{2L}\sqrt{\frac{T}{m}} \tag{4.1}$$

The Equation (4.1) is arranged to obtain the axial load on a cable (T) as in Equation 4.2.

$$T = \frac{4w(f_n L)^2}{n^2 g} \tag{4.2}$$

However, dynamic behavior of a real cable system has some complexities such as modulus of elasticity, cross-sectional area, moment of inertia, additional mass of couplers, and boundary conditions. Equation 4.2 was modified and developed by Hiroshi Zui, Tohru Shinke, and Yoshio Namita in 1996 (Equation 4.3 through Equation 4.8) [6].

50

$$T = \frac{4w}{n^2 g}(f_n L)^2 \left[1 - 2.20\frac{c}{f_n} - 0.550(\frac{c}{f_n})^2\right] \qquad 17 \le \xi \qquad (4.3)$$

$$T = \frac{4w}{n^2 g}(f_n L)^2 \left[0.865 - 11.60(\frac{c}{f_n})^2\right] \qquad 6 \le \xi \le 17 \qquad (4.4)$$

$$T = \frac{4w}{n^2 g}(f_n L)^2 \left[0.828 - 10.50(\frac{c}{f_n})^2\right] \qquad 0 \le \xi \le 6 \qquad (4.5)$$

$$T = \frac{4w}{n^2 g}(f_n L)^2 \left[1.00 - 4.40\frac{c}{f_n} - 1.10(\frac{c}{f_n})^2\right] \qquad 60 \le \xi \qquad (4.6)$$

$$T = \frac{4w}{n^2 g}(f_n L)^2 \left[1.03 - 6.33\frac{c}{f_n} - 1.58(\frac{c}{f_n})^2\right] \qquad 17 \le \xi \le 60 \qquad (4.7)$$

$$T = \frac{4w}{n^2 g}(f_n L)^2 \left[0.882 - 85.00(\frac{c}{f_n})^2\right] \qquad 0 \le \xi \le 17 \qquad (4.8)$$

$$c = \sqrt{\frac{EIg}{wL^4}} \qquad (4.9)$$

$$\xi = \sqrt{\frac{T}{EI}}L \qquad (4.10)$$

Where,

L   : Total length of the cable,   T : Axial load in the cable

w   : Unit weight of cable,   g : Gravitation acceleration

n   : Vibration mode referring to f_n,   I : Moment of inertia

m   : mass of the vibrating cable=$\frac{w}{g}$,   E : Modulus of elasticity

f_n : Measured resonant vibration frequency

51

The following constants are used to determine the existing cable forces

$E=2.05E11N/mm^2$ $g=9.81m/sec^2$ $I=2.39531E-7m^4$ $\rho=14.10kg/m$

$w=\rho^*g=14.10^*9.81=138.321kg/sec^2$ $A=1.735E-3m^2$

ρ : Unit weight of the cable

A : Cross-section area of the cable

Cable free vibration responses are recorded for all cables and axial load values are obtained using Equation 4.2 for different mode numbers (n). A sample response obtained from cable #1 is shown in Figure 4-13. It may be possible to miss one or two modal frequencies at the low frequency end causing a discrepancy between axial load calculations. The mode number variable 'n' can be modified to start from 2 or 3 to make the axial load (T) calculated similar for all 'n' values. The axial tensile forces are obtained for all cables using dynamic measurements and listed in Table 4-2. Note that shorter length cables (#10, #11, and #11) were not properly measured and excluded from the list. Also note that cable excitation and vibration measurements were conducted at an arm height distance from the cable support; therefore, results may be improved if the cables were to be excited and monitored from a higher distance.

Axial forces computed using higher natural vibration frequencies (larger n values) yield larger values. Equation 4.2 ignores contribution of bending stiffness of the cable, however cable used in METU bridge has a solid cross

section which starts to have a significant contribution to the vibration at
higher mode shapes with many bending cycles along the length of the cable.
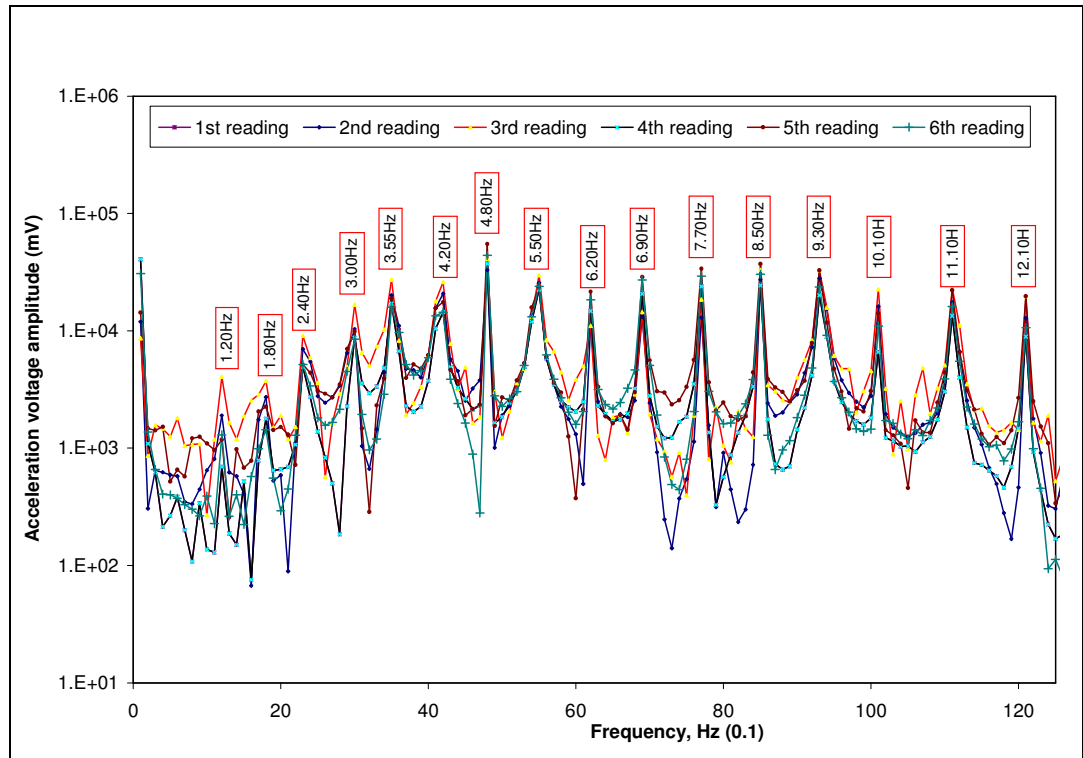
Figure 4-13: Sample frequency response of cables (cable #1).

Table 4-2: Measured cable vibration frequencies and calculated axial loads-1

n	Cable#1 L_1=62.22m		Cable#2 L_2=62.22m		Cable#3 L_3=54.75m		Cable#4 L_4=54.75m		Cable#5 L_5=47.48m		Cable#6 L_6=47.48m		Cable#7 L_7=39.22m		Cable#8 L_8=39.22m		Cable#9 L_9=32.63m	
	f (Hz)	T (ton)	f (Hz)	T (ton)	f (Hz)	T (ton)	f (Hz)	T (ton)	f (Hz)	T (ton)	f (Hz)	T (ton)	f (Hz)	T (ton)	f (Hz)	T (ton)	f (Hz)	T (ton)
1	-	-	0.6	7.90	0.80	10.90	-	-	-	-	0.70	6.30	0.80	5.60	-	-	-	-
2	1.20	7.90	1.20	7.90	1.60	10.90	1.40	8.30	1.60	8.20	1.40	6.30	1.60	5.60	-	-	-	-
3	1.80	7.90	1.80	7.90	2.40	10.90	2.10	8.30	2.40	8.20	2.10	6.30	2.40	5.60	2.70	7.10	1.80	2.20
4	2.40	7.60	2.40	7.90	3.20	10.90	2.80	8.30	3.30	8.70	2.80	6.30	3.20	5.60	-	-	2.70	2.76
5	3.00	7.90	3.10	8.50	4.00	10.90	3.50	8.30	4.10	8.60	3.90	7.80	4.00	5.60	4.00	5.60	-	-
6	3.55	7.70	3.70	8.40	4.85	11.10	4.30	8.70	5.00	8.90	4.80	8.20	4.80	5.60	5.30	6.82	3.80	2.43
7	4.20	7.90	4.30	8.30	5.70	11.30	5.00	8.70	5.85	8.90	5.80	8.80	6.10	6.60	-	-	4.90	2.96
8	4.80	7.90	5.00	8.60	6.50	11.20	5.80	8.90	7.00	9.80	6.80	9.30	7.30	7.30	6.65	6.04	-	-
9	5.50	8.10	5.60	8.50	7.35	11.40	6.80	9.70	7.40	8.70	8.10	10.40	8.70	8.20	8.00	6.90	6.20	2.87
10	6.20	8.50	6.10	8.20	8.20	11.40	7.55	9.70	8.00	8.20	9.10	10.60	10.10	8.90	-	-	7.60	3.49
Selected		7.90		7.90		10.90		8.30		8.70		6.30		5.60		6.60		2.50

Results presented in Table 4-2 is obtained by using simplistic Equation 4.2. Contribution of the bending stiffness can be incorporated using Equation 4.3 through Equation 4.8 created by using the advanced formulas that include bending stiffness of cables. The axial loads calculated using the second approach is different but fairly close to the results obtained in Table 4-2. A comparison of axial tensile cable forces calculated using two approaches is given in Figure 4-14. The difference between two approaches is approximately 3.3kN on the average which is caused by the ignored bending stiffness of the cables.

Table 4-3: Measured cable vibration frequencies and calculated axial loads-2

N	Cable#1		Cable#2		Cable#3		Cable#4		Cable#5		Cable#6		Cable#7		Cable#8		Cable#9	
	L_1=62.22m		L_2=62.22m		L_3=54.75m		L_4=54.75m		L_5=47.48m		L_6=47.48m		L_7=39.22m		L_8=39.22m		L_9=32.63m	
	f (Hz)	T (ton)	f (Hz)	T (ton)	f (Hz)	T (ton)	f (Hz)	T (ton)	f (Hz)	T (ton)	f (Hz)	T (ton)	f (Hz)	T (ton)	f (Hz)	T (ton)	f (Hz)	T (ton)
1	-	-	0.60	7.20	0.80	9.95	-	-	-		0.70	5.44	0.80	4.64	-	-	-	-
2	1.20	7.56	1.20	7.56	1.60	10.42	1.40	7.93	1.60	7.72	1.40	5.86	1.60	5.12	-	-	-	-
3	1.80	7.68	1.80	7.68	2.40	10.58	2.10	8.07	2.40	7.84	2.10	5.99	2.40	5.28	2.70	6.72	1.80	1.94
4	2.40	7.74	2.40	7.74	3.20	10.66	2.80	8.14	3.30	8.51	2.80	6.07	3.20	5.36	-	-	2.70	2.56
5	3.00	7.77	3.10	8.31	4.00	10.71	3.50	8.18	4.10	8.42	3.90	7.61	4.00	5.40	4.00	5.40	-	-
6	3.55	7.58	3.70	8.24	4.85	10.97	4.30	8.60	5.00	8.73	4.80	8.04	4.80	5.43	5.30	6.64	3.80	2.30
7	4.20	7.82	4.30	8.19	5.70	11.15	5.00	8.57	5.85	8.80	5.80	8.65	6.10	6.49	-	-	4.90	2.85
8	4.80	7.83	5.00	8.50	6.50	11.12	5.80	8.84	7.00	9.68	6.80	9.13	7.30	7.14	6.65	5.91	-	-
9	5.50	8.13	5.60	8.43	7.35	11.25	6.80	9.62	7.40	8.55	8.10	10.25	8.70	8.04	8.00	6.79	6.20	2.78
10	6.20	8.38	6.10	8.11	8.20	11.35	7.55	9.62	8.00	8.10	9.10	10.50	10.10	8.80	-	-	7.60	3.40
Average Axial Load Value of the Cables (n=1 through n=5)																		
	7.69		7.70		10.46		8.08		8.12		6.19		5.16		6.06		2.25	
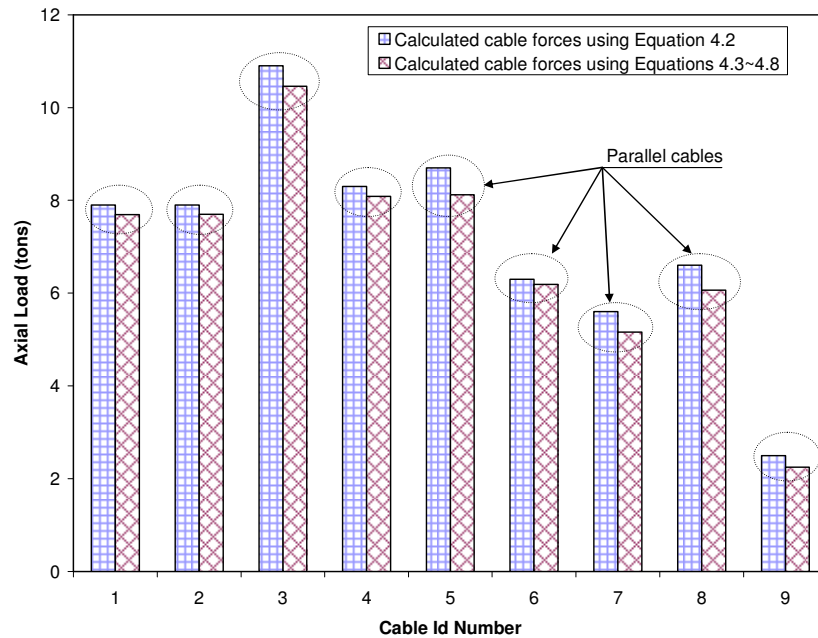
Figure 4-14: Comparison of cable forces

The results of the dynamic field test measurements on the cables show large axial load differences between parallel placed cables with the exception of cable #1 and #2. The cables numbered as 3 and 5 carry approximately 23% more axial load than their symmetrical members, cable #4 & #6. Also, cable #7 carries 15% less load than the cable numbered as #8. Those comparisons show indications that either the post-tensioning of cables was not properly done or the connections have relaxed over time. One of the possibilities is that the parallel cables are not post-tensioned simultaneously: When two parallel cables are tensed one after the other, post-tensioning the second cable after tensioning the first cable would cause relaxation on the first cable and reduction in its axial force. The exceptionally equal forces in cables #1 and #2 may be due to the fact that they are very close to the support at DSI side. The support would not permit transverse direction movement when cables are tensed one at a time.

4.4.3 Vibration Measurements of the Tower

The tower frequency analysis is divided into two main groups:

1. Longitudinal direction measurement
2. Transverse direction measurement

PCB 393C brand piezoelectric type accelerometer, CR10X data logger, data transmission cables, and notebook computer were used for this testing. The location of accelerometer was at about 15m elevation from base of the tower. The location of accelerometer is shown in Figure 4.15.
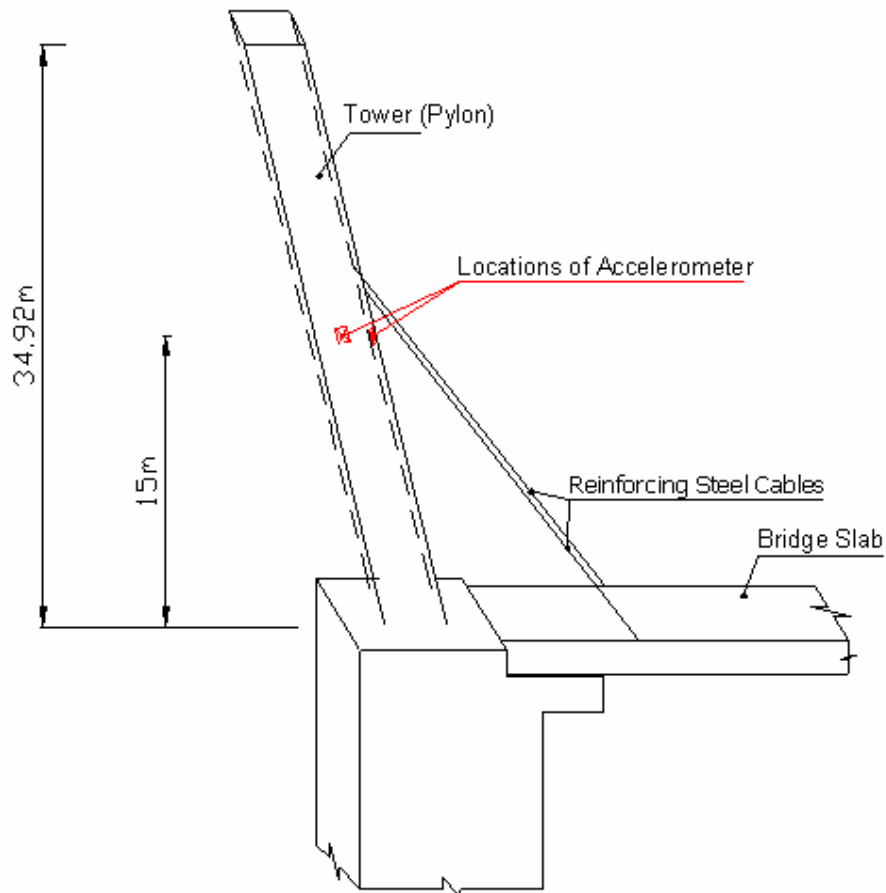
Figure 4-15: Transverse and longitudinal locations of the accelerometer

Data were post-processed using Artemis and Excel programs. The dominant frequencies of the tower along the transverse and longitudinal directions are plotted in Figure 4-16 and Figure 4-17, respectively using Artemis dynamic analysis program. Stable modal frequencies are listed in Table 4-4.
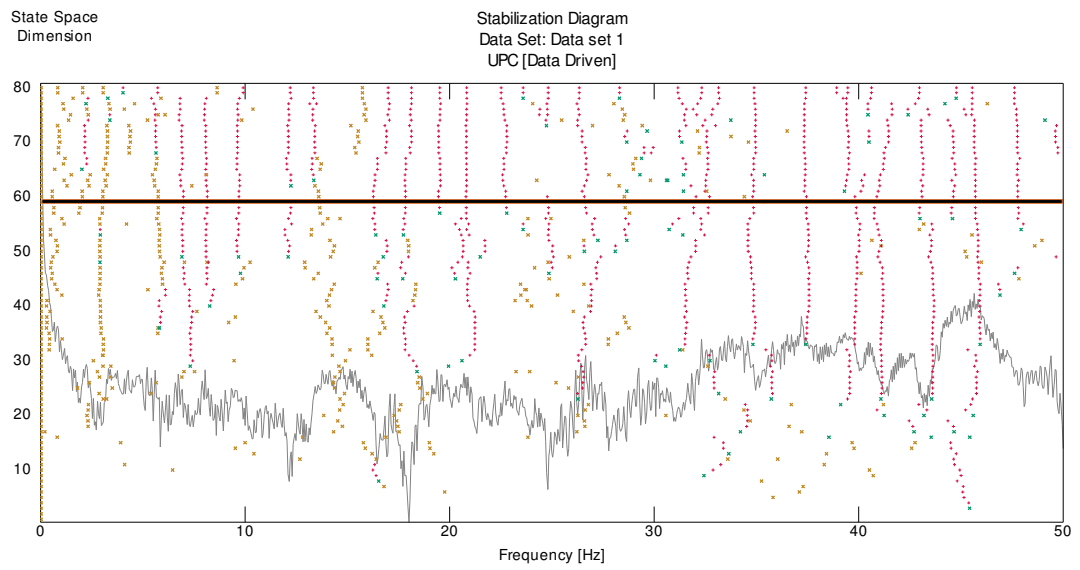
Figure 4-16: Resonant natural frequencies of the tower in longitudinal direction
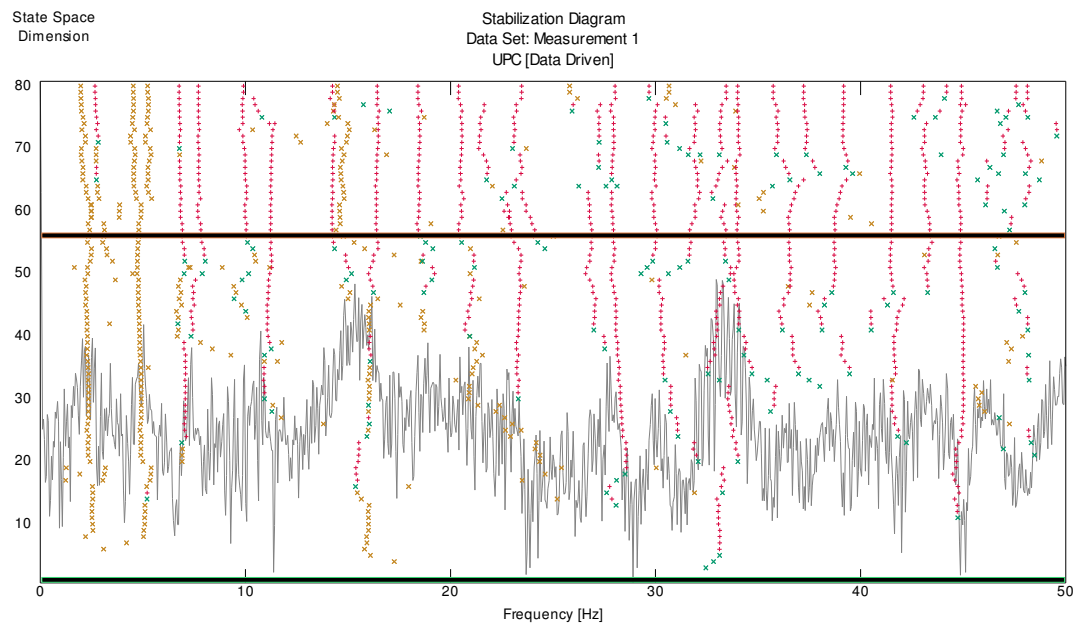
Figure 4-17: Resonant natural frequencies of the tower in transverse direction

Table 4-4: Natural frequencies and mode shapes of the tower for longitudinal and transverse directions.

n	Frequency (Hz)	
	@ Longitudinal direction	@ Transverse direction
1	3.65	6.91
2	6.98	11.23
3	12.25	14.24
4	16.30	16.40

CHAPTER 5

STRUCTURAL MODELLING & UPDATING

5.1 Introduction

Finite element modeling is a mathematical tool which may be used to simulate the physical behavior of the structures. Using FE modeling, the structure is divided into several small members. The finite element models contain the information, which is about the structure materials, geometry and constraints, to be analyzed. Construction of model geometry and updating of the FE models are the most difficult process in FE modeling. Construction of the load cases and analysis cases take place after developing the geometric representation of the structure to be analyzed and defining the geometric analysis domain, including boundary conditions.

Finite element models should be checked to see members are properly connected to each other and material properties are properly assigned without unit errors. A preliminary analysis would reveal obvious errors in the modeling.

The structural analysis of the METU Bridge is conducted using two different levels of complexity. Static and dynamic analyses are conducted for both

finite element models. Staged construction analysis is performed on the simplistic FEM as a third model. The FE models are listed as follows;

1. Simplistic FE model: This model is used only for modal analysis. This FE model represents the final stage of the construction where all of the cables are in place and temporary supports are removed.

2. Simplistic FE model (staged construction): This model is used only for staged construction analysis. Incremental linear analysis steps are carried out for a nonlinear loading analysis of the bridge to simulate various stages during cabling and temporary support removal. This model was an attempt to better estimate the cable forces analytically for zero displacement at cable supports on the deck.

3. Complex FE model: This model is used for both static and dynamic (modal) analysis.

The three-dimensional finite element models are constructed using shell and frame elements for the tower, deck, and cables. Body constraints are used to connect different parts of the model which are not aligned properly (e.g. frame element used for pipe section is connected to the transverse frame's web using constraints). Dynamic analysis of the models is performed by using eigenvalue analysis, which is used to calculate the natural vibration frequencies (eigenvalues) of the FE model and corresponding mode shapes (eigenvectors).

Frame members are used to simulate beam and truss behavior. Moment releases about 2nd and 3rd axis (Figure 5-1) are applied to ends of the cables and truss members (located under the bridge deck) so that they carry only axial loads. Sign convention of a frame element is given in Figure 5-1 [15].
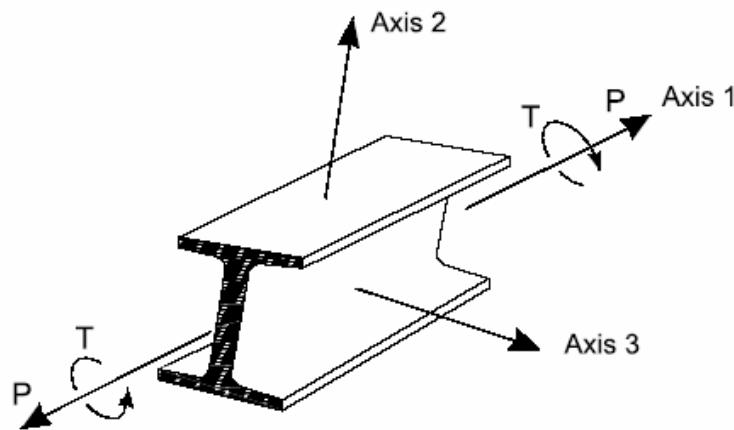
Figure 5-1: Positive sign convention of a frame member internal forces [15]

Shell members are used to simulate membrane and plate behavior of thin plates such as slab and webs of beams with variable height. Triangular shaped shell members are used for transitions between sharp corners towards flat surfaces. General view of triangular and quadrilateral shell members and their face and joint definitions are given in Figure 5-2.
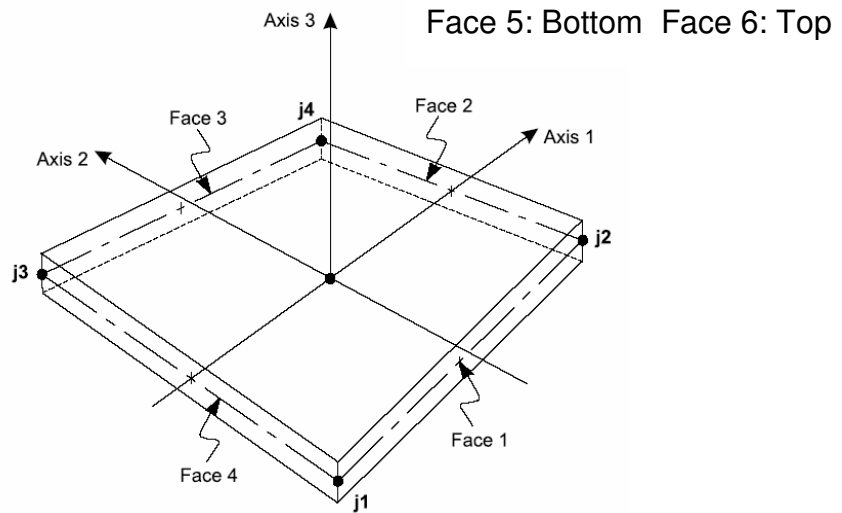
a) Quadrilateral shell member face and axis definitions
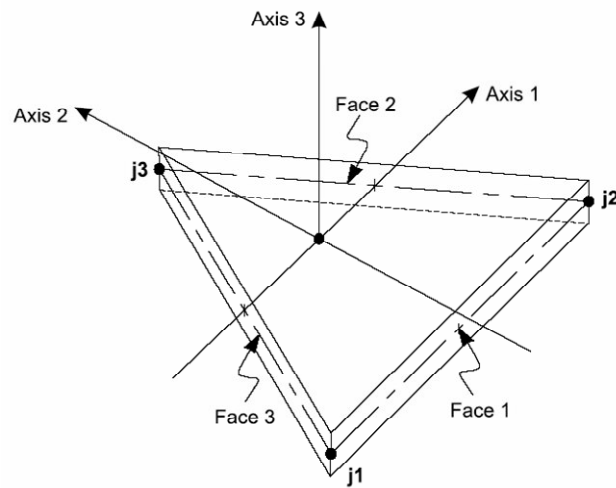
b) Triangular shell member face and axis definitions

Figure 5-2: Shell element joint connectivity and face definitions [15]

5.2 Calibration (Model Updating) of the FE Models

Modeling idealizations or assumptions are integral parts of analytical models. Initial values of geometry, material properties, support conditions and similar parameters are assigned to members from the plans when creating the initial FE models, which usually do not exactly reflect actual properties. Time

dependent stiffness and support condition changes are also unknown for many structures which require model calibration using experimentally measured data. The FE model updating studies involve modification of model input parameters within SAP2000 structural analysis program. Parameters of updating are selected to be: a) boundary conditions of the deck and tower, b) modulus of elasticity of the cables, c) mass of the deck and tower members[*]. Calibration process was carried out until a relatively good match between analytical model and experimental results was obtained. Mode shapes, modal frequencies, and cable forces were selected to be the comparison parameters. Assumptions and idealizations made for the FE models are listed as follows:

1. Modulus of elasticity (E) in tension and compression are equal.

2. The effect of residual stress is negligibly small.

3. The simplistic and complex FE models are analyzed for four different load cases: DL, COVERL, COUPLERL, and PRESTRESSL. Live load is not considered for load combination.

4. The multiplier values for all load cases are taken as 1. Static and dynamic analysis are performed in terms of this load combination (1.00*DL+1.00*COVERL+1.00*COUPLERL+1.00* PRESTRESSL).

5. The deck supports are idealized as springs. The tower at its base and cable connections at anchor blocks are assumed to be fixed. Also, hinge connections are assumed for the temporary pier base supports.

---

[*] Only in the simplistic model.

6. Non-linear analysis is performed for staged construction of the bridge. Staged construction analysis is performed to distinguish the cable force differences and effect on the structure between each cabling stages.

7. The temporary piers are fully connected to the bridge deck (not idealized as pin connection) since the connection was performed by means of welding.

8. The modulus of elasticity (E) is assumed to be different for the cables from that of steel (210000 MPa). (Cable data sheet indicates that E value changes between 205000 MPa and 215000 MPa.)

9. Poisson's ratio (μ) and unit density are taken as 0.30 and 7850 kg/m^3, respectively.

10. 9.81 kN (1 ton) axial prestressing load is applied to the cables which connects the bridge deck to the tower. 29.43 kN (3 tons) prestressing load is applied to the cables which tie the tower and anchor block.

5.3 Definition of the Models

Two level of complexity is used to generate four different 3D-FE models: complex, simplistic (staged construction), and simplistic (plain), using SAP2000 program. The general views of the models are shown in Figure 5-3, Figure 5-4, Figure 5-5 and Figure 5-6 respectively. The bridge geometry is modeled according to the available drawings. In the simplistic, "staged construction" FE model; the pylon (tower), cables, temporary piers, pipe sections, and 250*10mm steel plates are modeled using frame members.

The three rectangular box girders are connected by a 10mm thick vertically placed steel plate in transverse direction and 10mm thick steel plate is placed over the girders at deck level using shell members. The simplistic finite element model has a total of 905 nodes, 596 frames, and 946 shell members with a total of 5193 degrees of freedom (dofs).
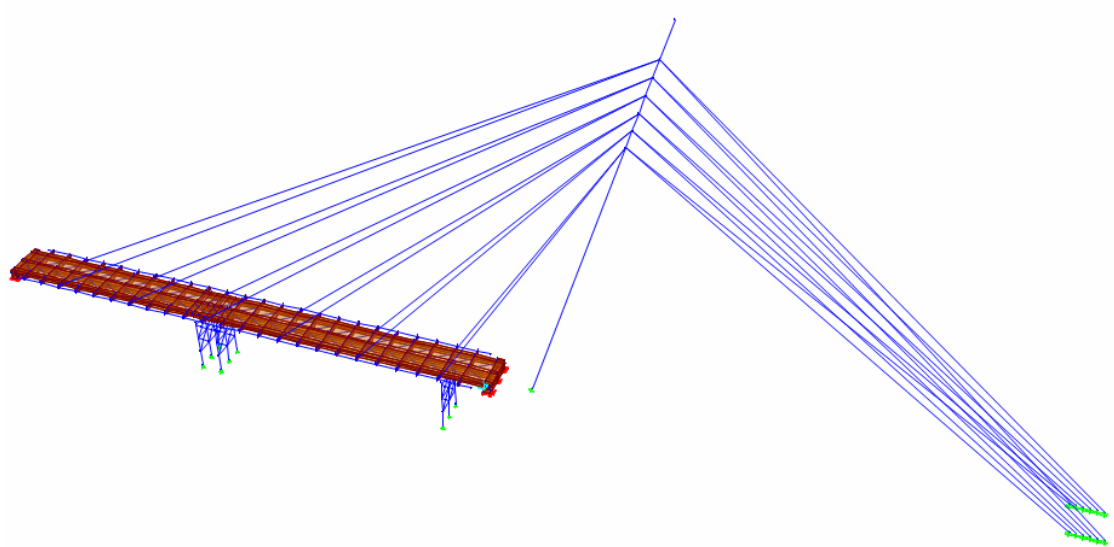
Figure 5-3: 3-D view of the simplistic FE model for staged construction analysis

The simplistic FE model is the same as the first model (staged construction) in terms of element meshing but the number of elements and dofs are different because temporary piers are not considered in this model. The simplistic finite element model has a total of 848 nodes, 494 frames and 946 shell members with a total of 4959 dofs and represents the last stage of the constructed bridge.
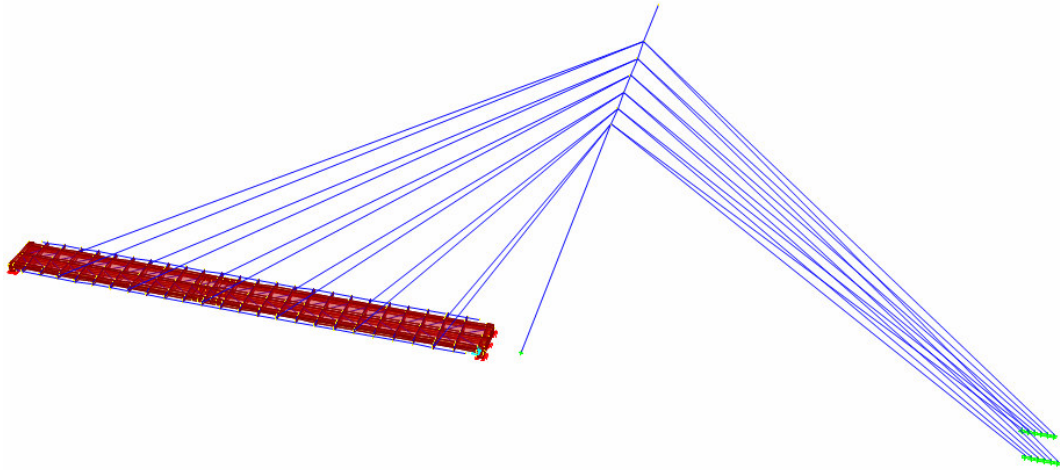
Figure 5-4: 3-D view of the simplistic FE model for modal analysis

In the complex FE model, the pylon (tower), the stiffening girder, which consists of three hollow box sections connected by a 10mm thick transverse steel plate, and 10mm thick steel deck are modeled using shell elements. On the other hand, cables, pipe sections and 250*10mm steel flanges of transverse beams are modeled using frame elements. The complex finite element model has a total of 4895 nodes, 866 frames and 5526 shell members with a total of 29214 dofs.
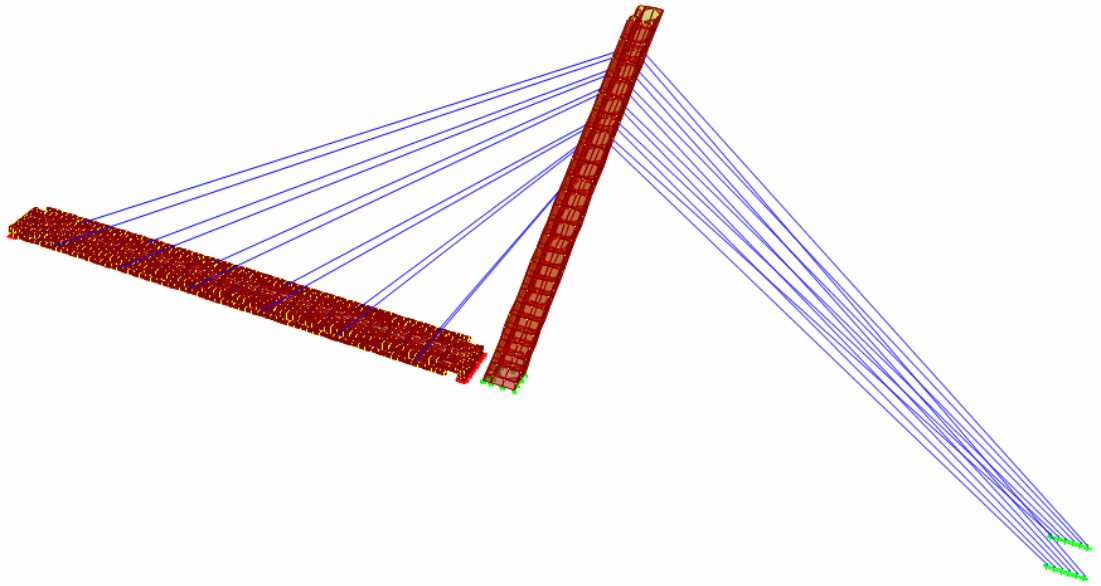
Figure 5-5: 3-D view of the complex FE model

Cable and tower support connections are defined using fixed supports while bridge supports are defined using springs. Properties of sections used in the analytical models are given in Table 5.1.

Moreover, one part of the bridge deck is modeled for determination of the strain levels during lifting process. This model (Figure 5-6) is formed using the simplistic FE model (Fig 5-4) and bridge deck segment FE model has a total of 405 nodes, 254 frames, and 451 shell members with a total of 2397 dofs. Level of strain obtained in analytical model is compared against measured values in Chapter-6 in Table 6-1 for five gages (gage#1 through gage#5), which were mounted at left segment (METU side) of the bridge deck. Three shell members located at the instrumented gage locations are examined to analytically obtain strain levels at these gage locations.

68
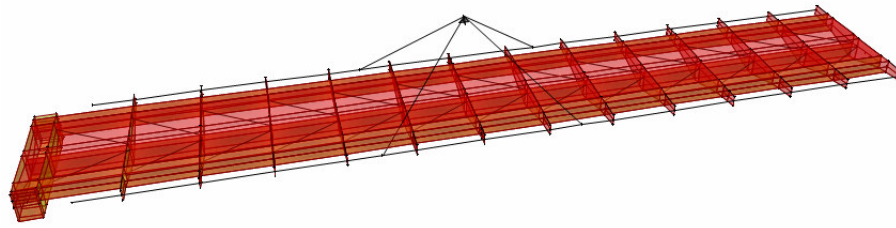
Figure 5-6: 3-D view of one the bridge deck segment FE model for lifting process

Table 5-1: Cross-sectional properties of frame members

SECTION PROPERTIES		FRAME SECTIONS				
		CABLE	PIPE-1	PIPE-2	PIPE-3	PLATE
1. Section type	-	Circular	Pipe	Pipe	Pipe	Rectangular
2. Member thickness	(cm)	-	0.70	0.60	0.45	1.00
3. Member width	(cm)	-	-	-	-	25.00
4. Diameter	(cm)	4.80	-	-	-	-
5. Outer diameter	(cm)	-	30.00	8.00	6.00	-
6. Cross-Sectional Area	(cm^2)	18.10	64.43	13.95	7.85	25.00
7. Torsional constant	(cm^4)	52.12	13836.89	192.21	60.82	8.12
8. Moment of inertia about 3 axis	(cm^4)	26.06	6918.45	96.11	30.41	2.08
9. Moment of inertia about 2 axis	(cm^4)	26.06	6918.45	96.11	30.41	1302.08
10. Shear area in 2 direction	(cm^2)	16.29	32.23	7.00	3.94	20.83
11. Shear area in 3 direction	(cm^2)	16.29	32.23	7.00	3.94	20.83
12. Section modulus about 3 axis	(cm^3)	10.86	461.23	24.03	10.14	4.12
13. Section modulus about 2 axis	(cm^3)	10.86	461.23	24.03	10.14	104.17
14. Plastic modulus about 3 axis	(cm^3)	18.43	601.06	32.93	13.89	6.25
15. Plastic modulus about 2 axis	(cm^3)	18.43	601.06	32.93	13.89	156.25
16. Radius of gyration about 3 axis	(cm)	1.20	10.36	2.62	1.97	0.29
17. Radius of gyration about 2 axis	(cm)	1.20	10.36	2.62	1.97	7.22
MATERIAL	-	CABLEMAT	STEEL	STEEL	STEEL	STEEL

In the simplistic FE models, the tower is modeled by using non-prismatic frame sections. Eight different hollow box sections are used to define the bridge tower and listed in Table 5-2. Variables t_2 and t_3 referred in Table 5-2 are defined in Figure 5-7.

In the used FE analysis program, (SAP2000), the changes of the bending stiffness values can be linear, parabolic, or cubic over each section's length. The axial, shear, torsional, mass, and weight properties change linearly at each section. Each non-prismatic section is defined using a start section and an end section. The changes of the bending stiffness values about 3 and 2 axes (Figure 5-7) are defined by specifying the parameters EIVAR33 and EIVAR22, respectively. A linear change in t_2 for the shape shown in Figure 5-6 would require that EIVAR33 to be linear. A linear change in t_3 would require EIVAR33 to be cubic. The changes of the bending stiffness about 2 axis is determined in the same manner by the parameter EIVAR22 [15].
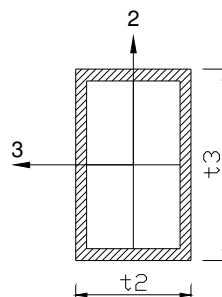
Figure 5-7: Hollow box section properties [15]

Table 5-2: Non-prismatic sections of the simplistic FE model tower

a) Edge prismatic sections to define non-prismatic sections

Prismatic Sections	Outside depth, t_3 (cm)	Outside width t_2 (cm)	Flange thickness (cm)	Web thickness (cm)
TSEC1	202.00	214.00	3.00	3.00
TSEC2	149.50	214.00	3.00	3.00
TSEC3	146.30	214.00	3.00	3.00
TSEC4	143.20	214.00	3.00	3.00
TSEC5	1400.10	214.00	3.00	3.00
TSEC6	136.94	214.00	3.00	3.00
TSEC7	133.80	214.00	3.00	3.00
TSEC8	127.30	214.00	3.00	3.00

b) Non-prismatic section properties

Non-Prismatic Sections	Non-Prismatic Section Properties					
	Start Section	End Section	Length	Length Type	EI33 Variation	EI22 Variation
VAR1	TSEC1	TSEC2	1	Variable	Parabolic	Cubic
VAR2	TSEC2	TSEC3	1	Variable	Parabolic	Cubic
VAR3	TSEC3	TSEC4	1	Variable	Parabolic	Cubic
VAR4	TSEC4	TSEC5	1	Variable	Parabolic	Cubic
VAR5	TSEC5	TSEC6	1	Variable	Parabolic	Cubic
VAR6	TSEC6	TSEC7	1	Variable	Parabolic	Cubic
VAR7	TSEC7	TSEC8	1	Variable	Parabolic	Cubic

5.4 Material Properties

Simplistic and complex FE models have the same material properties. The defined material constants are mass per unit volume, weight per unit volume, modulus of elasticity, shear modulus, poisson's ratio, and coefficient of thermal expansion. All material variables are assumed to be constant during the entire loading and unloading of the structure. Two materials called

CABLEMAT and STEEL are used for structural members. Material properties are given in Table 5-3.

Table 5-3: Material properties

ANALYSIS PROPERTY DATA	MATERIAL			
	STEEL		CABLEMAT	
Mass Per Unit Volume	7.85E-09	N/mm^3	7.85E-09	N/mm^3
Weight Per Unit Volume	7.70E-05	N/mm^3	7.70E-05	N/mm^3
Modulus of Elasticity	2.10E+05	N/mm^2	2.15E+05	N/mm^2
Shear Modulus	8.08E+04	N/mm^2	8.28E+04	N/mm^2
Poisson's Ratio	0.30		0.30	
Coeff. of Thermal Expansion	1.17E-05		1.17E-05	

5.5 Boundary Conditions

The boundary conditions of the tower at its base and cable connections at the anchor block are assumed to be fixed. Hinge supports are assigned to the bases of temporary supports. Joint springs are assigned to at the abutments as shown in Figure 5-8. The stiffness values of the joint springs are given in Table 5-4.
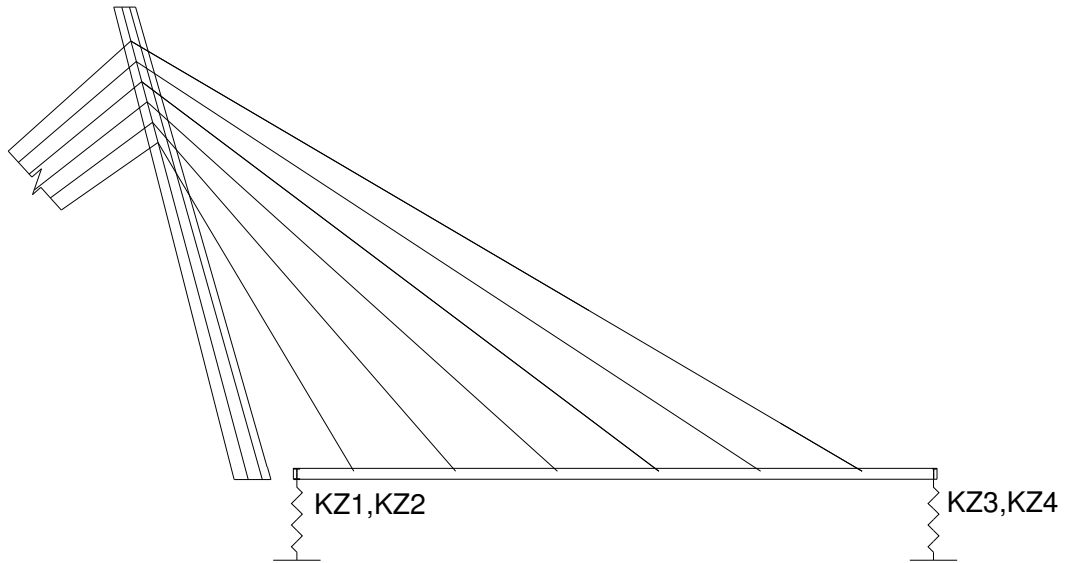
Figure 5-8: Supports of the bridge deck in FE models

Table 5-4: Each spring constant of the supports

Supports	VALUE OF STIFFNESS		
	U_X (N/m)	U_y (N/m)	U_z (N/m)
K_{Z1}	1.47E+08	1.47E+08	1.47E+08
K_{Z2}	**9.81E+07**	**9.81E+07**	**9.81E+07**
K_{Z3}	4903325	4903325	1.47E+08
K_{Z4}	**4412993**	**4412993**	**9.81E+07**

K_{Z1} and K_{Z3} represent the simplistic FE model deck supports; whereas, K_{Z2} and K_{Z4} represent the complex FE model deck supports. The difference is due to the fact that complex model has more support nodes and springs relative to the simplistic model.

73

5.6 Loading

The structure self weight (DL) is applied to the FE model automatically by taking self weight multiplier as 1. Uniformly distributed cover load (COVERL) ($50kg/m^2$) is applied to the deck members. The cables used on the bridge are connected to each other using couplers. The couplers' mass is approximately 10kg which is applied to the cables as nodal loads using loading COUPLERL in –Z direction parallel to the gravity. Prestressing load is given to the cables using temperature loading to simulated prestressing forces. The level of prestressing load on the cables to obtain zero displacements at the cable–deck connection was determined using the simplistic model. The required temperature forces are converted to prestressing forces using Equation (5.1).

$$F = \Delta T * E * A * \alpha \tag{5.1}$$

where;

F   : Prestressing load

ΔT : Temperature difference (^{o}C)

E   : Modulus of Elasticity

A   : Cross-sectional area

α : Coefficient of thermal expansion ($1.17*10^{-5}$)

5.7 Staged Construction Analysis

Staged construction analysis considers the deformations and member force changes between each construction stage. The member forces caused by gravitational load and post tensioning at earlier stages of construction are

74

subjected to changes when the other members are added to or removed from the system. Staged construction analysis is performed to calculate cable force variations at each stage (temporary piers removal and cabling processes) of the construction. The analysis was only possible in the simplistic FE model due to software limitations. 11 different construction stages are defined and force changes are calculated. All defined stages of construction are shown in Figure 5-9 [15].
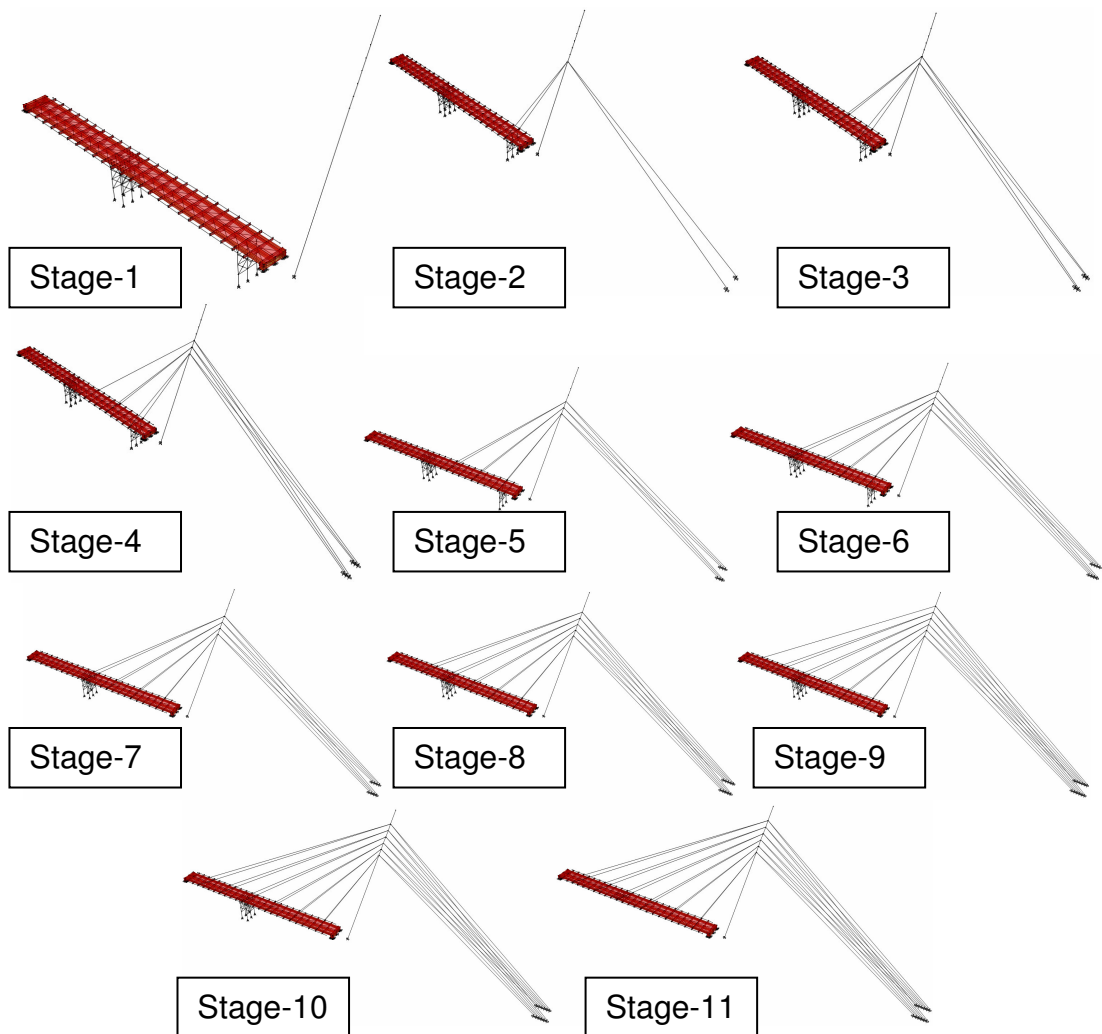
Figure 5-9: Stages of cabling and temporary support removal process

Three staged construction analyses are performed for 1) 9.81 kN initial prestressing in cables (as described in bridge plans), 2) for zero deck deflections at cable to deck connections, and 3) without any prestressing on cables. The variations of cable axial forces at each stage for analysis cases 1 and 2 above are given in Table 5-5 and Table 5-6, respectively. In both of the tables, it is clearly seen that application of additional cables causes reduction in cable forces for the existing cables. The existing cable forces are affected from the additional deformations caused by addition of new members.

Table 5-5: Staged construction analysis results for 9.81 kN initial axial post-tension in cables.

Stages	Cable Forces (kN)							
	Cable 11&12	Cable 9&10	Cable 7&8	Cable 6	Cable 5	Cable 4	Cable 3	Cable 1&2
1st Stage	-	-	-	-	-	-	-	-
2nd Stage	**9,81**	-	-	-	-	-	-	-
3rd Stage	7,16	**9,81**	-	-	-	-	-	-
4th Stage	5,89	10,99	**9,81**	-	-	-	-	-
5th Stage	5,10	10,10	8,14	**9,81**	-	-	-	-
6th Stage	5,89	10,50	8,83	10,99	**9,81**	-	-	-
7th Stage	27,37	10,50	5,10	12,36	**11,18**	-	-	-
8th Stage	27,17	10,69	3,83	10,50	9,03	**9,81**	-	-
9th Stage	26,78	10,50	4,22	11,28	10,01	11,09	**9,81**	-
10th Stage	25,90	10,20	4,22	11,09	9,81	11,18	9,91	**9,81**
11th Stage	15,50	31,78	73,38	93,49	98,79	44,05	47,48	6,67

Table 5-6: Staged construction analysis results for flat deck final shape

Stages	Cable Forces (kN)							
	Cable 11&12	Cable 9&10	Cable 8	Cable 7	Cable 5&6	Cable 3&4	Cable 2	Cable 1
1st Stage	-	-	-	-	-	-		
2nd Stage	**57,68**	-	-	-	-	-	-	-
3rd Stage	42,58	**135,48**	-	-	-	-	-	-
4th Stage	38,46	113,01	**120,07**	-	-	-	-	-
5th Stage	34,48	106,54	112,82	**120,17**	-	-	-	-
6th Stage	25,56	100,85	103,20	110,46	**137,10**	-	-	-
7th Stage	21,68	98,44	102,71	110,07	**137,29**	-	-	-
8th Stage	16,73	96,68	97,12	104,57	123,02	**146,12**	-	-
9th Stage	14,91	95,70	94,37	102,42	118,06	137,14	**130,18**	-
10th Stage	13,29	94,76	92,31	99,67	113,26	128,41	123,02	**130,18**
11th Stage	13,13	95,74	93,86	100,14	115,03	129,49	123,06	**130,17**

where:

Stage 1: The structural system examined in this stage is formed by the bridge deck, tower and temporary pier members.

Stage 2: The cables numbered as 11 and 12 are added to the structural system mentioned in Stage #1.

Stage 3: The cables numbered as 9 and 10 are added to the structural system mentioned in Stage #2.

Stage 4: The cable numbered as 7 is added to the structural system mentioned in Stage #3.

Stage 5: The cable numbered as 8 is added to the structural system mentioned in Stage #4.

Stage 6: The cables numbered as 5 and 6 are added to the structural system mentioned in Stage #5.

Stage 7: Temporary support at METU side is removed.

Stage 8: The cables numbered as 3 and 4 are added to the structural system mentioned in Stage #7.

Stage 9: Cable #2 is added to the structural system mentioned in Stage #8.

Stage 10: Cable #1 is added to the structural system mentioned in Stage #9.

Stage 11: Temporary mid-support is removed.

The 11th stage of the analysis represents the final stage of the construction. The cable forces calculated for the analytical models and analysis cases are listed in Table 5-7. Comparison of cable forces is discussed in Chapter 6.

Table 5-7: Cable forces obtained from different models and analysis cases

	Cable Forces (kN)	Staged Construction Analysis			Single Step Analysis				Field Measured (Average)
		Simplistic FE model			Complex	Simplistic	Complex	Simplistic	
		$\delta=0$	9.81 kN Pre.Load	0 kN Pre.Load	9.81 kN Pre. Load (Single Step)		0 kN Pre. Load (Single Step)		
Cable Forces (kN)	Cable 1&2	127.6	6.7	1.9	32.2	29.1	16.9	14.5	75.5
	Cable 3&4	127.0	47.5	69.9	83.5	83.6	77.1	77.6	90.9
	Cable 5&6	112.8	95.6	130.7	110.4	111.4	109.7	111.0	70.2
	Cable 7&8	95.1	73.4	102.2	111.0	110.6	112.4	112.0	55.0
	Cable 9&10	93.9	31.8	62.9	86.9	86.4	87.3	87.0	33.4
	Cable 11&12	12.9	15.5	42.5	32.4	30.4	27.2	25.1	-

5.8 Modal Analysis

Dynamic analyses of the analytical models are performed using eigenvalue analysis. The eigenvalue analysis is used to calculate the natural vibration frequencies (eigenvalues) of the FE models and the corresponding mode shapes (eigenvectors). First 13 modes are obtained from the complex and first 11 modes from the simplistic analytical models. The mode shapes of complex and simplistic modes are given in Figure 5-10, Figure 5-11, and Figure 5-12. The characteristics and frequencies of mode shapes are summarized in Table 5-8.

3.07Hz

1st bending M.D

5.00Hz

2nd bending M.D

7.85Hz

3rd bending M.D

11.10Hz

4th bending M.D

4.43Hz

1st lateral M.D

6.67Hz

1st torsional M.D

9.95Hz

2nd torsional M.D

14.32Hz

3rd torsional M.D
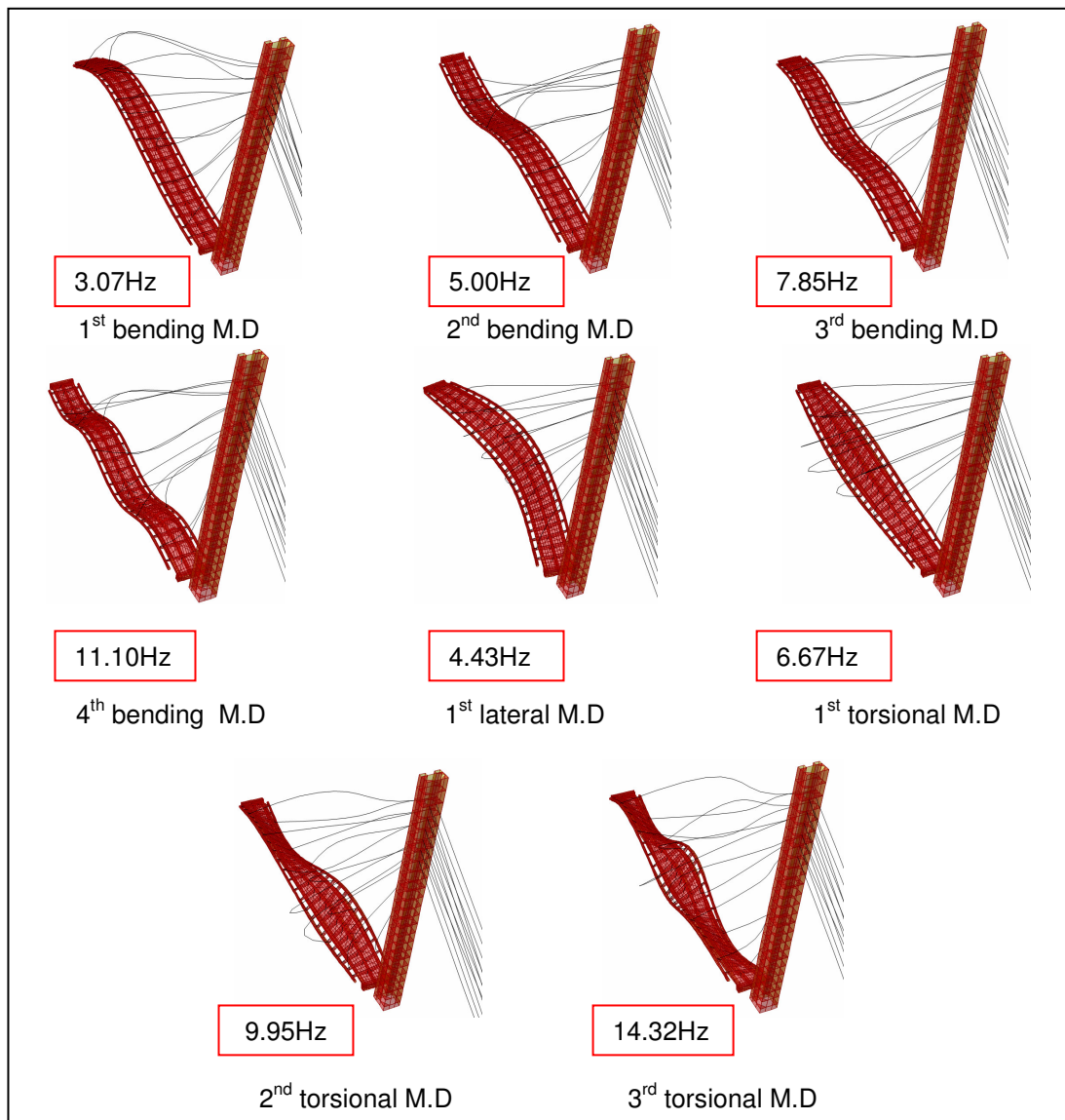
Figure 5-10: The complex FE model mode shapes of the bridge deck
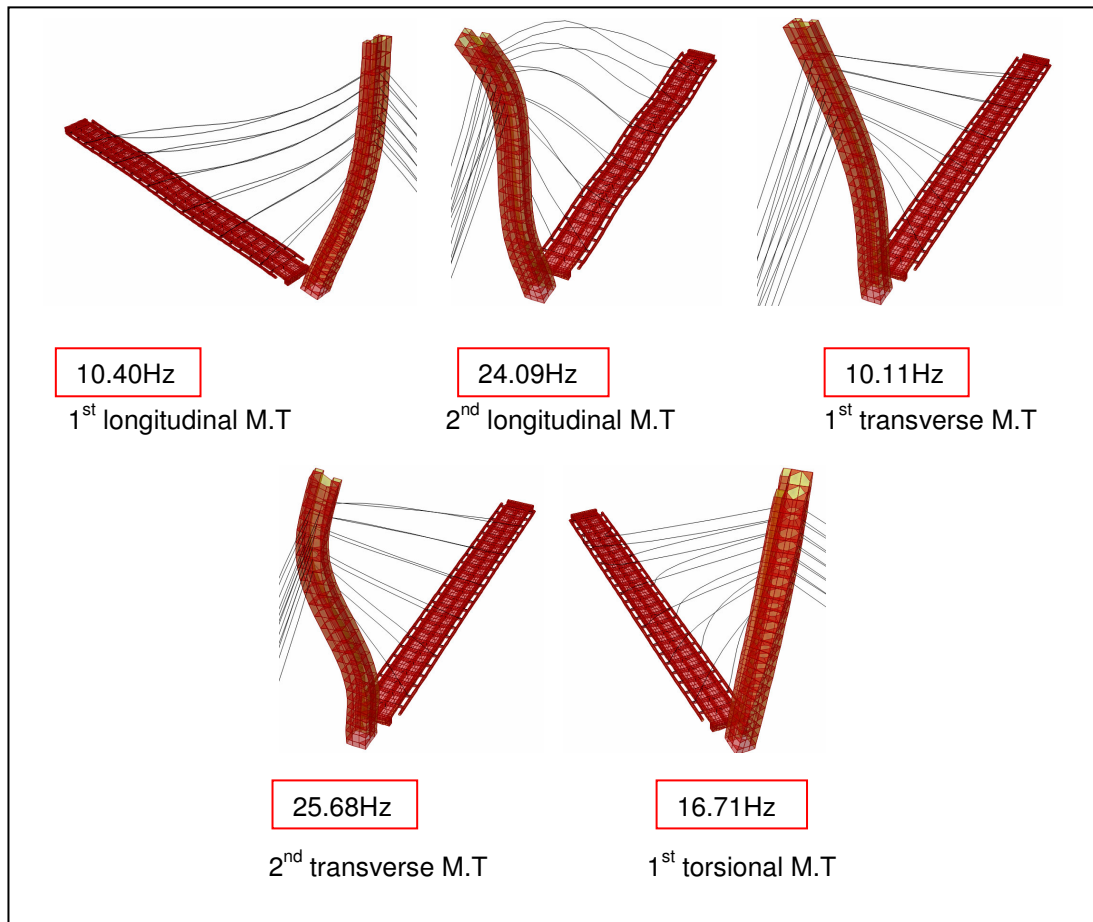
Figure 5-11: The complex FE model mode shapes of the tower

In Figure 5-10, Figure 5-11, and Figure 5-12, M.D represents the dominant motion of the deck resembling "Mode of the Deck", while "M.T" represents the mode shape of the tower. The comparison of analytical and experimental mode shapes and modal frequencies are discussed in Chapter 6.

| 2.97Hz | 4.84Hz | 7.90Hz |
| 1st bending M.D | 2nd bending M.D | 3rd bending M.D |

| 10.93Hz | 4.03Hz | 6.73Hz |
| 4th bending M.D | 1st lateral M.D | 1st torsional M.D |

| 9.43Hz | 14.01Hz | 11.27Hz |
| 2nd torsional M.D | 3rd torsional M.D | 1st longitudinal M.T |

12.05Hz

1st tranverse M.T
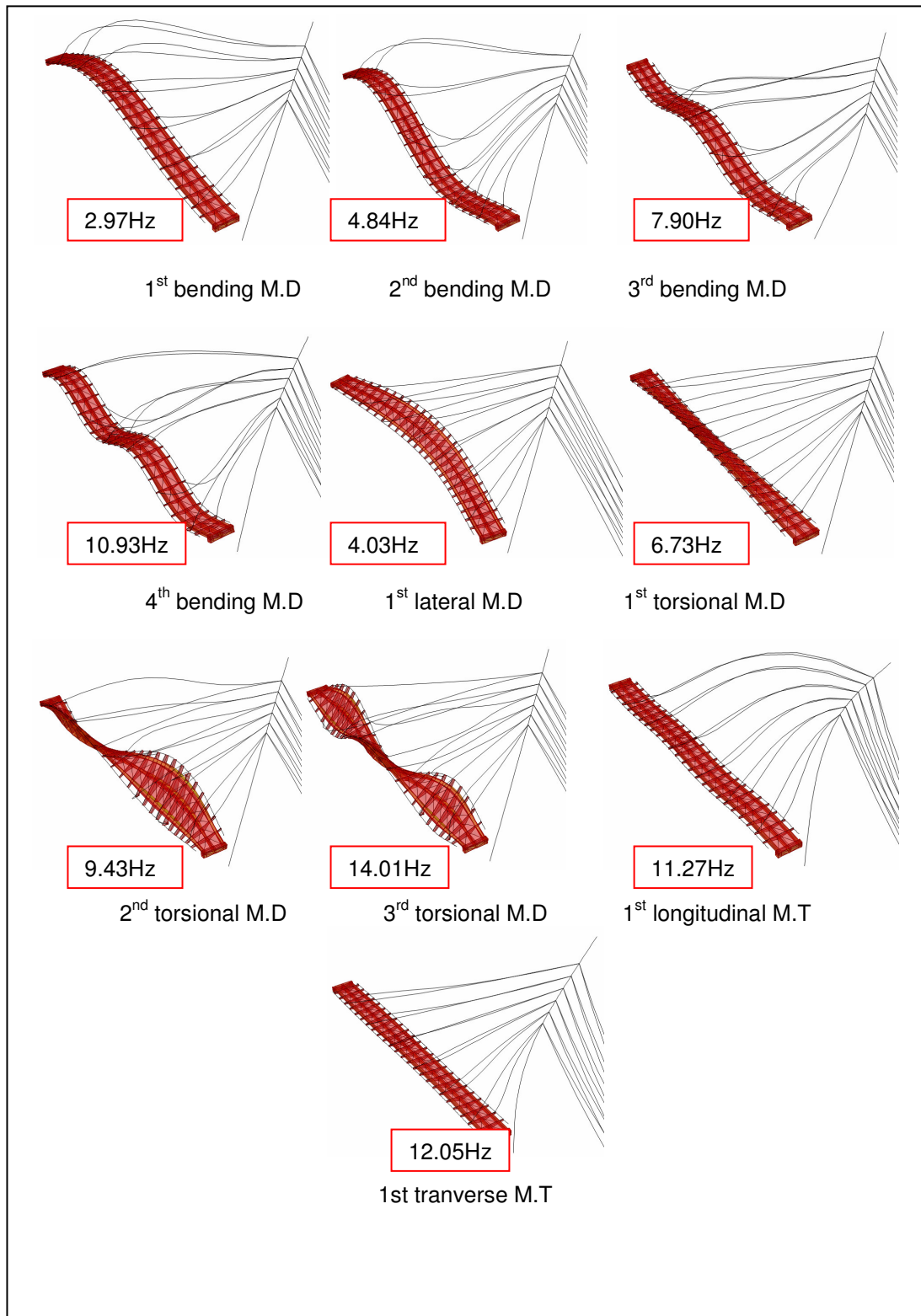
Figure 5-12: The simplistic FE model mode shapes

Table 5-8: Dynamic analysis of the FE models

Location of dynamic analysis	Mode Type	The simplistic FE model computed frequencies (Hz)	The complex FE model computed frequencies (Hz)	Difference (%)	Characteristics of the Mode Shapes
Modes of the bridge deck	Vertical Modes	2.97	3.07	3.38	1st bending mode; deck in one sine wave
		4.84	5.00	3.10	2nd bending mode; deck in two sine waves
		7.90	7.85	0.64	3rd bending mode; deck in three sine waves
		10.93	11.10	1.53	4th bending mode; deck in four sine waves
	Lateral Mode	4.03	4.43	9.03	1st lateral mode; deck in lateral swaying
	Torsional Modes	6.73	6.67	0.90	1st torsional mode; deck in one sine wave
		9.43	9.95	5.23	2nd torsional mode; deck in two and a half sine waves
		14.01	14.32	2.16	3rd torsional mode; deck in two sine waves
Modes of the bridge tower	Longitudinal Modes	11.27	10.40	8.42	1st longitudinal bending mode
		-	24.09	-	2nd longitudinal bending mode
	Transverse Modes	12.05	10.11	19.19	1st transverse bending mode
		-	25.68	-	2nd transverse bending mode
	Torsional Mode	-	16.71	-	1st torsional mode of the tower and deck in a half sine wave

CHAPTER 6

COMPARISON AND DISCUSSION OF RESULTS

The results obtained from each different analytical model and experimental studies are compared and discussed in this chapter. The strain measurements, cable forces, mode shapes, and modal frequencies are the comparison parameters.

6.1 Strain Reading Comparisons

The three months of strain gage readings are processed and maximum strain changes during major events are determined. A sample strain readings window during the transportation and lifting process on March 16th, 2003 is shown in Figure 4-5. The maximum of the responses are obtained during lifting process at gage locations #1 and #4, which are located at the bottom flange of girders at sections A-A and B-B, respectively (Figure 4-4). The cabling process is the next important event from a strain point of view. Largest strain difference is obtained at location #1 at bottom flange of the center girder at section A-A (Table 4-1). Although, gages 7 and 8 are symmetrically located at the bottom flange of section C-C (Figure 4-4), the cabling and support removal effects are measured up to 60% differences between channels 7 and 8 in measured strain values, which is an indication of transverse direction bridge bending or unequal cable tension application at

both sides of the bridge. Due to the inclined nature of cables, the bridge has also experienced axial loads during the cabling process. During the lifting and cabling processes, the gages recorded large strains close to 400 $\mu\varepsilon$ which converts in to 82.4 MPa and is close to about 60% of the materials allowable design stress. At critical portions of the bridge, the effects of each event might be cumulatively added up causing unexpected yielding or partial bridge collapse.

Measured strain levels during lifting process are compared against analytical model results in Table 6.1. All gages placed on the girders were parallel to the bridge length which corresponds to the S11 stress directions of the shell members that were used in the analytical models. Strain level differences between analytical and experimental results are between 4$\mu\varepsilon$ to 78$\mu\varepsilon$. The differences between the measured and simulated results may be due to spacing and height of the cables which were tied to the bridge deck segment, approximations made by discrete members of the FE model, and possible noise in the readings.

Table 6-1: Comparisons of strain levels between analytical and experimental results

Shell Member No	Gage ID	Location of gage at girders	Normal Stress Type	Stress Values (kg/cm^2)	E (kg/cm^2)	Calculated Ave.Strain ($\mu\varepsilon$)	Measured Strain ($\mu\varepsilon$)
159	1	Bottom	S11	636.86	2100000	303	381
159	2	Top	S11	135.70	2100000	65	21.1
207	4	Top	S11	668.06	2100000	318	348
207	5	Bottom	S11	136.67	2100000	65	88.8
870	3	Bottom	S11	68.92	2100000	33	28.9

6.2 Cable Force Comparisons

The cable forces are computed for 7 different analytical simulations as listed below and tabulated in Table 5-7:

1) Last stage of staged construction analysis using simplistic model to obtain zero deformation at all cable to deck connection points.

2) Application of 9.81 kN (1 ton) post tensioning to all cables using staged construction analysis and simplistic model,

3) Directly placing cables without any post-tensioning with staged construction analysis using simplistic model,

4) Single step analysis for 9.81kN (1 ton) post-tensioning using complex model,

5) Single step analysis for 9.81kN (1 ton) post-tensioning using simplistic model,

6) Single step analysis for zero post-tensioning using complex model.

7) Single step analysis for zero post-tensioning using simplistic model.

The comparison of cable forces show large differences between different analysis cases showing that the cable forces are highly sensitive to the selected analysis type or used post-tensioning method. Comparison between the analysis cases and measured cable forces show similarities; however, it is not possible to claim that any of the analysis results fully match against the field measured cable forces. The minimum difference between the measured and analysis cable forces is obtained for the second analysis case: "staged construction with 9.81kN (1 ton) post-tensioning", which happens to be the

construction sequence described in bridge projects by Kipman Inc. The construction stages of post-tensioning application were not observed during this thesis. The differences between the measured and simulated results may be due to inaccurate post-tensioning application or assumptions inherent to the analytical model. The field measurements were conducted 7 months after the construction which would leave a time frame for relaxation due to vibrations and temperature variations.

The large difference obtained for cable #1 and cable #2 might be due to the nonlinear nature of the cable since large sagging was observed at the site during measurements. Cables 1 & 2 being the longest cables (62.22 m) and having the smallest inclination ($\approx 30.45^{\circ}$) might affect the cable force calculation based on linear FE modeling analysis.

Experimentally obtained cable forces given in Table 5-7 are the average forces obtained for symmetric cables. Measured forces are listed in Table 4-2 and Table 4-3 for two different levels of complexity formulations. The results which are given in Table 4-2 use simple formulation ignoring the bending stiffness of cables. The results which are listed in Table 4-3 incorporate modifications to the formulation to include bending stiffness effects. The comparison of experimentally obtained cable forces are shown in Figure 4-14 for both simple and complex formulas. The difference between the forces obtained using two different level of complexity has small significance since the cables are long enough to ignore their bending stiffness.

The comparison of the experimentally obtained forces on parallel cables shows large variations which are probably due to the construction sequence of cables. The differences in parallel cable forces are in the range of 20% to 25%. The cable force differences between parallel cables get smaller when the cables are close to the supports. The difference between parallel cable forces is dominantly generated when the bridge deflects sideways as one of the cables is post-tensioned and the other one is not placed yet. The lateral deflection of the bridge deck is minimal when the cables are close to the abutments.

6.3   Mode Shape and Modal Frequency Comparisons

The dynamic analysis results show that the analytical models, simplistic and complex, adequately represents experimentally measured modes and frequencies. The comparisons of the dominant mode shapes and frequencies of the bridge and tower are given in Table 6-2. The differences in modal frequencies range between 1% and 11%.

The comparison of dynamic measurement obtained at center line versus side location of the bridge deck reveals that the torsional mode shape is located at 6.6 Hz (Figure 6-1). Although other torsional modes located at 9.10 Hz and 15.50 Hz show up in both measurements, the separation of mode shapes can be achieved by comparison against analytical model dynamic analysis as listed in Table 6-2.

Four different dominant vertical modes are found from the experimental measurements at 3.10 Hz, 4.90 Hz, 7.80 Hz and 12.10 Hz and these modes are compared against the analytical results. All vertical modes with the exception of the last mode (12.10 Hz) show close correlation between the analytical and experimental analysis.

Experimentally obtained vertical mode at 12.10 Hz and the torsional mode at 15.50 Hz are matched experimentally with about 1Hz difference (Table 6-2). The experimental frequencies are smaller than the experimentally measured counterparts for high frequency modes which is an indication of higher amount of moving mass or lower stiffness used in the analytical models for higher frequency mode shapes.

The lateral bridge vibration measurement conducted at the about 2/3 of the bridge length. The FFT of the recorded data is shown Figure 4-10. Although three different lateral modes were captured from the experimental data, analytical models were able to simulate only the first lateral bending mode of the bridge deck at 4.03Hz and 4.43Hz from the simplistic and complex FE model, respectively.

Vibration measurements of the tower were conducted at longitudinal and transverse directions using an accelerometer located at 15.00m of elevation inside the tower. Longitudinal and transverse direction natural frequencies of the tower were obtained experimentally (Figure 4-16 and Figure 4-17) and

listed in Table 4-4. The excitations of experimental modes were difficult due to massive size of the tower. Artemis software was used to post process experimental data in order to obtain hidden modes using ambient and impact force data. Only two modes were obtained in each longitudinal and transverse direction using the complex FE model. The simplistic model gave only one mode in each direction. Longitudinal modes of the tower are found in from the complex FE model at 10.40 Hz and 24.09 Hz, and in the simplistic model at only 11.27 Hz. The transverse modes of the tower are obtained at 10.11 Hz and 25.68 Hz for the complex FE model and 12.05 Hz for the simplistic FE model. The accelerometer was placed at mid location of the tower to eliminate torsional tower modes. Although torsional mode of the tower was not captured, complex FE model simulated a torsional tower mode at 16.71 Hz. (Table 6-2).

Table 6-2: Comparisons of dynamic analysis

| Location of dynamic analysis	Mode Type	The simplistic FE model computed frequencies (Hz)	The complex FE model computed frequencies (Hz)	Measured Frequencies (Hz)	Error (%) of the simplistic FE model results	Error (%) of the complex FE model results	Nature of Mode Shapes
Dominate modes of the bridge deck	Vertical Modes	2.97	3.07	3.10	4.19	0.84	1st bending mode; deck in one sine wave
		4.84	5.00	4.90	1.22	1.94	2nd bending mode; deck in two sine waves
		7.90	7.85	7.80	1.28	0.64	3rd bending mode; deck in three sine waves
		10.93	11.10	12.10	9.67	8.26	4th bending mode; deck in four sine waves
	Lateral Mode	4.03	4.43	4.50	1.97	1.06	1st lateral mode; deck in lateral swaying
	Torsional Modes	6.73	6.67	6.50	3.54	2.62	1st torsional mode; deck in one sine wave
		9.43	9.95	9.10	3.63	9.34	2nd torsional mode; deck in two and a half sine waves
		14.01	14.32	15.50	9.61	7.61	3rd torsional mode; deck in two sine waves
Dominate modes of the bridge tower	Longitudinal Modes	11.27	10.40	10.50	7.33	1.00	1st longitudinal mode;1st bending mode
		-	24.09	26.00	-	7.35	2nd longitudinal mode;2nd bending mode
	Transverse Modes	12.05	10.11	10.80	11.57	6.39	1st transverse mode; 1st bending mode
		-	25.68	23.10	-	11.17	2nd transverse mode; 2nd bending mode
	Torsional Mode	-	16.71	-	-	-	1st torsional mode of the tower and deck in a half sine wave
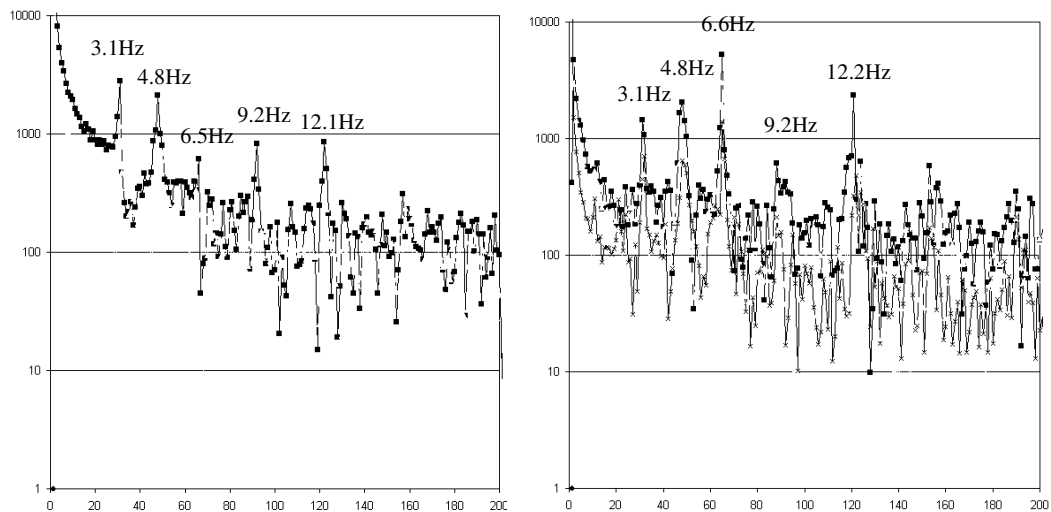
Figure 6-1: Torsional vibration measurements of the bridge deck [14]

The comparisons of the initial and calibrated analytical models for three vertical and three torsional mode frequencies of the bridge deck are given in Table 6-3. All mode frequencies are improved (2% to 29.75%) with the exception of the third torsional mode of the deck. The average improvement from initial to calibrated FEM results is approximately 20% (Table 6-3).

Table 6-3: Improvement of FEM results

Mode type	Nominal FEM Results (Hz)	Calibrated FEM Results (Hz)	Measured Frequencies (Hz)	% Improvement
1st bending	2.58	3.07	3.10	15.96
2nd bending	4.64	5.00	4.90	7.20
3rd bending	5.84	7.85	7.80	25.61
1st torsional	6.60	6.67	6.50	-1.05
2nd torsional	9.63	9.43	9.10	2.12
3rd torsional	10.06	14.32	15.50	29.75
			Ave. Improvement =	19.90

92

CHAPTER 7

SUMMARY AND CONCLUSIONS

This study targeted monitoring of construction stage strains, indirect measurements of axial forces on bridge cables, and dynamic tests on the bridge deck and tower. A cable-stayed steel pedestrian bridge in Ankara-Turkey is selected as a case study. The bridge parts were instrumented at the factory after manufacturing and strains were measured during transportation, erection, and service stages. The level of strains for each major event are obtained and discussed. Dynamic measurements were conducted at the bridge deck, cables and tower. Transverse, longitudinal, and vertical direction measurements were conducted to capture bridge modes and modal frequencies as many as possible, and comparisons against analytical models were performed. Cable dynamic measurements are carried out in order to obtain the cable forces indirectly using resonant vibration frequencies. Two different levels of complexity is used for analytical FE models. Staged construction analyses are performed in addition to single step linear analysis (Table 5-7). Cable forces and bridge modal frequencies are compared against analytical model simulations.

Following conclusions are drawn based on the conducted analytical and experimental studies:

- Large quantities of strains are measured during construction stages such as lifting bridge segments with crane and cabling processes. Individual events generated close to a maximum of 400 $\mu\varepsilon$ strains, while the largest total strain measured in the course of 3 months monitoring is 492 $\mu\varepsilon$ at gage location #1, 504 $\mu\varepsilon$ at gage location #4, 548 $\mu\varepsilon$ at gage location #6. The measured strain values at the bridge deck indicate that the METU bridge experiences up to 80% of its design strains during construction and 3 months of service stages, although most probably design load conditions were not occurred.

- Experimental (indirect) measurements of cable forces show that there are significant differences between parallel cables, especially the cables located close to the middle part of the bridge deck. The tension cable force differences change between 1 kN to 23.8 kN which refers to about 3% to 38% difference between parallel cables. The large difference between the middle span cables is due to cabling sequence: the bridge deck bends laterally when the first one of the two parallel cables is post tensioned. Application and tensioning of the second cable causes the bridge to bend back into its center line causing the first cable to carry more load relative to the second cable.

94

• Post-tensioning force of the cables should be checked a) after all cables are placed in their locations and first round of post-tensioning is applied and b) at certain intervals (e.g. semi-annually or annually) to investigate and correct possible cable force variations and relaxations that occur over time.

• The comparison of experimental and analytical cable forces show large differences based on the type of analysis. Largest differences are obtained for single step construction which does not simulate changes in cable forces during construction phases. Staged construction analysis gives better results as compared to single step analysis. Variations between the measured and simulated cable forces are attributed to relaxation of cable forces after construction (due to vibrations, traffic etc) and possible non linear effects on experimental cable vibration measurements (such as sagging, lumped mass of couplers, bending stiffness of cables, support conditions, bridge cable interaction, etc.), and uncertainities associated with the temporary supports.

• Analytical modal analysis and experimental measurements correlate well for the mode shapes and frequencies. The experimentally obtained modal frequencies were partially identified simply by changing the accelerometer measurement location and direction. The actual (complete) mode shapes were obtained using FEM modal analysis and matched against experimental modes by comparing modal frequencies (Table 6-2). The

complex FE model results better match against the experimental measured frequencies and modes, except for the second torsional mode of the bridge deck. The average of the frequency errors are 4.85% and 5.40% for the complex and simplistic models, respectively. The complex model was able to simulate two additional modes of the tower (2nd bending in x and y directions) and torsional tower mode while simplistic model was not able to simulate them.

- The support conditions of the bridge deck are modeled using springs instead of pin or roller supports to simulate the bearing conditions better. Calibrations of simplistic and complex models are performed by changing spring stiffness coefficients, cable modulus of elasticity, and deck surface mass until experimentally obtained modal frequencies and mode shapes are matched against their analytical counterparts. The modulus of elasticity of cables that gives better correlation is $2.15*10^5$ MPa (which is also the same as in the cable specifications provided by the manufacturer). The improvrevement in average differences of modal frequencies is 20% (Table 6-3) after the FEM calibration.

- Based on the experimental & analytical experience obtainedin this study, bridge monitoring and testing systems may include long-term strain readings, short-term dynamic tests, and indirect cable force measurements by measuring natural vibration frequencies. Displacement & tilt measurement may also be added for a comprehensive study.

96

• Multiple accelerometers might be used to better obtain resonant frequencies and mode shapes; however, larger numbers of accelerometers require more initial expenses for more advanced data acquisition systems and transducers.

• The equipment (data logger, gages, accelerometer, cables, etc.) for instrumented monitoring costs about 8.000 to 13.000 USD; however, the knowledge obtained from monitoring is very valuable. Especially construction of large and important structures should incorporate similar monitoring systems to understand construction and service loading conditions as well as aging process of the structure for maintenance purposes.

REFERENCES

1. Iain A. M., "Analytical Modeling of Structural Systems", Ellis Horwood Limited, 1990.

2. Smith, J. D., "Vibration Measurement and Analysis", Butterworth Co. Ltd, 1989.

3. Troitsky M. S., "Cable-Stayed Bridges: An Approach to Modern Bridge Design", 2nd edition, Van Nostrand Reinhold Company Inc., New York, 1988.

4. Podolny W., Scalzi J. B., "Construction and Design of Cable-Stayed Bridges", Wiley J. & Sons, New York (USA), 1976.

5. Gimsing N. J., "Cable Supported Bridges: Concept and Design", Wiley J. & Sons, New York, 1983

6. Lee Z. K., Chang K. C., Loh C. H., Chen C. C., and Chou C. C., "Cable Force Analysis of Gi-Lu Cable-Stayed Bridge after Gi-Gi Earthquake", National Taiwan University, Taipei, Taiwan.

7. Computers and Structures, Inc., Berkeley, California, USA, SAP2000 Static and Dynamic FE Analysis of Structures Non-Linear Version 8.0.8, Structural Analysis Program.

8. Brauer J. R., "What Every Engineer Should Know about Finite Element Analysis", 2nd ed. rev. and expanded, Marcel Dekker, Inc., New York.

9. Galindez N., Marulanda J., Thomson P., Caicedo J. M., Dyke S. J., and Orozco A., "Implementation of a Modal Identification Methodology on the Pereirados Quebrasdas Cable-Stayed Bridge", 16th ASCE Engineering Mechanics Conference, July 16-18,2003, University of Washington, Seattle.

10. Caicedo J. M., Turan G., Dyke S. J., and Bergman L. A., " Comparison of Modeling Techniques for Dynamic Analysis of a Cable-Stayed Bridge", Washington University, St. Louis, Missouri 63130, University of Illinois, Urbana, Illinois 61820.

11. Mehrabi A. B., and Ciolko A. T., "Health Monitoring and Problem Solving for Cable Supported Bridges", Construction Technology Laboratories, Inc., Skokie, IL (USA).

12. Hartley M. J., Pavic A., and Waldrom P., "Investigation of Pedestrian Walking Loads on a Cable Stayed Footbridge Using Modal Testing and FE model updating", University of Sheffield, IMAC-XVII Proceedings, the Society for experimental Mechanics, Inc., 1999.

13. Chang C. C., Chang T. Y. P, and Zhang Q. W., "Ambient Vibration of Long-Span Cable Bridge", Journal of Bridge Engineering, Vol. 6, No. 1, January/February, 2001.

14. Türer A., and Özerkan T., "Strain and Vibration Measurements of a Cable-Stayed Pedestrian Bridge", Civil Engineering Dept., Middle East Technical University, Ankara, Turkey, 2004.

15. Computers and Structures, Inc., Berkeley, California, USA, "SAP2000 Integrated Finite Element Analysis and Design of Structures, Analysis Reference Manual, Version 8.0.8, July 2002.

16. Kaya Ö., "Finite Element Modeling and earthquake Simulation of a Highway Bridge Using Measured Earthquake Data", Thesis, Civil Engineering Dept., Middle East Technical University, Ankara, Turkey, April 2003.

17. Slope Indicator, http://www.slopeindicator.com, CR10X datasheets, July 2003.

18. Campbell Scientific, Inc., http://www.campbellsci.com, cr10x, July 2003.

19. Geokon, Inc., http://www.geokon.com, strain gages, July 2003.

20. PCB Piezotronics, Inc., http://www.pcb.com, pcb 393c spec_sheet, August 2003.

21. Bartleby. com, http://www.bartleby.com, May 2005.

22. DYWIDAG-Systems International, www.dywidag-systems.com, docs, March 2005.

STRAIN AND TEMPERATURE READING GRAPHS AND BATTERY

CHARGE CHANGE GRAPH ACCORDING TO TIME

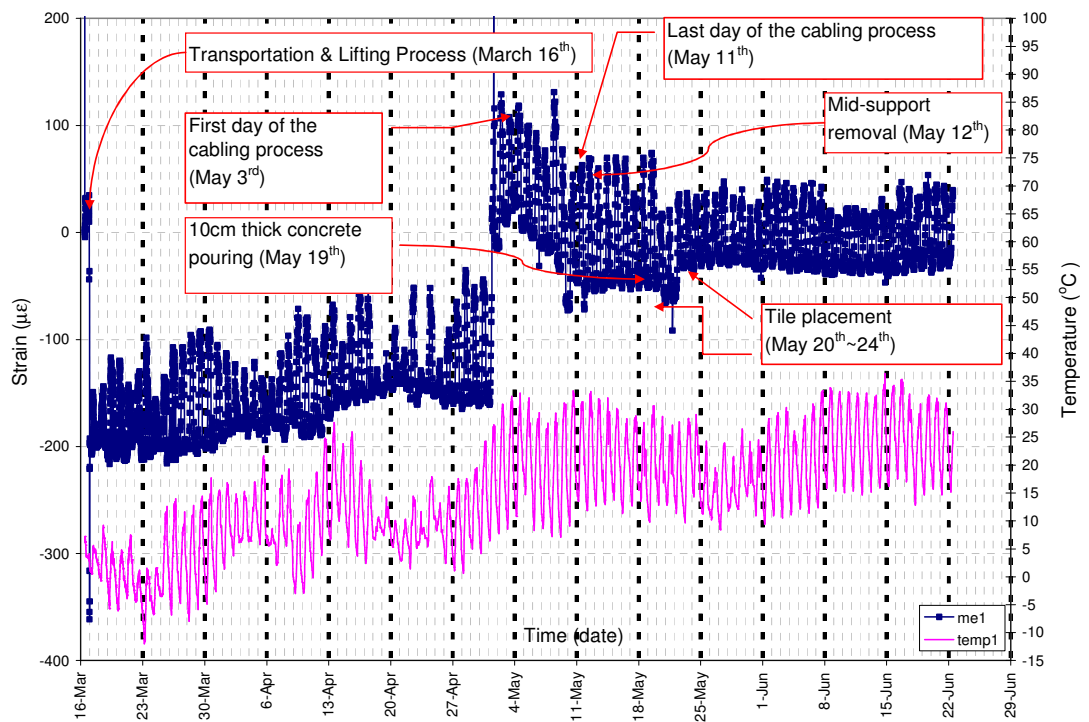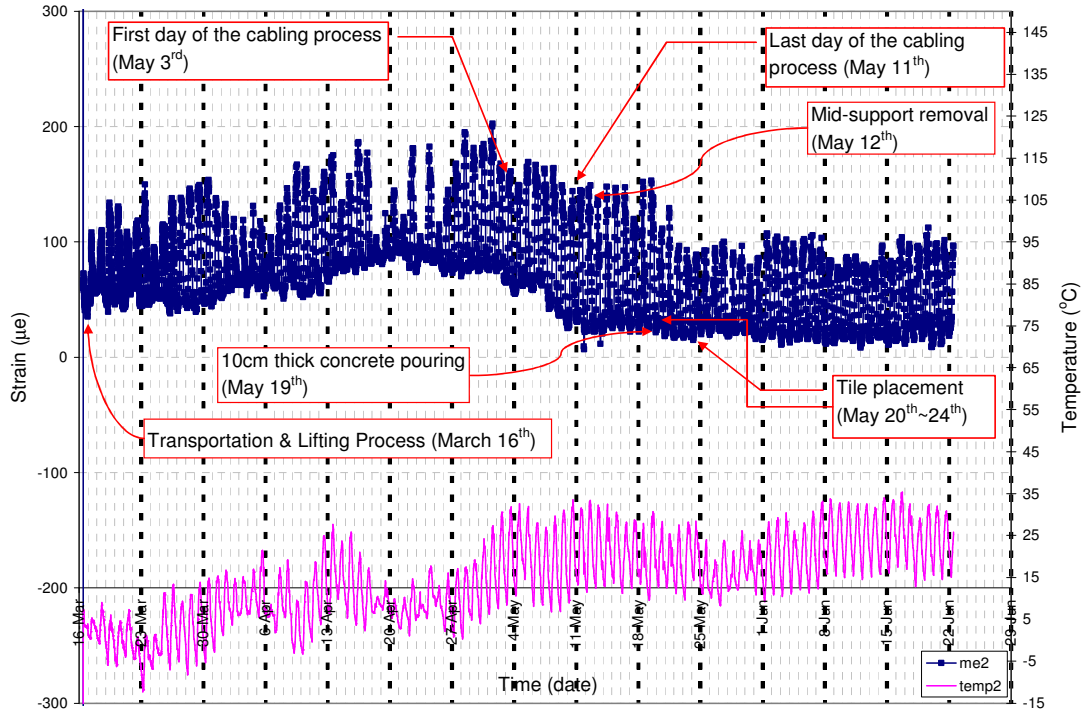Figure A.1: Strain and temperature changes for strain gage-1
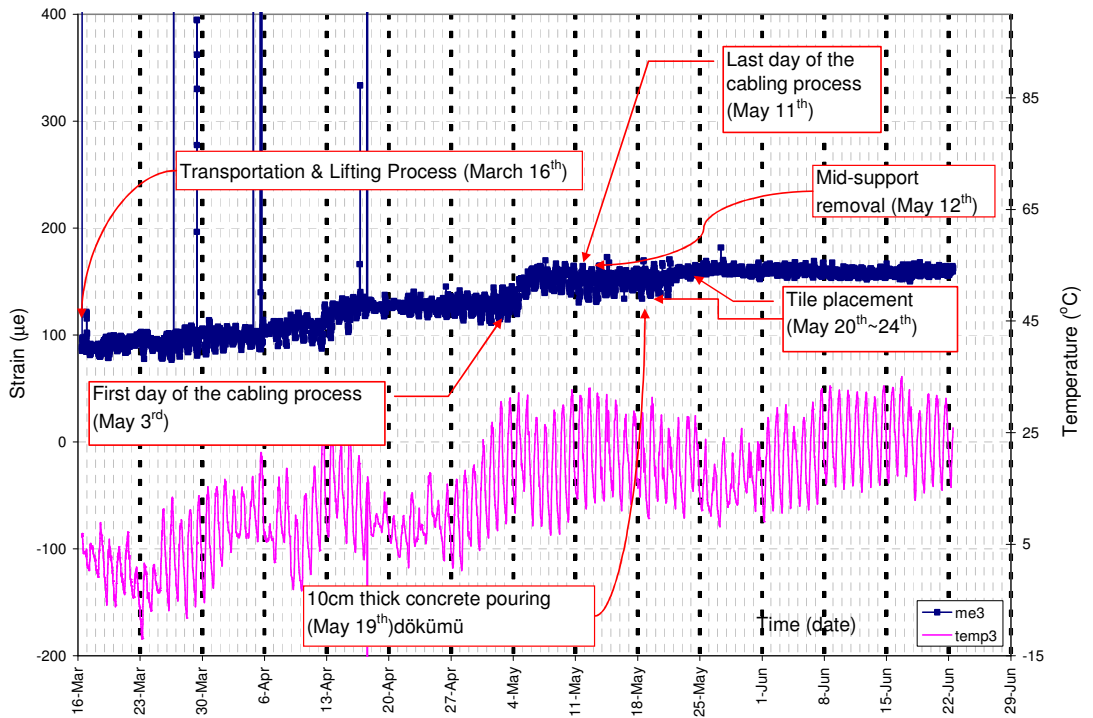
Figure A.2: Strain and temperature changes for strain gage-2

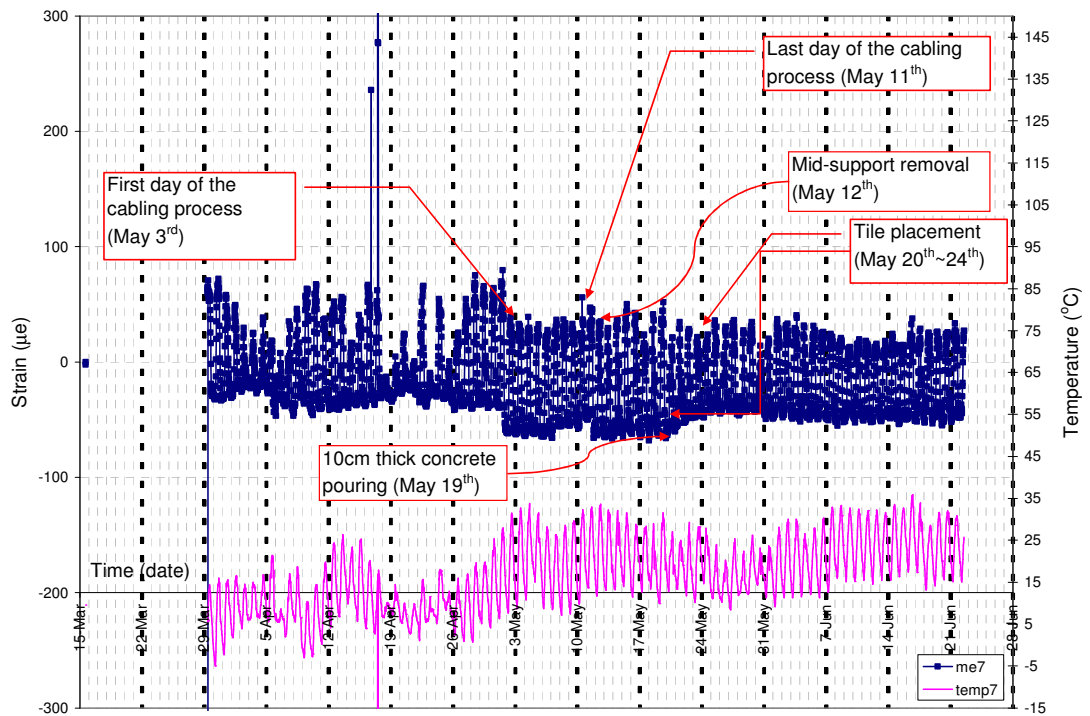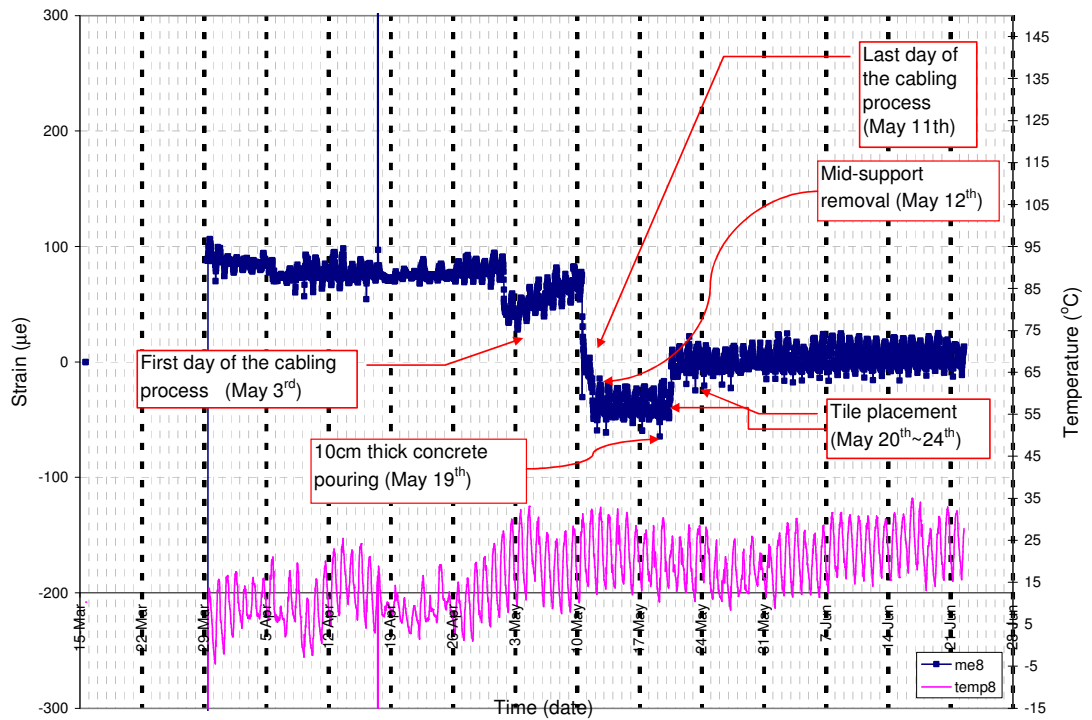Figure A.3: Strain and temperature changes for strain gage-3
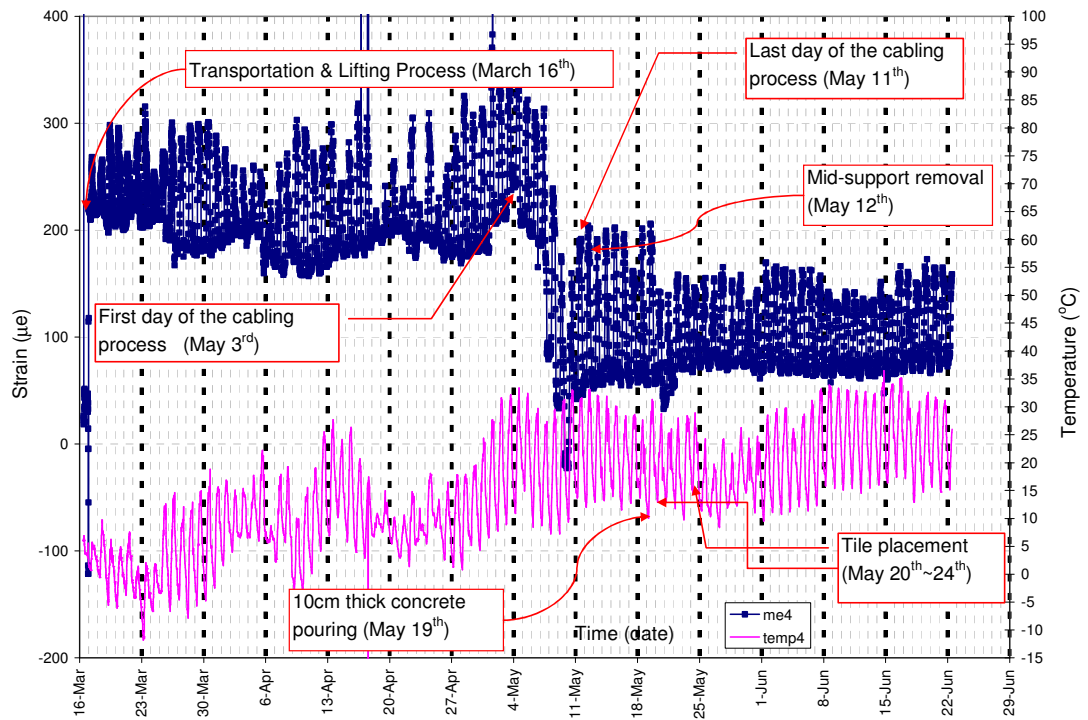
Figure A.4: Strain and temperature changes for strain gage-4
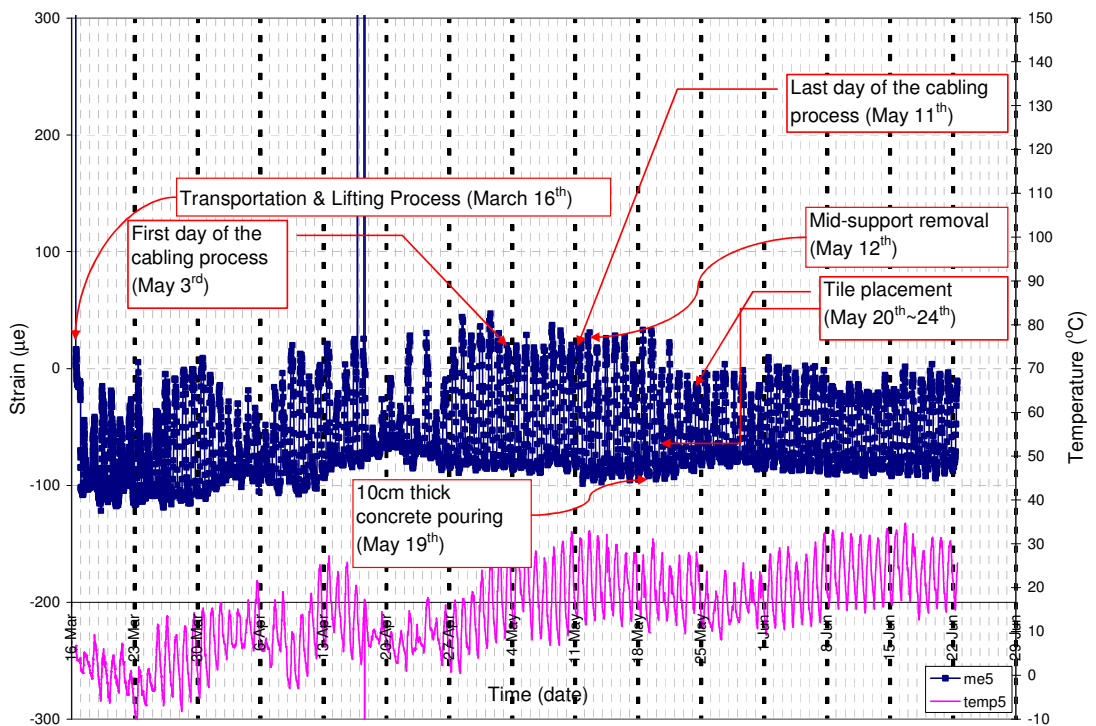
Figure A.5: Strain and temperature changes for strain gage-5

103
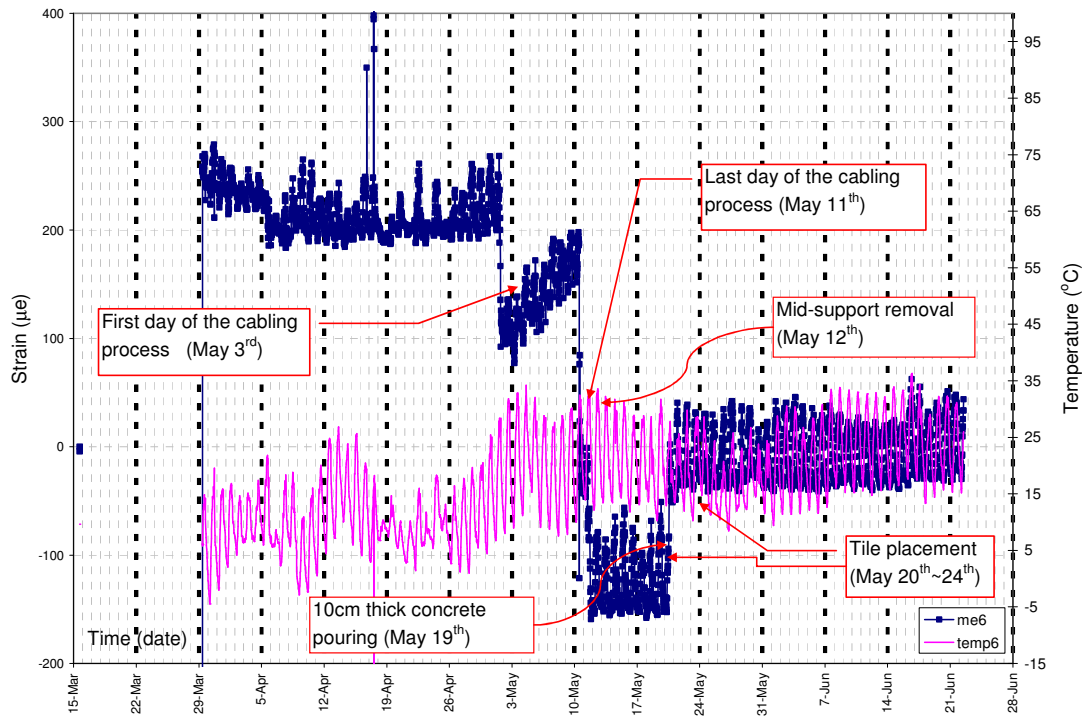
Figure A.6: Strain and temperature changes for strain gage-6

Figure A.7: Strain and temperature changes for strain gage-7

104

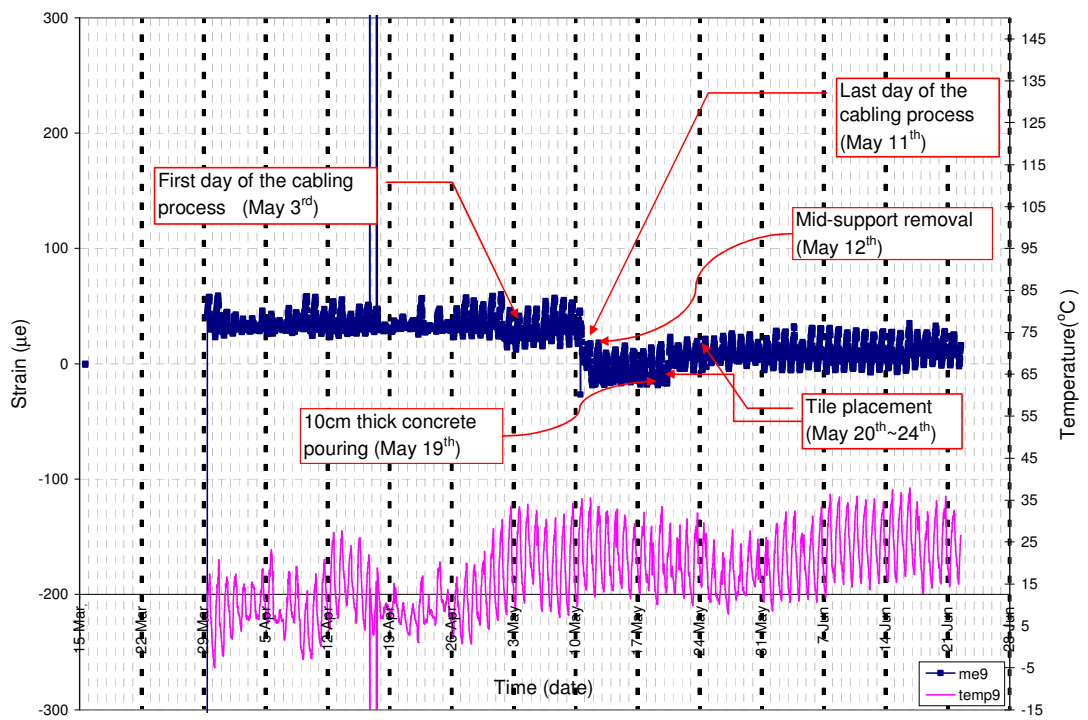Figure A.8: Strain and temperature changes for strain gage-8

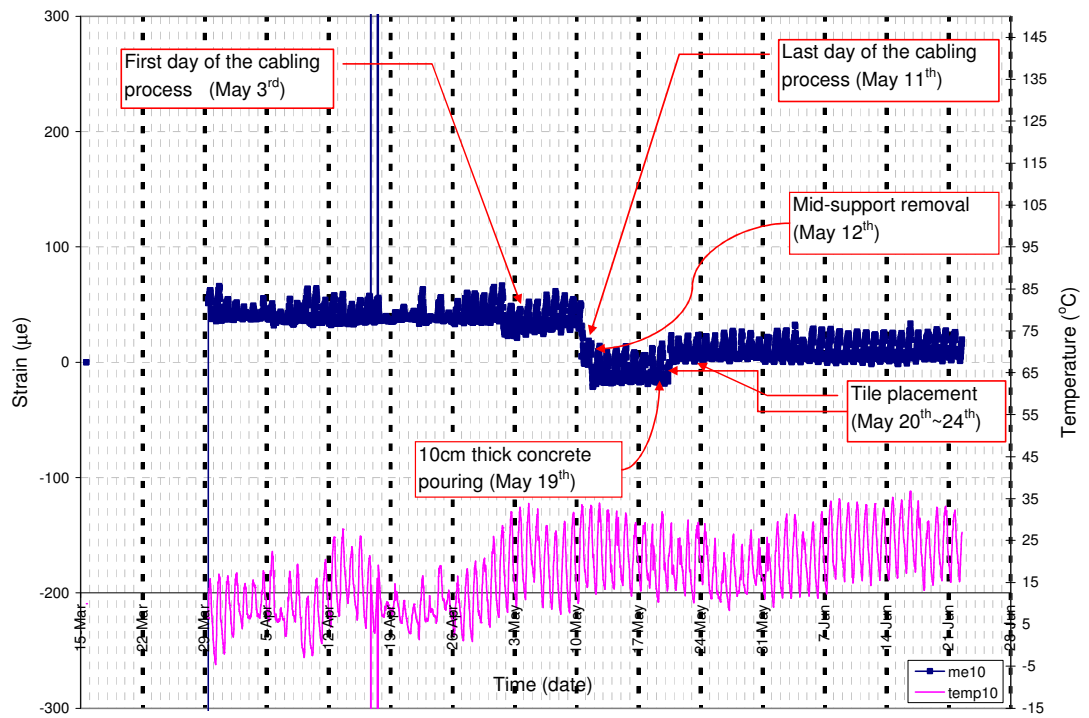Figure A.9: Strain and temperature changes for strain gage-9

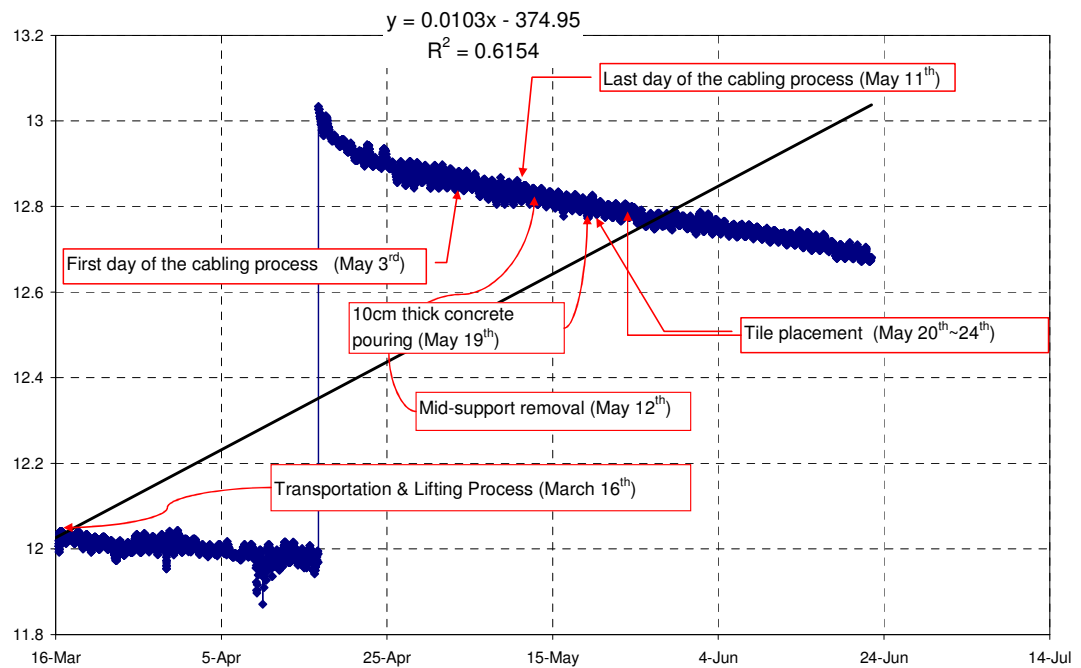Figure A.10: Strain and temperature changes for strain gage-10

Figure A.11: Battery voltage range

APPENDIX- B

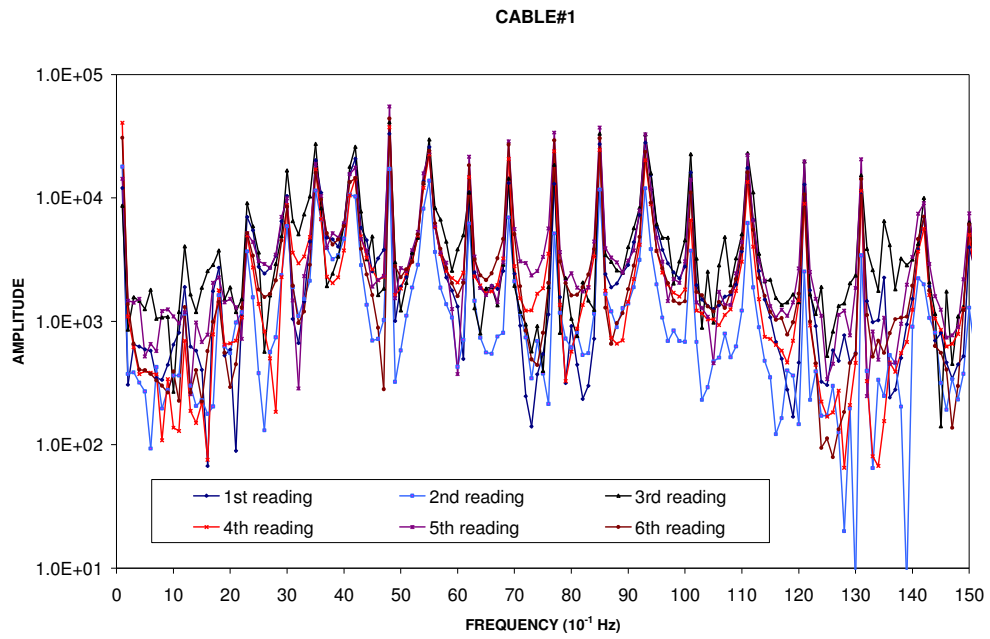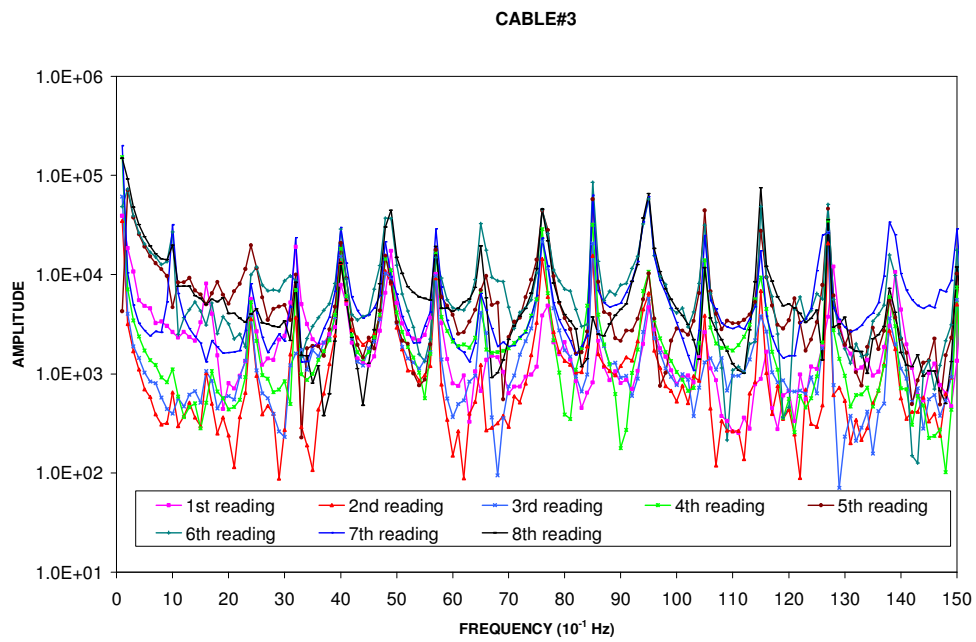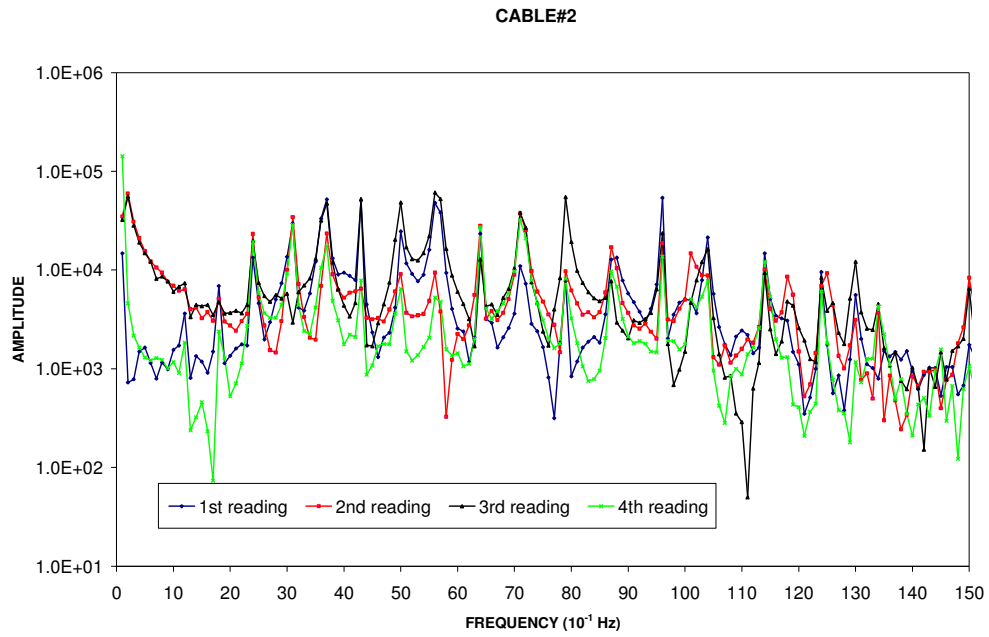## SAMPLE FREQUENCY RESPONSE GRAPHS OF THE CABLES

CABLE#1

Figure B.1: Sample frequency response of cables (cable #1)

CABLE#2

Figure B.2: Sample frequency response of cables (cable #2)

CABLE#3

Figure B.3: Sample frequency response of cables (cable #3)

CABE#4

Figure B.4: Sample frequency response of cables (cable #4)

CABLE#5

Figure B.5: Sample frequency response of cables (cable #5)

CABLE#6

Figure B.6: Sample frequency response of cables (cable #6)

CABLE#7

Figure B.7: Sample frequency response of cables (cable #7)

CABLE#8

Figure B.8: Sample frequency response of cables (cable #8)

CABLE#9

Figure B.9: Sample frequency response of cables (cable #9)

111

CABLE#10

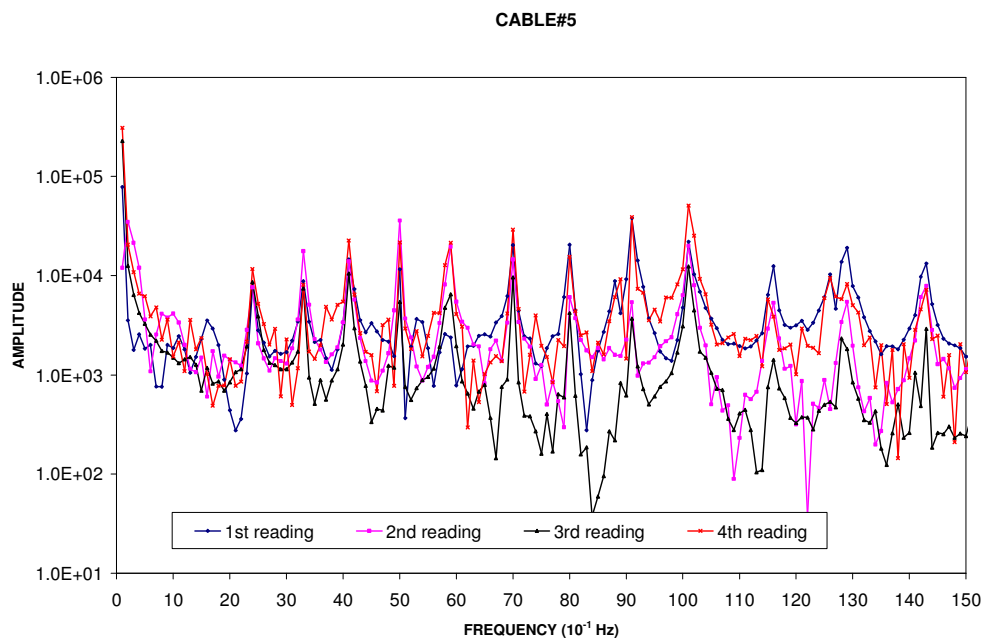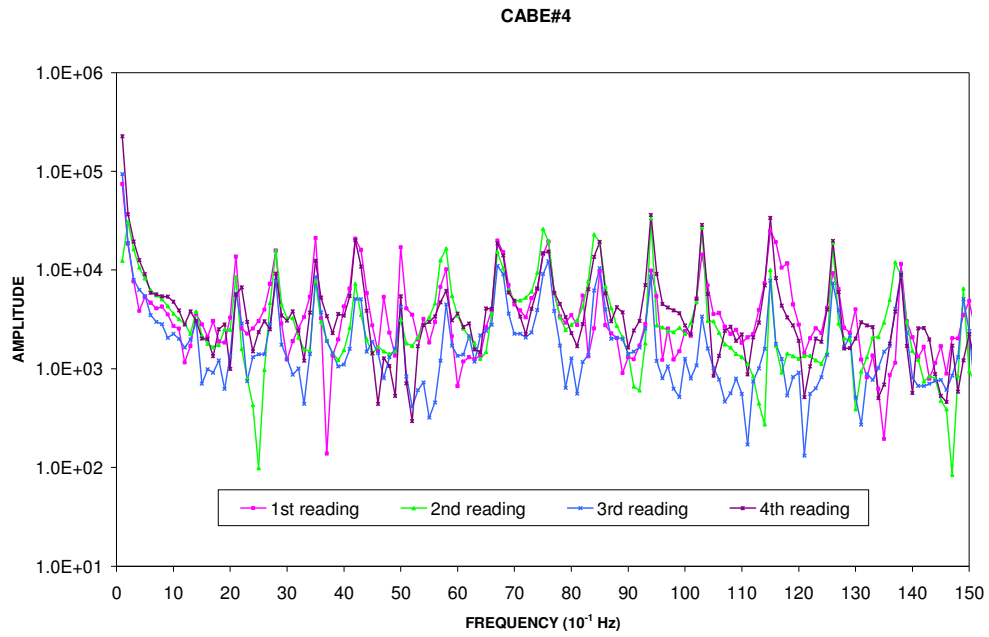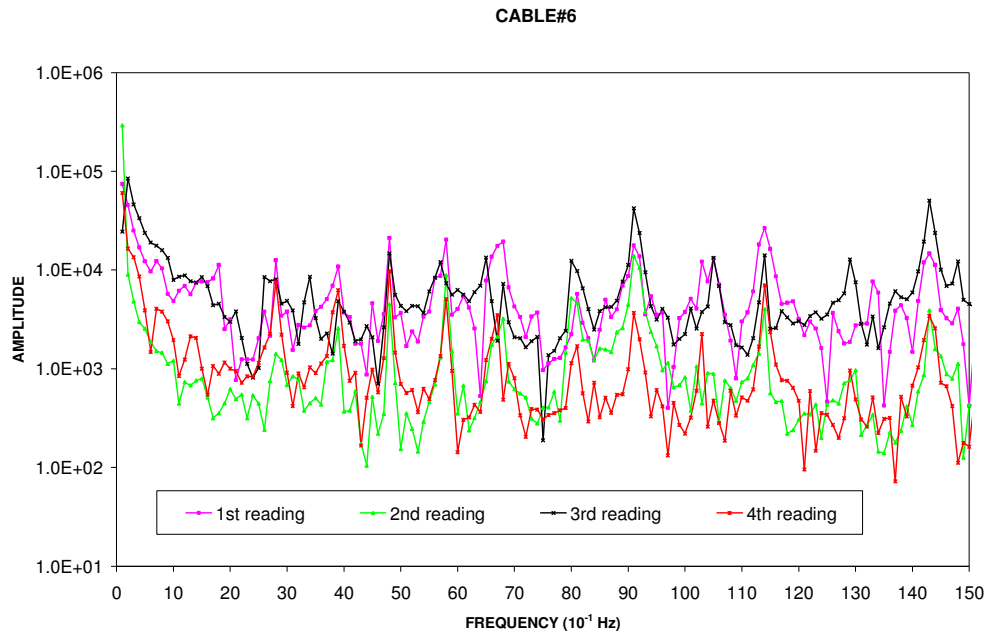Figure B.10: Sample frequency response of cables (cable #10)

CABLE#11

Figure B.11: Sample frequency response of cables (cable #11)
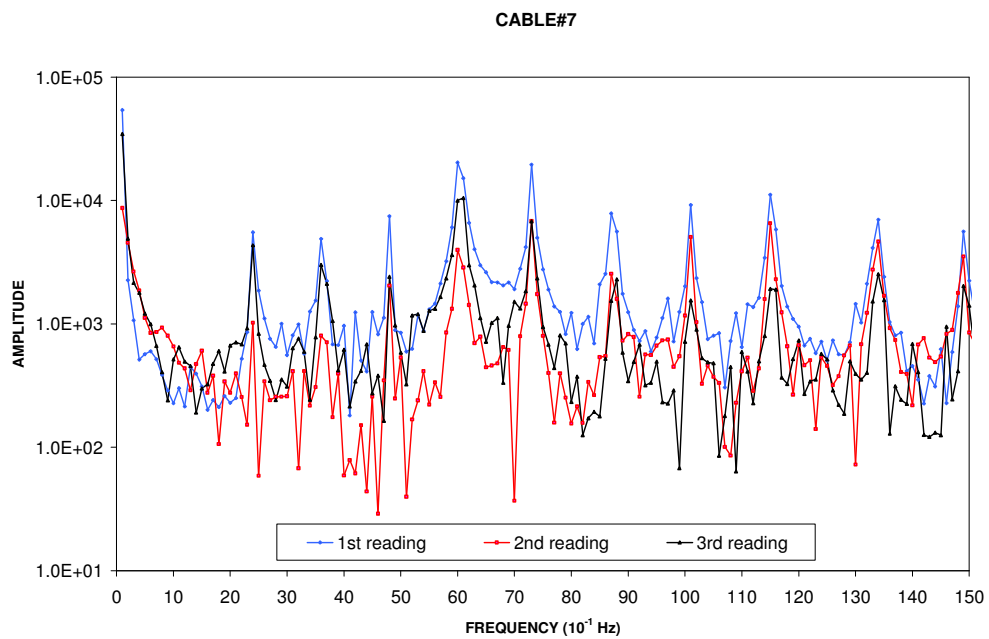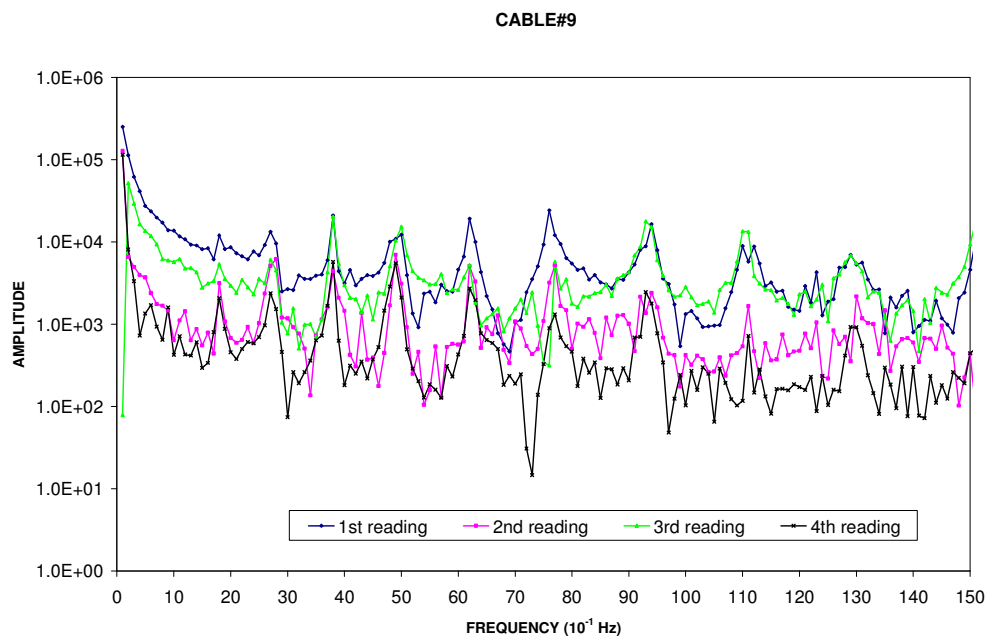
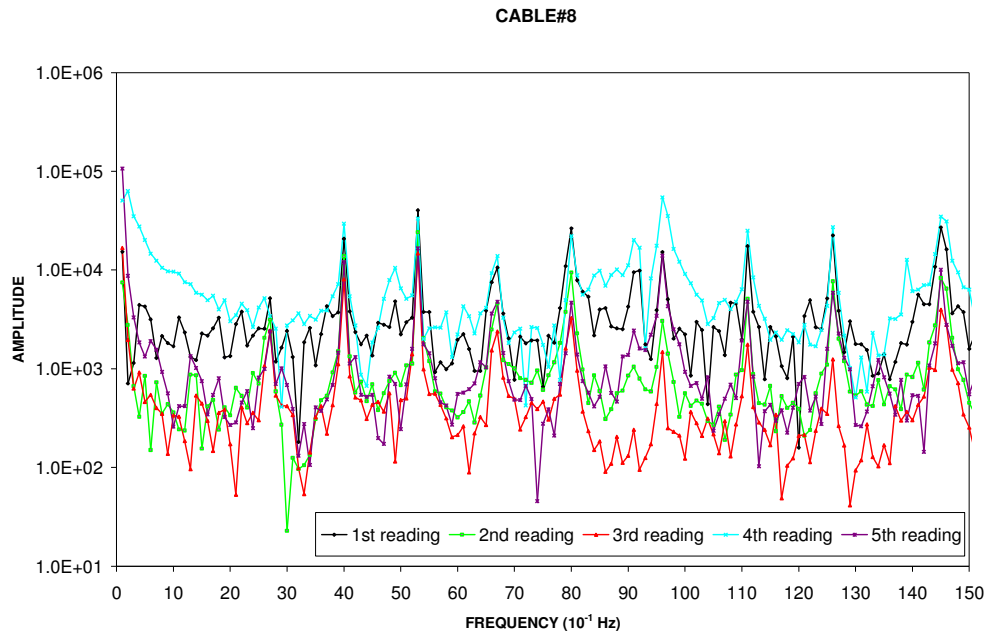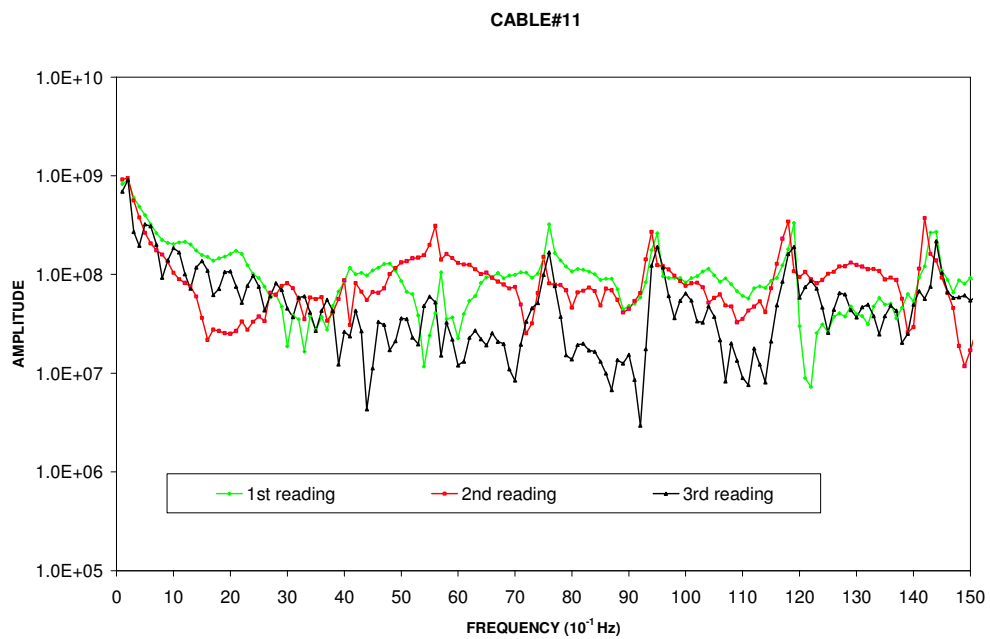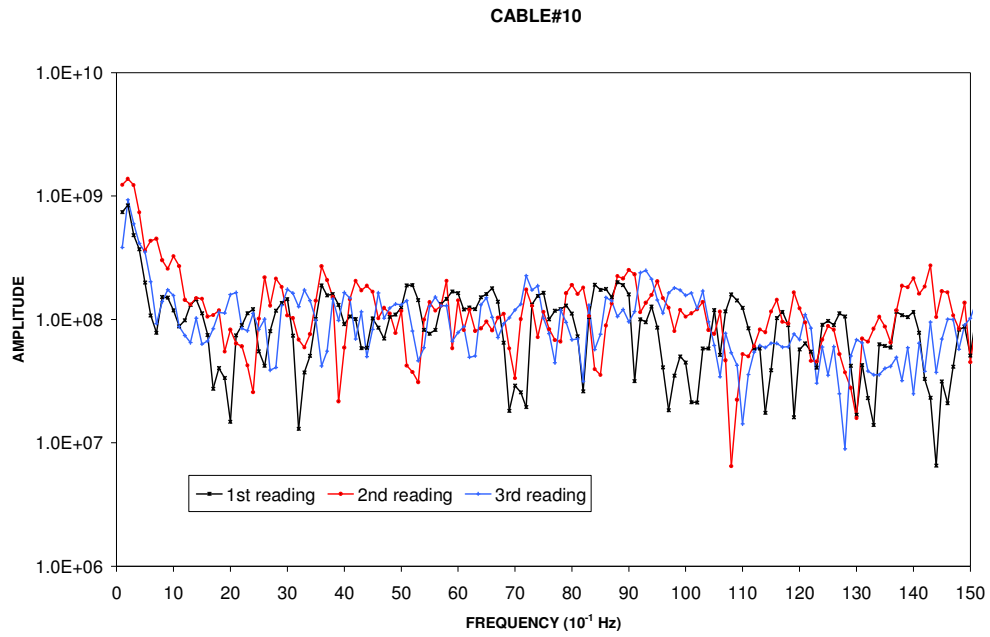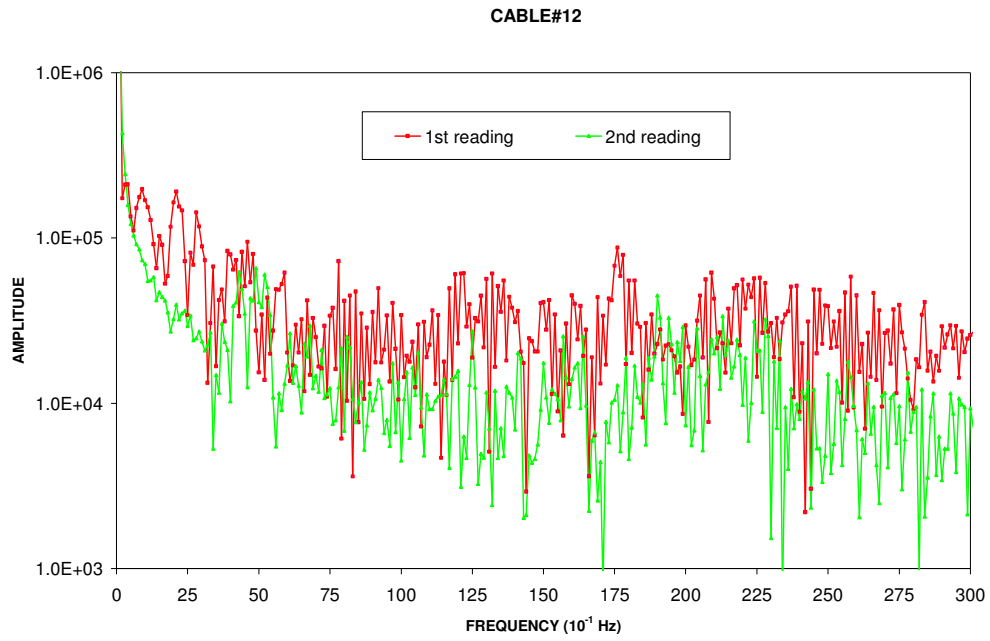Figure B.12: Sample frequency response of cables (cable #12)

113

APPENDIX-C

TECHNICAL SPECIFICATIONS OF INSTRUMENTS

C.1 Technical Specifications of Vibrating Wire Strain Gage

Standard Range   : 300$\mu\varepsilon$,   Accuracy   : $\pm0.1\%$ ~ $\pm0.5\%$ F.S.

Sensitivity   : 1.0$\mu\varepsilon$,   Nonlinearity : < 0.5% F.S.

Temperature Range: -20°C to + 80°C   Active Gage Length: 150mm

Range   : Set of values of force for which the error of a measuring instrument is intended to lie within specified limits

Sensitivity   : Full scale output divided by the <u>rated capacity</u> of a given transducer.

Rated capacity   : The maximum force that a force transducer is designed to measure.

Accuracy   : Closeness of the agreement between the result of a measurement and true value of the force.

Nonlinearity   : The deviation of measured transducer outputs from a best-fit line giving output in terms of force.
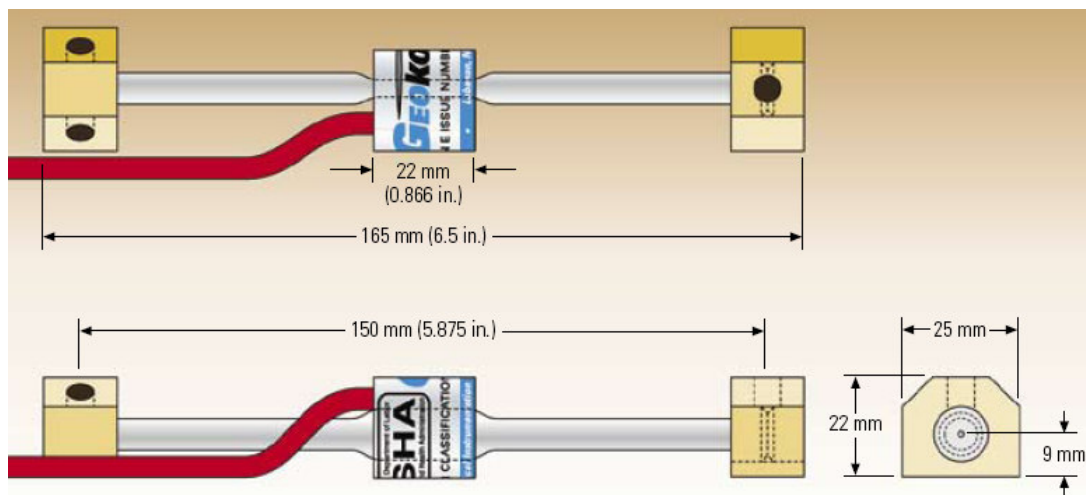
Figure C.1: Longitudinal and cross sections of vibrating wire strain gage

C.2 Technical Specifications of CR10X Data Logger
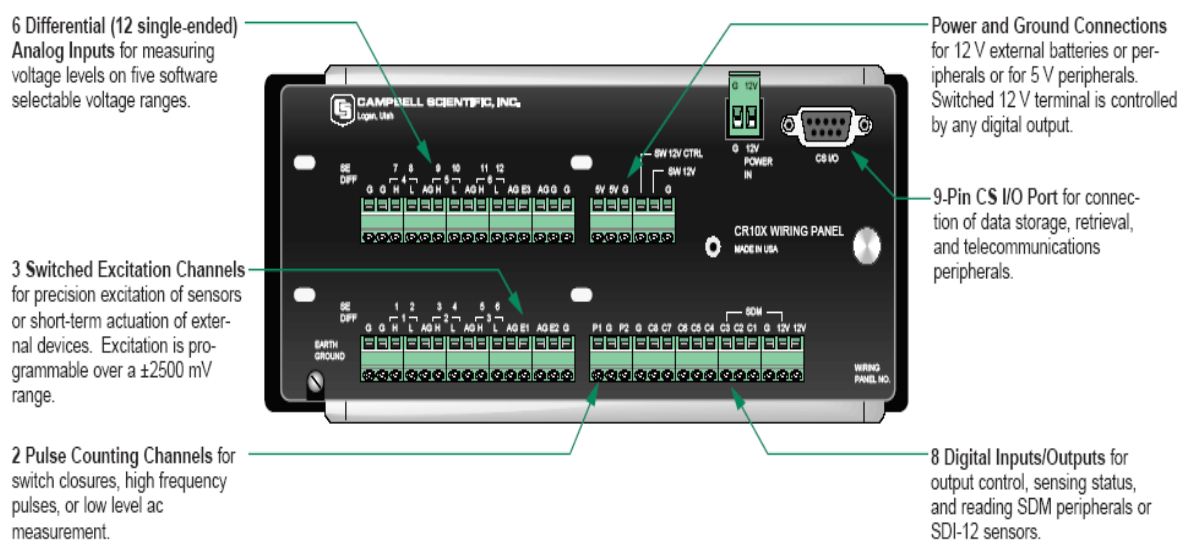
Figure C.2: CR10X data logger

PROGRAM EXECUTION RATE

Program is synchronized with real-time up to 64 Hz. One channel can be measured at this rate with uninterrupted data transfer. Burst measurements up to 750 Hz are possible over short intervals.

ANALOG INPUTS

NUMBER OF CHANNELS: 6 differential or 12 single ended, individually configured. Channel expansion provided by AM16/32 or AM416 Relay Multiplexers and AM25T Thermocouple Multiplexers.

ACCURACY : ±0.10% of FSR (-25° to 50°C);

: ±0.05% of FSR (0° to 40°C);

e.g., ±0.1% FSR = ±5.0 mV for ±2500mV range

Table C.1: Range and resolution

Full Scale Input Range (mV)	Resolution (µV)	
	Differential	Single-Ended
±2500	333.00	666.00
±250	33.30	66.60
±25	3.33	6.66
±7.5	1.00	2.00
±2.5	0.33	0.66

INPUT SAMPLE RATES: Includes the measurement time and conversion to engineering units. The fast and slow measurements integrate the signal for 0.25 and 2.72 ms, respectively. Differential measurements incorporate two integrations with reversed input polarities to reduce thermal offset and common mode errors.

Fast single-ended voltage   : 2.6 ms

Fast differential voltage   : 4.2 ms

Slow single-ended voltage   : 5.1 ms

Slow differential voltage   : 9.2 ms

Differential with 60 Hz rejection   : 25.9 ms

Fast differential thermocouple   : 8.6 ms

INPUT NOISE VOLTAGE (for ±2.5 mV range):

Fast differential   : 0.82 µV rms

Slow differential   : 0.25 µV rms

Differential with 60 Hz rejection   : 0.18 µV rms

COMMON MODE RANGE   : ±2.5 V

DC COMMON MODE REJECTION   : >140 dB

NORMAL MODE REJECTION   : 70 dB

INPUT CURRENT   : ±9 nA maximum

INPUT RESISTANCE   : 20 Gohms typical

ANALOG OUTPUTS

DESCRIPTION :3 switched, active only during measurement, one
at a time

RANGE : ±2.5 V

RESOLUTION : 0.67 mV

ACCURACY : ±5 mV; ±2.5 mV (0° to 40°C)

CURRENT SOURCING : 25 mA

CURRENT SINKING : 25 mA

FREQUENCY SWEEP FUNCTION:

The switched outputs provide a programmable swept frequency, 0 to 2.5 V square wave for exciting vibrating wire transducers.

RESISTANCE MEASUREMENTS

The CR10X provides ratio-metric bridge measurements of 4- and 6-wire full bridge, and 2-, 3-, and 4-wire half bridges. Precise dual polarity excitation using any of the switched outputs eliminates dc errors. Conductivity measurements use a dual polarity 0.75 ms excitation to minimize polarization errors.

ACCURACY : ±0.02% of FSR plus bridge resistor error.

PERIOD AVERAGING MEASUREMENTS

The average period for a single cycle is determined by measuring the duration of a specified number of cycles. Any of the 12 single-ended analog

input channels can be used. Signal attenuation and ac coupling are typically required.

Table C.2: Input frequency range

Signal peak-to-peak[1]		Min. Pulse w.	Max. Freq.[2]
Min.	Max.		
500 mV	5.0 V	2.5 µs	200 kHz
10 mV	2.0 V	10 µs	50 kHz
5 mV	2.0 V	62 µs	8 kHz
2 mV	2.0 V	100 µs	5 kHz

[1]Signals centered around datalogger ground
[2]Assuming 50% duty cycle

RESOLUTION   : 35 ns divided by the number of cycles measured

ACCURACY   : ±0.01% of reading (number of cycles ≥100)

                         ±0.03% of reading (number of cycles <100)

TIME REQUIRED FOR MEASUREMENT: Signal period times the number of cycles measured plus 1.5 cycles + 2 ms

PULSE COUNTERS

NUMBER OF PULSE COUNTER CHANNELS

2 eight-bit or 1 sixteen-bit; software selectable as switch closure, high frequency pulse, and low level ac.

119

MAXIMUM COUNT RATE

16 kHz, eight-bit counter; 400 kHz, sixteen-bit counter. Channels are scanned at 8 or 64 Hz (software selectable).

SWITCH CLOSURE MODE

Minimum Switch Closed Time: 5 ms Minimum Switch Open Time: 6 ms

Maximum Bounce Time: 1 ms open without being counted

HIGH FREQUENCY PULSE MODE

Minimum Pulse Width   : 1.2 μs

Maximum Input Frequency   : 400 kHz

Voltage Thresholds: Count upon transition from below 1.5 V to above 3.5 V at low frequencies. Larger input transitions are required at high frequencies because of input filter with 1.2 μs time constant. Signals up to 400 kHz will be counted if centered around +2.5 V with deviations ≥ ±2.5 V for ≥ 1.2 μs.

Maximum Input Voltage: ±20 V

LOW LEVEL AC MODE

Typical of magnetic pulse flow transducers or other low voltage, sine wave outputs.

Input Hysteresis   : 14 mV

Maximum ac Input Voltage   : ±20 V

Table C.3: Minimum AC input voltage and its range

Minimum AC Input Voltage (Sine wave mV RMS)	Range (Hz)
20	1.0 to 100
200	0.5 to 10000
1000	0.3 to 16000

DIGITAL I/O PORTS

8 ports, software selectable as binary inputs or control outputs. 3 ports can be configured to count switch closures up to 40 Hz.

OUTPUT VOLTAGES (no load): high 5.0 V ±0.1 V; low < 0.1 V

OUTPUT RESISTANCE   : 500 ohms

INPUT STATE   : high 3.0 to 5.5 V; low -0.5 to 0.8 V

INPUT RESISTANCE   : 100 kohms

SDI-12 INTERFACE STANDARD

Digital I/O Ports C1-C8 support SDI-12 asynchronous communication; up to ten SDI-12 sensors can be connected to each port. Meets SDI-12 Standard version 1.2 for datalogger and sensor modes.

CR10XTCR THERMOCOUPLE REFERENCE

POLYNOMIAL LINEARIZATION ERROR: Typically <±0.5°C (-35° to +50°C), <±0.1°C (-24° to +45°C).

INTERCHANGEABILITY ERROR: Typically <±0.2°C (0° to +60°C) increasing to ±0.4°C (at -35°C).

CPU AND INTERFACE

PROCESSOR   : Hitachi 6303

PROGRAM STORAGE

Up to 16 kbytes for active program; additional 16 kbytes for alternate programs. Operating system stored in 128 kbytes Flash memory.

DATA STORAGE

128 kbytes SRAM standard (approximately 60,000 data values). Additional 2 Mbytes Flash available as an option.

OPTIONAL KEYBOARD DISPLAY: 8-digit LCD (0.5" digits)

PERIPHERAL INTERFACE

 9 pin D-type connector for keyboard display, storage module, modem, printer, card storage module, and RS-232 adapter.

CLOCK ACCURACY: ±1 minute per month

SYSTEM POWER REQUIREMENTS

VOLTAGE: 9.6 to 16 Vdc

TYPICAL CURRENT DRAIN

1.3 mA quiescent, 13 mA during processing, and 46 mA during analog measurement.

BATTERIES

Any 12 V battery can be connected as a primary power source. Several power supply options are available from Campbell Scientific. The Model CR2430 lithium battery for clock and SRAM backup has a capacity of 270 mAhr.

C.3 Technical Specifications of PCB 393C Accelerometer

- Sensitivity: (±15%) 1000mV/g (101.9mV/(m/s²))
- Broadband Resolution: (10000 to 1 Hz) 0.0001g rms (0.001m/s² rms)
- Electrical Connector: 10-32 Coaxial Jack
- Weight: 31.2oz (885gm)

Table C.4: Technical properties of 393C model accelerometer

Performance	
Sensitivity (± 15 %)	1000 mV/g
Measurement Range	2.5 g pk
Frequency Range (± 5 %)	0.025 to 800 Hz
(± 10 %)	0.01 to 1200 Hz
Resonant Frequency	≥ 3.5 kHz
Broadband Resolution (1 to 10,000 Hz)	0.0001 g rms
Non-Linearity	≤ 1 %
Transverse Sensitivity	≤ 5 %
Environmental	
Overload Limit (Shock)	± 100 g pk
Temperature Range	-65 to +200 °F
Temperature Response	<0.03 %/°F
Base Strain Sensitivity	0.001 g/µε
Electrical	
Excitation Voltage	18 to 30 VDC
Constant Current Excitation	2 to 20 mA
Output Impedance	<100 ohm
Output Bias Voltage	3.0 to 4.5 VDC
Discharge Time Constant	≥ 20 sec
Settling Time	300 sec
Electrical Isolation (Base)	$\geq 10^8$ ohm
Physical	
Sensing Element	Quartz
Sensing Geometry	Compression
Housing Material	Stainless Steel
Sealing	Hermetic
Size (Diameter x Height)	2.25 in x 2.16 in
Weight	31.2 oz
Electrical Connector	10-32 Coaxial Jack
Electrical Connection Position	Side
Mounting Thread	10-32 Female

APPENDIX-D

CR10X DATA LOGGER SOFTWARE PROGRAM EXAMPLE

The following software program example is used in burst mode.

```
;{CR10X}
;

*Table 1 Program
01: 5  Execution Interval (seconds)
 1: If Flag/Port (P91)
 1: 13 Do if Flag 3 is High
 2: 88 Call Subroutine 88
 2: Do (P86)
 1: 23 Set Flag 3 Low

*Table 2 Program
02: 0.0000 Execution Interval (seconds)

*Table 3 Subroutines
 1: Beginning of Subroutine (P85)
 1: 88         Subroutine 88
 2: Burst Measurement (P23)
 1: 1          Input Channels per scan
 2: 15         2500 mV Fast Range
 3: 4          In Chan
 4: 0000       Trig/Trig/Dest/Meas Options
 5: 10         Time per Scan (msec)
 6: 1          Scans (in thousands)
 7: 0          Samples before Trigger
 8: 0          mV Limit
 9: 0          mV Excitation
10: 2          Loc [acc_1]
11: 1000       Mult
12: 0.0        Offset
 3: Do (P86)
 1: 10         Set Output Flag High (Flag 0)
 4: Resolution (P78)
 1: 1 High Resolution
 5: Sample (P70)
 1: 1000      Reps
 2: 2         Loc [acc_1]
 6: End (P95)


 End Program
```